University of Tennessee, Knoxville
Trace: Tennessee Research and Creative Exchange

Masters Theses Graduate School

12-2011

STRUCTURAL AND STRATIGRAPHIC RELATIONSHIPS NEAR THE SOUTHERN TERMINUS OF THE PULASKI FAULT, NORTHEAST TENNESSEE

Phillip Michael Derryberry
pderryb2@utk.edu

Recommended Citation
Derryberry, Phillip Michael, "STRUCTURAL AND STRATIGRAPHIC RELATIONSHIPS NEAR THE SOUTHERN TERMINUS OF THE PULASKI FAULT, NORTHEAST TENNESSEE. " Master's Thesis, University of Tennessee, 2011.
https://trace.tennessee.edu/utk_gradthes/1065

This Thesis is brought to you for free and open access by the Graduate School at Trace: Tennessee Research and Creative Exchange. It has been accepted for inclusion in Masters Theses by an authorized administrator of Trace: Tennessee Research and Creative Exchange. For more information, please contact trace@utk.edu.

To the Graduate Council:

I am submitting herewith a thesis written by Phillip Michael Derryberry entitled "STRUCTURAL AND STRATIGRAPHIC RELATIONSHIPS NEAR THE SOUTHERN TERMINUS OF THE PULASKI FAULT, NORTHEAST TENNESSEE." I have examined the final electronic copy of this thesis for form and content and recommend that it be accepted in partial fulfillment of the requirements for the degree of Master of Science, with a major in Geology.

Robert D. Hatcher, Jr., Major Professor

We have read this thesis and recommend its acceptance:

Micah J. Jessup, Linda C. Kah, Peter J. Lemiszki

Accepted for the Council:
Carolyn R. Hodges

Vice Provost and Dean of the Graduate School

(Original signatures are on file with official student records.)

STRUCTURAL AND STRATIGRAPHIC RELATIONSHIPS NEAR THE SOUTHERN TERMINUS OF THE PULASKI FAULT, NORTHEAST TENNESSEE

A Thesis
Presented for the
Master of Science Degree
The University of Tennessee, Knoxville

Phillip M. Derryberry

December, 2011

DEDICATION

This thesis is dedicated to my amazing parents, Ginny and Gary Derryberry, for their love, encouragement, and friendship

ACKNOWLEDGMENTS

First and foremost, I sincerely thank Dr. Robert D. Hatcher, Jr., for all his support and guidance throughout this process and for helping me toward becoming a well-rounded and skilled field geologist/scientist. Special thanks to Dr. Peter J. Lemiszki for his valuable help in the field, critiques of my map, and thought-provoking discussions. I am also grateful to Dr. Linda C. Kah and Dr. Micah J. Jessup for providing me with great advice and for being excellent teachers.

This research would not have been possible without funding from the UTK Department of Earth and Planetary Sciences, UTK Science Alliance Center of Excellence, and the EDMAP component (G09AC00126) of the National Cooperative Geologic Mapping Program from the U.S. Geological Survey. Additional thanks to Dr. Robert D. Hatcher, Jr. for the George D. Swingle Award in 2010 and all who have contributed to it.

I am very grateful to Nancy Meadows for her masterful editing skills and our good conversations, and to Andrew Wunderlich, the GIS genie, for making life a lot easier when compiling my map. Of course, I also thank my fellow graduate students, past and present, who have helped and talked with me about many aspects of geology and my research: Matt Huebner, Chris Howard, Arthur Merschat, William Gilliam, Carissa Snyder, Justin Reher, Brittany Davis, and Heather Byars. Much appreciation to Peter Robertson, Chris Howard, Ginny Derryberry, and Norman Rivera for spending several days with me, helping with fieldwork and enjoying God's amazing countryside. And last but not least, the beautiful and talented Jennifer Brouner for her assistance in the field and keeping me sane for nearly three years.

ABSTRACT

The Pulaski fault is one of the master thrust faults in the Appalachian Alleghanian fold-thrust belt. Detailed geologic mapping of Cambrian and Ordovician strata in northeastern Tennessee revealed key structural and stratigraphic characteristics for distinguishing the Pulaski thrust sheet from its footwall, the Saltville thrust sheet. Unlike most thrust systems in the Valley and Ridge, the Pulaski records at least two deformation phases. Geometric and crosscutting relationships along parts of the Pulaski thrust sheet in this study area and in southwestern Virginia suggest hanging wall and possibly some footwall deformation prior to the emplacement of the thrust sheet.

The initial deformation in the Pulaski sheet, which consists of northwest-vergent, tight to overturned, pre-faulting macroscopic folds, may be a manifestation of the previously recognized late Mississippian to Pennsylvanian Lackawanna phase of the Alleghanian orogeny. Transport of the earlier deformed strata, analogous to deformation sequences that occurred in the Pulaski sheet near the Roanoke recess, would therefore be associated with the main (Early Permian) phase of the Alleghanian orogeny. In the study area, these two phases likely represent small changes in orientation during a single event of continued shortening. Type 3 fold interference patterns in the Pulaski thrust sheet here further support this notion.

Substantially different facies occur on opposite sides of the fault. Upper Conasauga and Knox Group strata in the Pulaski thrust sheet consist predominantly of limestone and contain few identifiable stratigraphic markers suitable for subdividing the Knox northwest of the fault. Lower Conasauga Group rocks in the thrust sheet are more dolomitic and are interbedded with thin shale units. Geologic mapping during this study has successfully subdivided Honaker Dolomite in parts of the Pulaski thrust sheet by the tracing of the Rogersville Shale.

Data suggest that the Pulaski fault was overridden by the thin-skinned Great Smoky fault. Kinematic and geometric interrelationships between the Pulaski and other Valley and Ridge faults provide useful insight into the processes of footwall/hanging wall deformation and thrust propagation in foreland fold-thrust belts. Findings here could also improve our understanding of deformation sequences between the southern and central Appalachians.

TABLE OF CONTENTS

LIST OF FIGURES

LIST OF ATTACHMENTS

CHAPTER I

INTRODUCTION

Present Investigation

The somewhat unusual characteristics of the Pulaski fault, relative to other Valley and Ridge faults, have influenced many workers to structurally and stratigraphically analyze specific regions that contain this fault. These characteristics include: (1) its large extent [563 km (350 miles)]; (2) relatively low dip; (3) structurally lower detachment indicated by the presence of Lower Cambrian clastics (Chilhowee Group) in parts of the hanging wall; and (4) complex, likely polyphase deformation. Most investigations, including Cooper and Cashion (1970), Rodgers (1970a), Bartholomew and Schultz (1980), and Bartholomew et al. (1980), have historically been in southwestern Virginia near the southern/central Appalachian transition. Work on the Pulaski fault in parts of the southern Appalachians, specifically near its southwestern terminus in East Tennessee, is less detailed. Rodgers (1953a, p. 160) suggested a possible future mapping project within this region:

> *Pulaski and associated faults southwest of Nolichucky River . . . The S-shaped curve of the Pulaski fault shown on the present map is based on scattered observations and needs verification.*

The purpose of this study was to produce a detailed (1:24,000-scale) geologic map near the southwestern terminus of the Pulaski fault to: (1) better define the location where the thin-skinned Great Smoky fault overlaps the Pulaski; (2) identify distinct facies changes that characterize the Pulaski and Saltville thrust sheets within the area; and (3) attempt to determine a deformational history that occurred within this segment of the Pulaski sheet. Rodgers' (1953b) 1:125,000 geologic map of East Tennessee lacks sufficient detail to resolve these objectives. Detailed 1:24,000 geologic mapping by Whitmer (2005), which was incorporated into this thesis with some remapping, contains the "S"-curve segment of the Pulaski fault, but does not include its terminus to the south in the Neddy Mountain quadrangle.

Fieldwork was completed during the winter, spring, and summer of 2009 and 2010. Mapping was accomplished with the assistance of a hand-held Trimble™ GeoXT 2005 Series GPS unit with data recorded in ArcPad™, which permitted direct recording of data in ESRI ArcMap™. Over 1,100 structural data stations (including orientations of strike and dip of bedding surfaces, cleavage, joints, and mesoscale folds) were collected and measured using a Brunton compass. The map was digitally compiled using ArcMap™ and Adobe Illustrator™ software.

Study Area

Research was conducted within an area encompassing parts of four 7.5-minute quadrangles: Cedar Creek, Parrottsville, Neddy Mountain, and Paint Rock, located near the Greene/Cocke County line in East Tennessee (Fig. 1-1). This study area is ~100 km east of Knoxville, Tennessee, and is located close to Newport, Tennessee (to the southwest), Greeneville, Tennessee (to the northeast), and the North Carolina state line (to the southeast; Fig. 1-1). Main roads in the area include U.S. and State Routes 70 and 321/411, permitting easy access via Interstate Highways 40 and 81. The Nolichucky and French Broad Rivers transect the area.

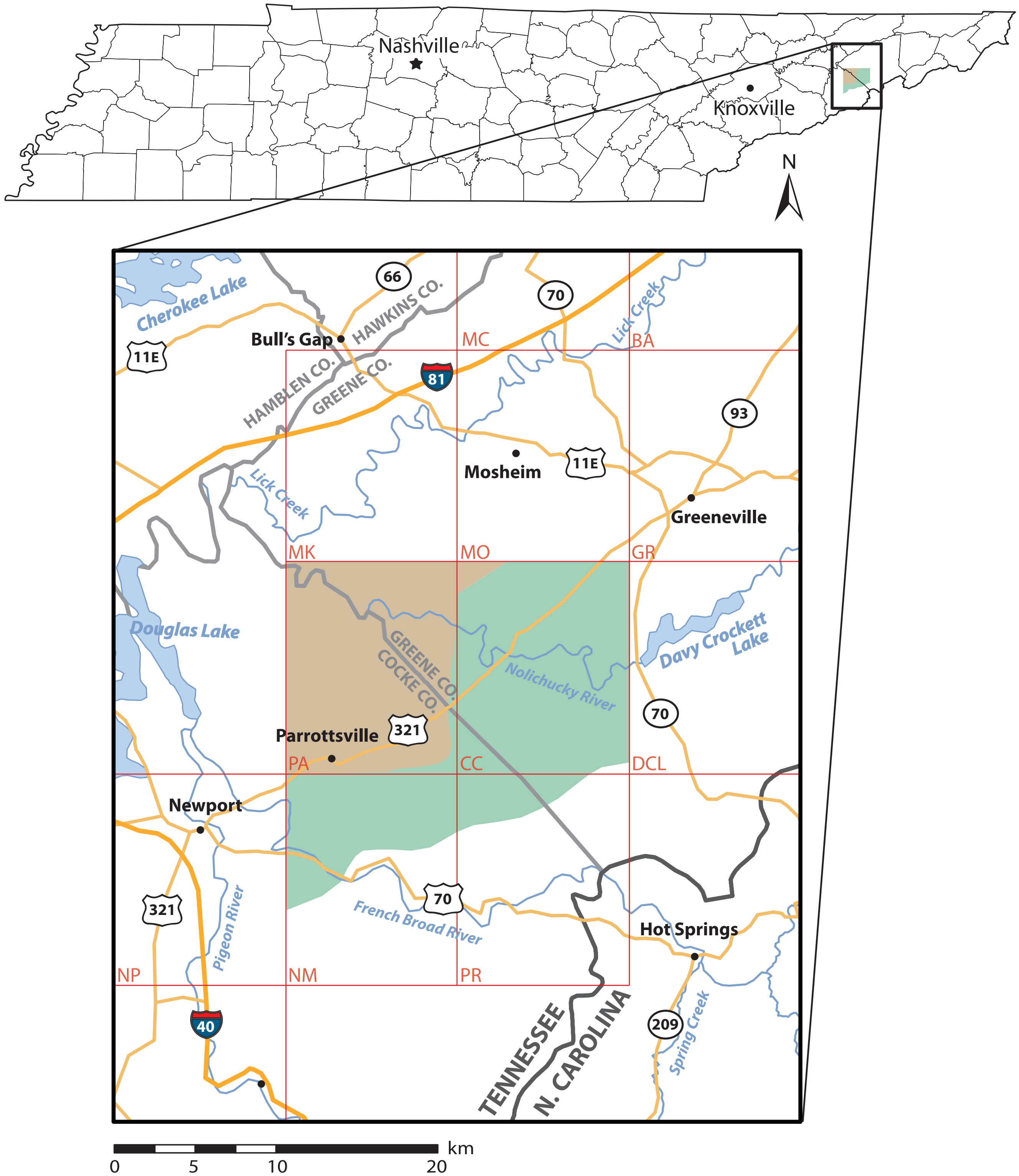

Figure 1-1. Location of field area [green—this study; brown—Whitmer (2005)] overlain with 7.5-minute quadrangle index (red). BA-Baileyton. CC-Cedar Creek. DC-Davy Crockett Lake. GR-Greeneville. MC-McCloud. MK-Mohawk. MO-Mosheim. NM-Neddy Mountain. NP-Newport. PA-Parrottsville. PR-Paint Rock.

The majority of the mapped area is situated southeast of the Bays Mountain synclinorium within the Valley and Ridge province, with a very small portion lying in the Blue Ridge province. In this region, the Blue Ridge can be distinguished from the Valley and Ridge by the exclusive appearance of Cambrian and Precambrian strata within its thrust sheets, as well as increasing metamorphic grade and complexity of deformation (Hatcher et al., 1989). Overall, stratigraphy of the study area ranges from Lower Cambrian to Middle Ordovician and consists of Chilhowee, Shady, Rome, Conasauga, Knox, and Chickamauga units. Elevations range from ~300 m (~1,000 ft) at the French Broad River to ~915 m (~3,000 ft) in the Meadow Creek Mountains in the Blue Ridge. Topography reflects the general northeast-southwest trend of the Valley and Ridge province and is heavily influenced by the great variation of lithologic units. Several karst features were observed, mostly within Knox carbonates. Alluvial, colluvial, and terrace deposits that are mostly related to the Quaternary Nolichucky River and the Blue Ridge topographic front were also mapped.

Geologic Setting

The Appalachian foreland fold-thrust belt in the Valley and Ridge province, which contains rock units ranging from Early Cambrian through early Pennsylvanian age, contains a wedge-shaped stack of mostly west-vergent, thin-skinned thrusts positioned above undeformed Mesoproterozoic basement (Hatcher et al., 2007a). In eastern Tennessee and southwestern Virginia, the sedimentary strata represent a progression from a passive platform margin to the development of a foreland (Sevier) basin, which had a clastic source to the southeast during the Blountian phase of the Taconic orogeny (Drake et al., 1989). The late Mississippian-Early Permian Alleghanian orogeny is the youngest and most pervasive tectonic event to affect the southern and central Appalachians. This event emplaced the Blue Ridge-Piedmont megathrust sheet indenter that drove foreland deformation in front of and beneath it (Hatcher et al., 1989, 2007a).

Most major thrust faults in the Valley and Ridge propagate from a basal detachment in the mechanically weak Lower Cambrian Rome Formation (Rodgers, 1970b). These faults increase in stratigraphic throw and displacement southwestward along strike, with the most significant structural transition occurring within the Roanoke recess (Hatcher et al., 1989). Here, Valley and Ridge structures undergo a gradual change in strike from ~N30°E (central Appalachians) to ~N60°E (southern Appalachians) over a broad displacement transfer zone (Rodgers, 1970b). The deformation style also changes from the central Appalachians, which are primarily fold-dominated (i.e., décollement folds overlying blind thrusts), to the southern Appalachians, which are primarily fault-dominated (Gwinn, 1964). These contrasting styles can be attributed to an oblique, and later head-on, rotational collision that initiated the zipper-like closing of the Paleozoic Theic ocean between Gondwana and Laurentia (including previously assembled Peri-Gondwanan and Gondwanan superterranes) during the Alleghanian orogeny (Hatcher, 2002). The associated Early Permian head-on collision, which drove the Blue Ridge-Piedmont composite crystalline thrust sheet, is responsible for the foreland deformation and tectonic style observed in the southern Appalachians (Hatcher, 2002).

Pulaski Fault

The Pulaski-Staunton fault (herein called Pulaski) is one of the master Alleghanian thrust faults in the southern Appalachian Valley and Ridge foreland fold-thrust belt (Fig. 1-2). It contains many unique attributes, both structurally and stratigraphically, relative to other Appalachian Valley and Ridge faults (e.g., Saltville, Copper Creek, and St. Clair faults). The Pulaski fault, for instance, is the only major fault that extends into the central Appalachians and can be traced entirely through the angular Roanoke recess in southwestern Virginia (Rodgers, 1970b). All other major faults of the southern Appalachians terminate as surface features near the 30° bend at Roanoke (Fig. 1-2; Bartholomew, 1987; Couzens and Dunne, 1994). The Pulaski fault's northern terminus lies in Rockingham County, north of Staunton, Virginia. The Greenwood and Seven Springs faults trace the main Pulaski fault to its southern terminus southwest of Greeneville in northeastern Tennessee (Cooper and Cashion, 1970).

Unlike most major Valley and Ridge faults, which propagate from a décollement in the Rome Formation, the Pulaski has been interpreted to have rooted in a lower structural level, based on the presence of Lower Cambrian Shady Dolomite and Chilhowee Group rocks in the hanging wall (Butts, 1933; Rodgers, 1970b; Bartholomew et al., 1980). The most prominent structural feature of the Pulaski fault in Tennessee is the Babbs Knobs flap, located in the southern Baileyton quadrangle and northwestern Greeneville quadrangle (Byerly, 1966; Bultman, 2005). Here, the fault trace irregularly encircles an area of ~26 km^2. The irregularity results from low-dip angles and post-emplacement folding of the Pulaski fault (Byerly, 1966).

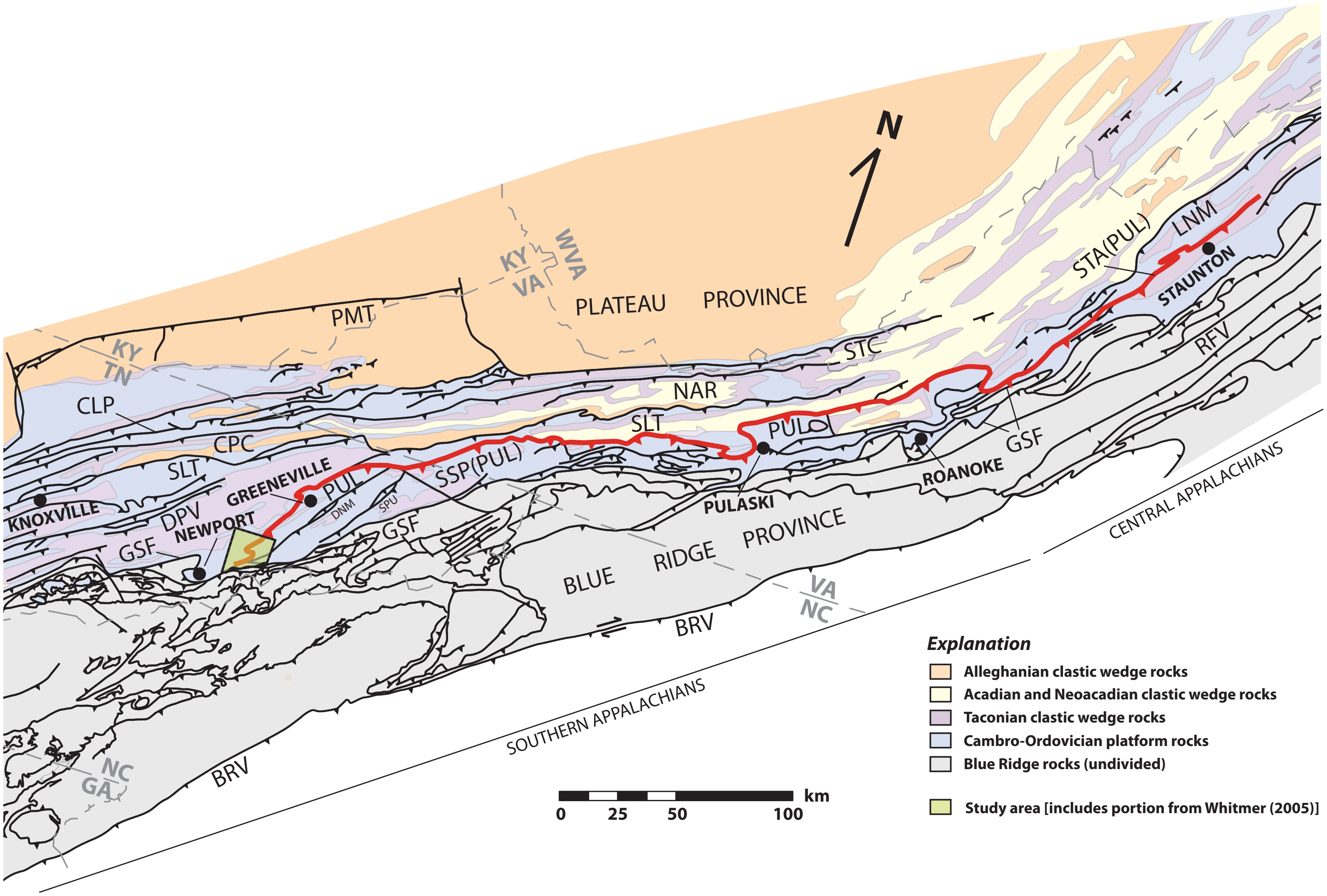

Figure 1-2. Tectonic map showing the Pulaski fault (bold red), in relation to other major faults within the southern and central Appalachian Valley and Ridge, Plateau, and Blue Ridge provinces. BRV-Brevard fault. CLP-Clinchport fault. CPC-Copper Creek fault. DNM-Dunham Ridge fault. DPV-Dumplin Valley fault. GSF-Great Smoky fault. LNM-Little North Mountain fault. NAR-Narrows fault. PMT-Pine Mountain thrust. PUL-Pulaski fault. RFV-Rockfish Valley fault. SLT-Saltville fault. STA-Staunton fault. SPU-Spurgeon fault. SSP-Seven Springs fault. STC-St. Clair fault. Modified from Hatcher et al. (2007b).

Bartholomew (1987) defined the Pulaski thrust sheet as a complex, composite sheet in which various plates were juxtaposed during different stages of Alleghanian thrusting. Near the Roanoke area, Bartholomew noted that a 300-500-m-thick “broken” formation, earlier identified by Schultz (1983), which contains the Max Meadows Breccia (Cooper and Haff, 1940), represents a lower-level décollement zone that formed earlier in the Alleghanian prior to ramping. Early deformation and later passive transport of this unit suggest two-phase Alleghanian deformation is recorded in the Pulaski sheet.

Previous Work

Previously published maps that contain all or portions of the quadrangles in the research area include Keith (1895, 1905a, 1905b), Rodgers (1953b), Brokaw et al. (1966), and Hardeman et al. (1966). Initially, the Pulaski fault was mapped from Marion to Blacksburg, Virginia, by Campbell (1925), who named the fault after exposures adjacent to the town of Pulaski in Pulaski County, Virginia. The fault was later traced by Butts (1933) northeastward near Purgatory Mountain and into the central Appalachian part of the Valley and Ridge. For years, the Seven Springs fault was misidentified as a separate and distinct fault from the Pulaski (Cooper, 1936). Later work and improved mapping (Rodgers, 1953b; Hardeman et al., 1966; Cooper and Cashion, 1970) confirmed that both faults are one in the same. This discovery sparked others to delineate previously suggested northern continuations of the Pulaski fault, such as the Staunton fault (Cooper, 1970; Harris, 1979), identified near Staunton, Virginia, where the Pulaski is believed to terminate (Fig. 1-2).

Rodgers (1953b; 1970a) further traced the Pulaski fault 120 km southwestward into Tennessee, where he and later Milici (1975) interpreted it to terminate and disappear beneath the Blue Ridge thrust sheet. Byerly (1966) produced a detailed geologic map of the Baileyton and Greeneville 7.5-minute quadrangles ~50 km northeast of the Pulaski terminus, focusing on the peculiar Babbs Knobs flap in the Pulaski sheet. Whitmer (2005) mapped the area within the Parrottsville and portion of the Cedar Creek quadrangles that contained the "S-curve" segment of the Pulaski fault, but did not map farther south to the terminus. The possibility that the fault continues as far southwest as the Newport quadrangle was first raised by Lemiszki (2008) based on certain key structural and stratigraphic differences between the Saltville and Pulaski thrust sheets. However, newer detailed (1:24,000-scale) mapping of the Neddy Mountain quadrangle (this study) reconfirms the site of the terminus previously mapped by Rodgers (1953b; 1970a).

Rodgers (1953a) first recognized key facies changes within lithologic units (Chickamauga, Knox, and Conasauga Groups) of the the Pulaski and Saltville thrust sheets in northeastern Tennessee and southwestern Virginia. The paucity of many stratigraphic markers did not permit Rodgers to successfully subdivide any of these groups within the Pulaski sheet. With the exception of the Ocoee Supergroup, no other stratigraphic unit in the southern Appalachians has been debated as much as the Chickamauga Group (Rodgers, 1953a). Successful subdivision of the Middle Ordovician Sevier Shale (Chickamauga Group) was accomplished for the first time by Lemiszki (2003), Bultman (2005), and Whitmer (2005).

CHAPTER II

STRATIGRAPHY

General Overview

Rock units of the study area range from the Lower Cambrian (Unicoi Formation) to the Middle Ordovician (Middle Sevier Shale), and occur in three major thrust sheets, the Saltville, Pulaski, and Blue Ridge–from northwest to southeast (Fig. 2-1). These strata include units from the Chilhowee, Conasauga, Knox, and Chickamauga Groups, along with Shady and Rome Formations. However, the majority of rocks in the Pulaski thrust sheet belong to the Conasauga and Knox Groups, both of which consist of observable, distinct facies that contrast with those in the same units in thrust sheets farther northwest (Rodgers, 1953a). For instance, limestone dominates the Knox Group in the Pulaski sheet, whereas dolomite and specific chert markers are more abundant in the Saltville sheet. Conversely, the Conasauga Group contains more limestone and shale in the Saltville sheet, as compared to the more dolomitic strata in the Pulaski sheet (Fig. 2-2). Therefore, because of a change in specific rock unit characteristics between the Saltville and Pulaski thrust sheets, this segment of the Pulaski fault in the study area represents both a structural and facies break.

Only the Knox and lower Chickamauga Groups are exposed on both sides of the Pulaski fault in the study area; thus Conasauga Group facies in the hanging wall were evaluated against previously described Conasauga rock units in the Saltville sheet (e.g., Rodgers, 1953a, Lemiszki, 2003; Bultman, 2005). Mapping of the Chilhowee Group and other Lower Cambrian formations in the composite Great Smoky thrust sheet was not

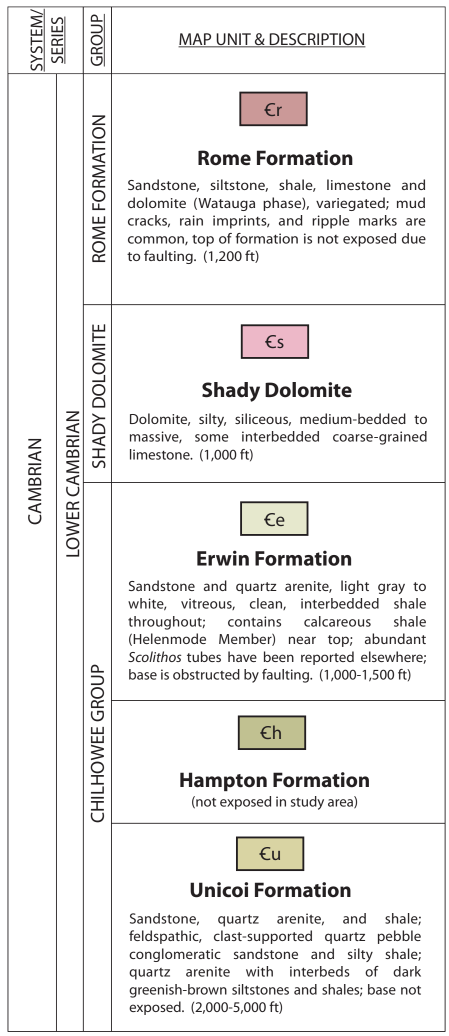

Figure 2-1 (Part A). Generalized stratigraphic column of the study area.

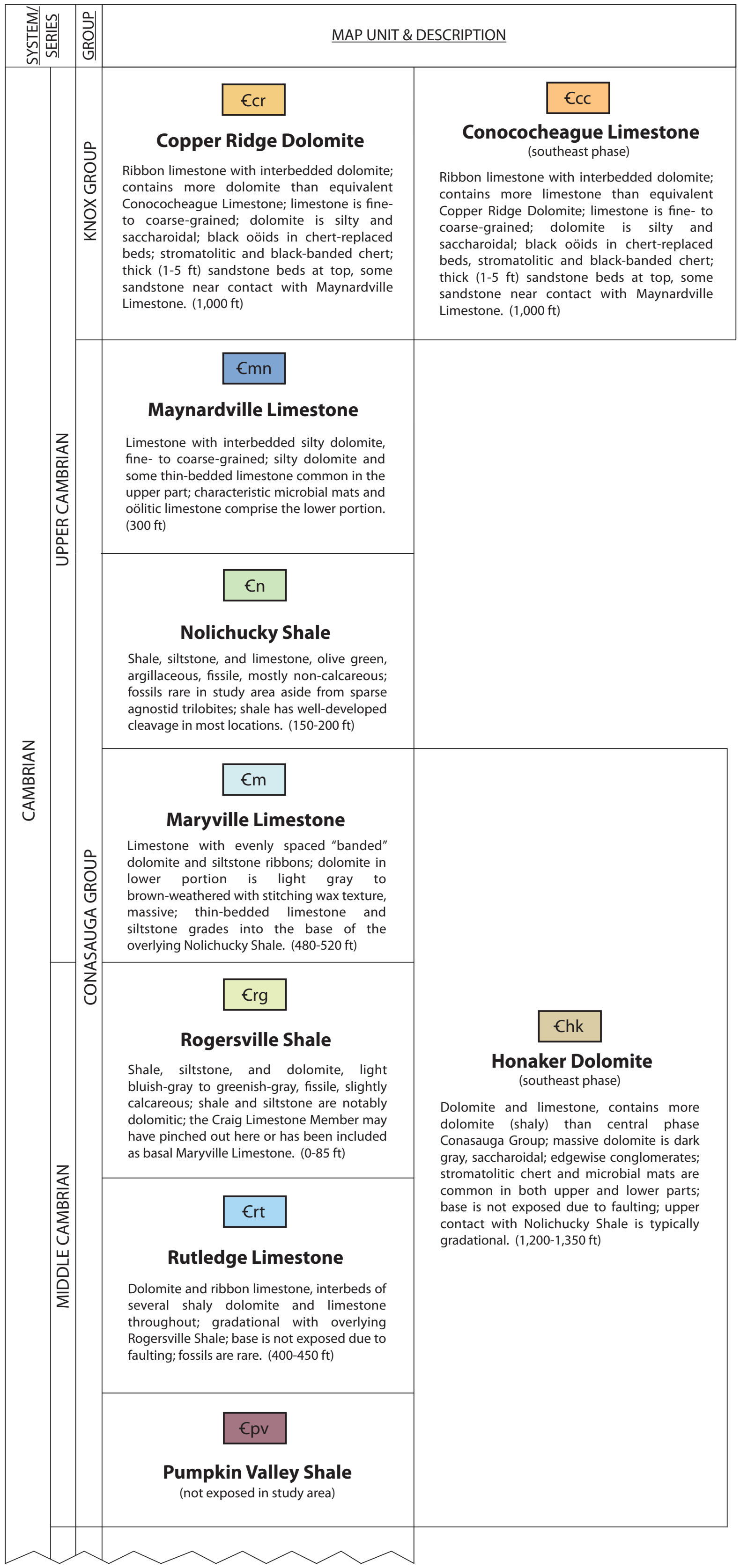

Figure 2-1 (Part B). Generalized stratigraphic column of the study area.

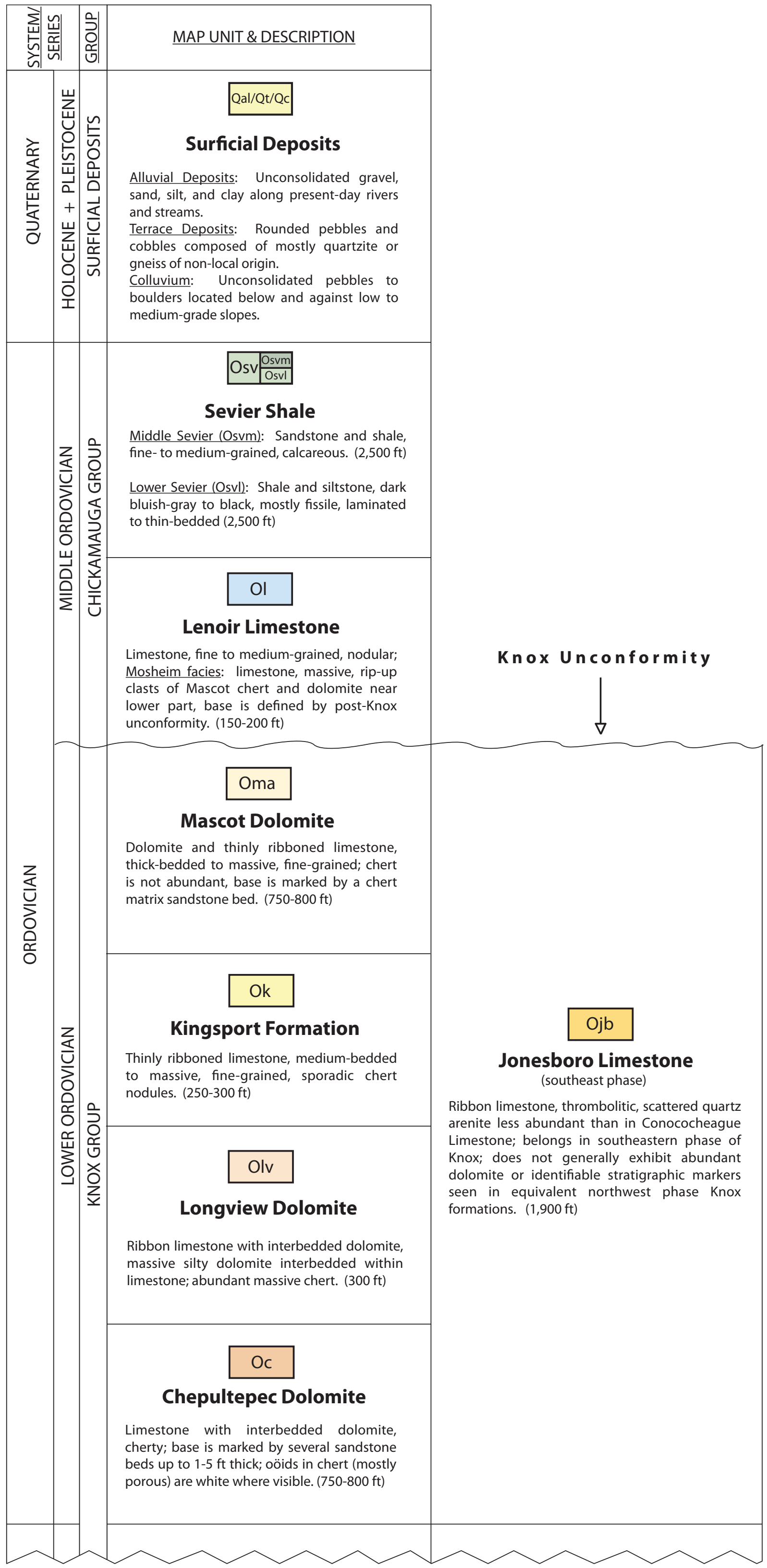

Figure 2-1 (Part C). Generalized stratigraphic column of the study area.

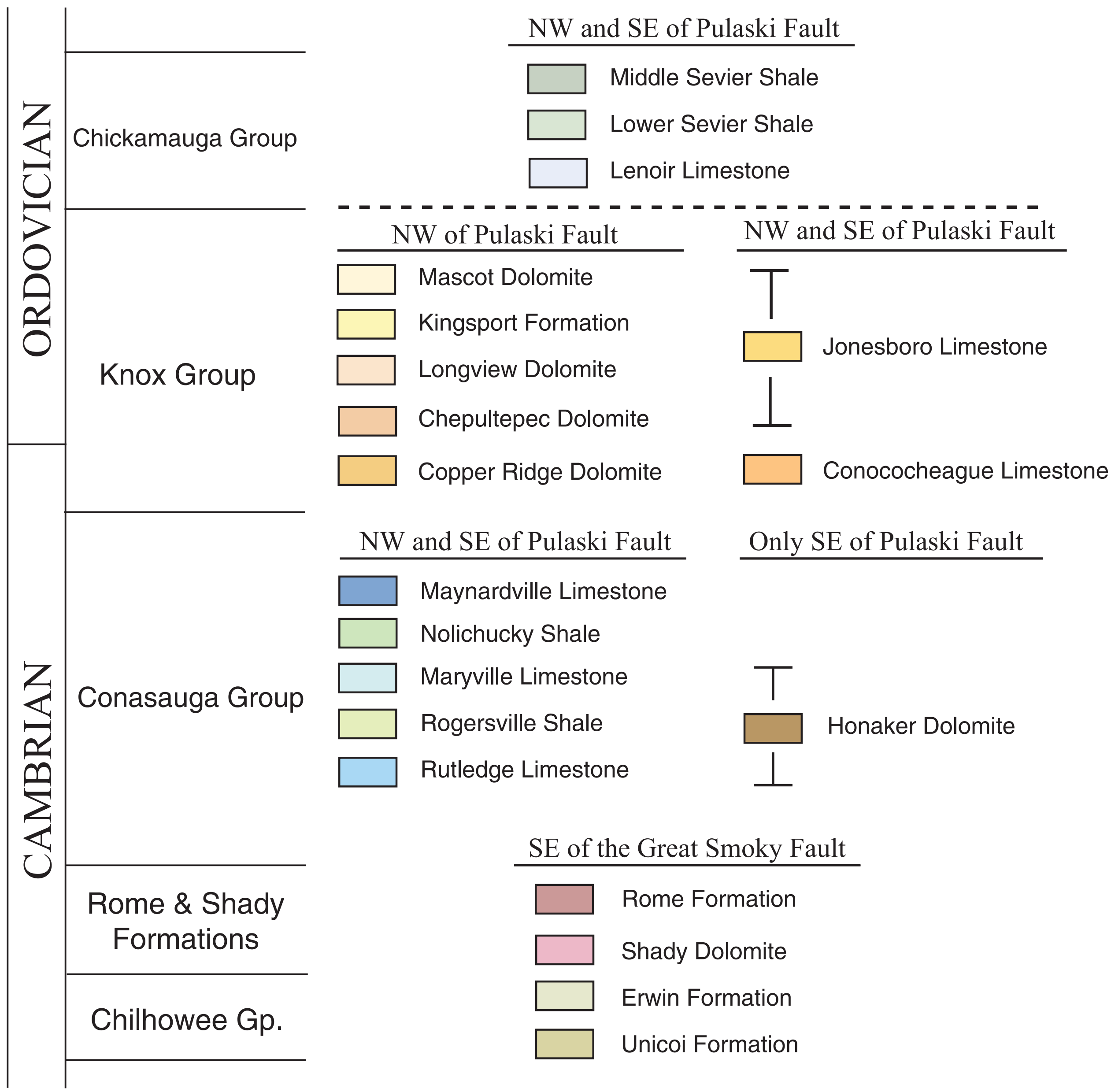

Figure 2-2. Simplified stratigraphic column showing distribution of formations and their rock types in relation to the two major faults located within the study area (i.e., Pulaski and Great Smoky faults). Colors correspond to geologic map units on Plate I.

extended further southward within the Neddy Mountain nor the Paint Rock quadrangles, because the stratigraphic focus of this study was principally confined to the Saltville and Pulaski thrust sheets.

Lithologic and Geomorphologic Overview

Limestone in the study area is commonly ribboned with both siltstone and dolomite, and is simply referred to as ribbon limestone throughout this chapter. Many formations in the Knox Group consist largely of ribbon limestone and interbedded massive dolomite. Weathered surfaces on the massive dolomite in both Conasagua and Knox Groups characteristically exhibit a “stitching-wax” texture, which is caused by differential weathering of calcite-filled fractures in the more resistant massive dolomite (Bucher, 1956; Little, 1969).

Grain size (in diameter) for unit descriptions is classified as fine (<0.10 mm), medium-fine (0.10-0.25 mm), medium (0.25-0.50 mm), medium-coarse (0.50-0.75 mm), coarse (0.75-1 mm), and very coarse (>1 mm). Bed thickness is classified as very thin (1-3 cm), thin (3-10 cm), medium (10-50 cm), thick (50 cm-1.5 m), and massive (>1.5 m).

Topographic signatures of several rock formations in the study area, especially those in the Knox Group, were used to help delineate map contacts. The Conococheague Limestone/Copper Ridge Dolomite, Longview Dolomite, and Mascot Dolomite are typically associated with prominent ridges, and the Chepultepec Dolomite and Kingsport Formation are underlain by valleys. Knobby (nonlinear) hills and short ridges are commonly seen in silty to shaly units, most notably the lower Sevier Shale. One of the best locations to observe this contrast in topography and lithology is along U.S. 321, just northeast of Parrottsville, Tennessee. The knobby hills of lower Sevier Shale can be seen looking to the northwest, whereas the "rolling hills" developed on Knox Group carbonate ridges are seen to the southeast.

Soils in the study area are indicative to certain lithologies. Carbonate-rich formations (e.g., Knox Group strata) are generally bright reddish-orange, cherty, and can be clay rich. These soils contrast with those of shaly formations (e.g., Nolichucky Shale), which are typically brown to yellowish-brown chippy soils and are usually sparsely vegetated.

Chilhowee Group

The Lower Cambrian Chilhowee Sandstone (Group), named by Safford (1869) for exposures along Chilhowee Mountain in Blount County, Tennessee, can be distinguished from the underlying Ocoee Supergroup by increased quartz content and regularity of unit thickness (Rodgers, 1953a). Keith (1903) subdivided the northeastern sequence of the Chilhowee Group into the Unicoi, Hampton, and Erwin Formations. These conformable and mostly clastic rocks were deposited on the eastern Laurentian margin during the rift-to-drift transition, comprising an upward-maturing succession of alternating sandstone and shale (Hatcher et al., 2007b).

In the study area, Chilhowee Group strata are confined to the composite Great Smoky thrust sheet. However, in parts of the Pulaski sheet between Pulaski and Marion, Virginia, both Shady Dolomite and Chilhowee Group rocks are mapped in stratigraphic continuity beneath the Rome Formation (Butts, 1933; Rankin et al., 1972). Because major faults west of the Pulaski propagated from basal detachments in the Rome Formation, the presence of rocks as old as the Chilhowee Group in the Pulaski sheet led Bartholomew et al. (1980) to suggest a structurally lower detachment (analogous to Blue Ridge faults) for the Pulaski fault in southwestern Virginia.

Unicoi Formation

The Unicoi and basal portion of the Hampton Formation (not exposed) represent the transition from the latest stages of Iapetan rifting to the onset of passive margin development (Simpson and Erikson, 1989). First named for Unicoi County, Tennessee, by Campbell (1899), the Unicoi Formation in northeastern Tennessee ranges from 610-1,524 m (2,000-5,000 ft) thick where top and base are present (Rodgers, 1953a). The portion of Unicoi Formation mapped near the southern edge of the study area is bounded by two faults: an unnamed Blue Ridge fault, which juxtaposes both Unicoi and Rome Formations, and the Great Smoky fault, which separates the Unicoi from Valley and Ridge rocks to the northwest. With no base exposed, thickness estimates for the Unicoi here cannot be reliably determined and would require further mapping to the south/southeast. Its southwestern equivalent, the Cochran Conglomerate, is well-exposed ~70 km (~44 mi.) southwest of the Neddy Mountain quadrangle along the south side of English Mountain. Although both the Cochran and Unicoi formations share similar lithologies, the Unicoi Formation contains more lithological variation and is generally thicker (maximum of ~1,500 m [~5,000 ft] in places) than the Cochran Conglomerate (Rodgers, 1953a).

The lower Unicoi Formation, although not well-exposed, consists of predominantly silty shale and feldspathic siltstone interbedded with medium- to coarse-grained feldspathic and conglomeratic sandstone. Sporadic layers of dark green amygdaloidal basalt, representing lava flows associated with rifting, have been observed from the Virginia State Line to the Nolichucky River (Rodgers, 1953b; Rankin, 1975), yet none of these volcanic layers are exposed in the study area. The upper Unicoi Formation (Fig. 2-3) contains tide- and wave-influenced, shallow-marine shelf deposits (Simpson and Eriksson, 1989). These layers are mostly thick-bedded to massive, vitreous, feldspathic coarse-grained sandstone, quartz arenite, and clast-supported, quartz pebble conglomerate (Fig. 2-3B). Frequent interbeds of dark greenish-brown siltstone and shale are also present.

Erwin Formation

Keith (1903) named the Erwin Formation after the town of Erwin in Unicoi County, Tennessee. Like the Unicoi Formation, accurate thickness of the Erwin Formation was not obtained in the study area, but the complete section of the formation ranges from 240-460 m (800-1,500 ft) thick in northeastern Tennessee, with an average thickness of 244 m (800 ft) on English Mountain (Greene, 1959) and a thickness of 396 m (1,300 ft) farther southwest on Chilhowee Mountain (Rodgers, 1953a). It consists of shallow-marine deposits of mostly light gray to white, vitreous, quartz arenite and sandstone interbedded with shaly siltstone, making this formation an important ridge-former in local Blue Ridge topography (Fig. 2-4). The underlying Hampton Formation, which is not exposed in the study area, can be distinguished from the Erwin Formation by

(A)

(B)

Figure 2-3. Exposures of Unicoi Formation along Yellow Spring Branch Road west of Neddy Mountain. (A) Thick-bedded and coarse-grained quartz arenite. (Hammer is ~30 cm). (B) Quartz pebble conglomerate interbedded with coarse-grained feldspathic sandstone. (Pen is ~14 cm).

the abundance of silty and sandy shale, abundant detrital mica, and interbeds of feldspathic sandstone (Rodgers, 1953a; Schwab, 1970).

King et al. (1944) split the Erwin into four members based on grain size. The most notable and thinnest member, the Helenmode, consists of mostly fine-grained, calcareous shale at the top of the Erwin Formation. Its soils are marked by characteristic leaching that reflect the soluble carbonate Shady Dolomite above and more resistant quartz arenite below (Rodgers, 1953a). Colluvial deposits of the Erwin Formation, however, obstruct the exposure of the Helenmode-Shady contact. Abundant *Scolithos* tubes have been reported in previous studies from northeast Alabama to central Virginia (Rodgers, 1953a; Schwab, 1970; Mack, 1980) although none were observed in the study area.

<u>Shady Dolomite</u>

The Shady Dolomite, named by Keith (1903) for Shady Valley near Elizabethton in Johnson County, Tennessee, records the start of carbonate sedimentation on the Lower Cambrian passive margin (Barnaby and Read, 1990). Like the overlying Rome Formation, it can be found in both the Valley and Ridge and Blue Ridge provinces (Rodgers, 1970b). Thickness of the Shady Dolomite varies from ~610 m (~2,000 ft) in southwestern Virginia (Byrd et al., 1973; Pfiel and Read, 1980), to ~305 m (~1,000 ft) in northeastern Tennessee (Rodgers, 1953a). The Shady Dolomite (Fig. 2-5) is mostly medium- to thick-bedded bluish-gray to white, silty dolomite with interbedded limestone.

Although the mapped area contains an incomplete section of Shady Dolomite, it clearly reveals the upper part of the formation, where massive light gray dolomite

Figure 2-4. Vitreous quartz arenite (float) of the Erwin Formation on the northeast slope of Neddy Mountain. (Hammer is ~30 cm).

Figure 2-5. Typical outcrop of Shady Dolomite consisting of light bluish-gray, coarse-grained and silty dolomite. Located west of Neddy Mountain along Long Creek Road. (Hammer is ~30 cm).

contains abundant chert and is overlain by shaly bluish-gray dolomite. In the study area, the Shady Dolomite is observed to be in stratigraphic contact with the underlying Erwin Formation, but not the overlying Rome Formation, from which it is separated by an unnamed Blue Ridge fault.

Rome Formation

Hayes (1891) named the Rome Formation for Rome in Floyd County, Georgia. The Rome Formation is widely distributed throughout East Tennessee and acts as the weak basal layer through which the master décollement propagated across the Valley and Ridge (Rodgers, 1970b; Chapple, 1978). The thickness of the Rome in northeast Tennessee averages 365 m (1,200 feet) and is estimated to be the same in the study area. However, incomplete sections are common due to: (1) frequent appearance of Rome directly above major thrusts; (2) general lack of a base; and (3) relatively sparse fossil indicators (Rodgers, 1953a). In the study area, the Rome Formation is located exclusively southeast of the Great Smoky fault and in the thin-skinned portion of the western Blue Ridge province. It underlies a prominent knobby ridge just to the northeast of where the Great Smoky sheet overrides the Pulaski sheet in the Neddy Mountain quadrangle (Fig. 2-6).

The lower Rome consists of variegated medium coarse-gained sandstone and siltstone with interbedded shale and occasional dolomite (“Watauga phase”) and limestone beds (Fig. 2-7). Colors range from light to medium gray, brown, maroon, dark red, reddish purple, to olive green. Brighter shades of green, red, purple, and yellowish-brown are also present, all of which are commonly found within the lower Apison Shale

Figure 2-6. Knobby ridge of Rome Formation (looking south) along Happy Hollow Road. Its location is 3 km northeast of the Pulaski fault's southwestern terminus.

Figure 2-7. Typical red and green coarse-grained sandstone of the Rome Formation showing a strongly cleaved layer (parallel to bedding) above hammer head. Location is on the east slope of the knobby ridge near Happy Hollow Road. (Hammer is ~30cm long).

Member (Rodgers, 1953a; Spigai, 1963; Samman, 1975). Sedimentary structures include mud cracks, raindrop imprints, and ripple marks, likely indicating shallow intertidal to supratidal environments. Rome soils are mostly dark reddish-brown, which starkly contrasts the yellowish-brown, shale chippy soils of the nearby lower Rutledge Limestone.

Conasauga Group

The Middle and Late Cambrian Conasauga Group, named by Hayes (1891) for the Conasauga River in Whitfield and Murray Counties, Georgia, has substantial lithologic variation throughout the Valley and Ridge, which led Rodgers (1953b) to divide the group into the northwestern, central, and southeastern phases (Fig. 2-8). All Conasauga facies in the mapped area, which include the Rutledge Limestone, Rogersville Shale, Maryville Limestone, Honaker Dolomite (which incorporates the previous three), Nolichucky Shale, and Maynardville Limestone, represent the southeastern phase.

Aside from certain exposures of Maynardville Limestone near the western boundary of the Neddy Mountain quadrangle, most Conasauga Group exposures in the study area are confined to southeast of the Pulaski fault. The Pulaski sheet in the study area rests on the interfingering and undefined transition between the divisible Middle Cambrian units and the Honaker Dolomite of the southeastern phase (Fig. 2-8). Depositional environments recorded for each phase of the Conasauga Group range from shale-dominated clastic subtidal in the northwest phase to carbonate peritidal in the southeastern phase (Hasson and Haase, 1988). The contact between the Maryville Limestone and Nolichucky Shale in this study area represents a sequence boundary on

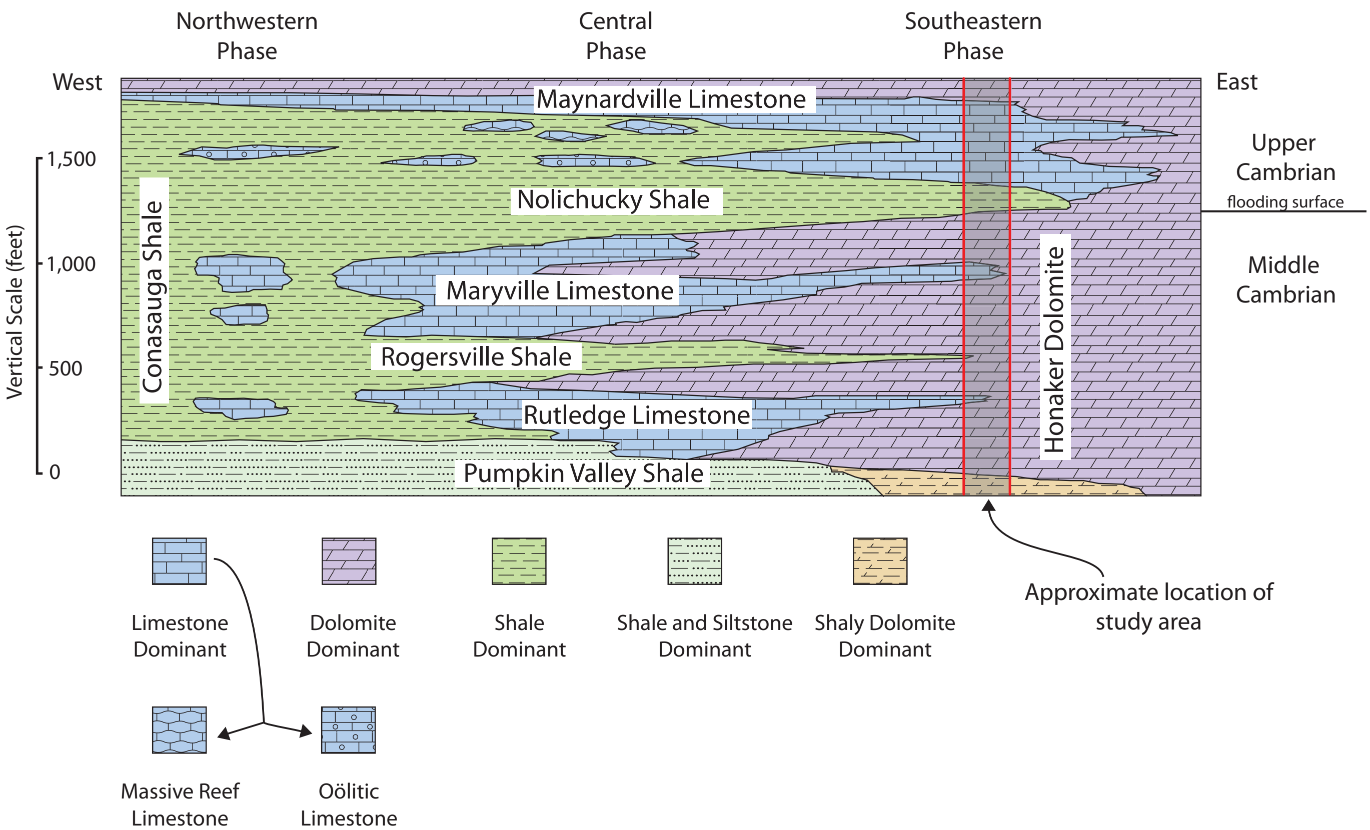

Figure 2-8. Facies relationships in the Conasauga Group in the East Tennessee Valley and Ridge. (Modified from Rodgers, 1953a).

the passive margin, marking a distinct shift from shallow-water carbonate deposition to deeper-water basinal siliciclastics (Foreman, 1991, Srinivasan, 1993, Srinivasan and Walker, 1993).

<u>Honaker Dolomite</u>

Originally named the Honaker Limestone by Campbell (1897) for Honaker in Russell County, Virginia, the Middle to Late Cambrian Honaker Dolomite (Butts, 1940) is equivalent to the Rutledge Limestone, Rogersville Shale, and Maryville Limestone. Its estimated thickness is ~370 m (1,220 ft), and it is justifiably designated a map unit where the Rogersville Shale cannot be separated in the study area. Prior to this study, the Honaker Dolomite, which is exposed in the Pulaski, Dunham Ridge, and Holston Mountain thrust sheets, had not been subdivided into its central phase equivalents southeast of the Pulaski fault (Rodgers, 1953b; Byerly, 1966; Hardeman et al., 1966; Little, 1969; Hasson and Haase, 1988; Whitmer, 2005). Little (1969) was able to successfully subdivide the Honaker Dolomite into three unnamed members but did not map them separately. On the presence of thin (<10-26 m) traceable Rogersville Shale, together with characteristic thin banded limestone of the Maryville Limestone in parts of the study area, the Honaker Dolomite was subdivided in the southwestern portion of the Pulaski sheet. Where the Rogersville Shale is not exposed, the unit was mapped as Honaker Dolomite.

The lower Honaker Dolomite, although incomplete, comprises dominantly dark bluish-gray, medium-bedded to massive, silty dolomite interbedded with some finely crystalline ribbon limestone and shaly dolomite. This part of the Honaker Dolomite contains abundant black and red massive and nodular chert, which is highly fractured. In the Pulaski sheet, the Honaker is the oldest unit present in the cores of several tightly folded anticlines. The base of the Honaker does not appear anywhere in the mapped area, but according to Rodgers (1953a) and Byerly (1966), the unit becomes thin-bedded and very shaly in the lower section, which may represent the southeastern phase equivalent of the Middle Cambrian Pumpkin Valley Shale. Rodgers (1953a) was the first to suggest that one of the shaly units in the Lower Honaker may have acted as a local detachment for the Pulaski fault in this area. Rodgers and Kent (1948) named the Pumpkin Valley Shale for exposures in Pumpkin Valley in Hawkins County, Tennessee. Originally named the Rome Shale by Hayes (1894) and Keith (1895), it was later determined to belong in the Conasauga Group based on fossil data and gradationally overlie the red and green shale, siltstone, and sandstone of the Rome Formation (Rodgers and Kent, 1948).

The upper Honaker Dolomite (Fig. 2-9) consists of mostly medium to dark bluish-gray, thin-bedded to massive saccharoidal dolomite and limestone with thickly laminated to ribboned, evenly spaced alternations of dolomite and limestone, which is analogous to the Maryville Limestone. Chert is less abundant in the upper Honaker Dolomite, but can still be found locally in generous quantities. The unit weathers mostly tannish-brown where dolomite is abundant, contrasting the medium to dark gray weathering surface of most limestone beds. Some of the fresher dark gray, saccharoidal layers of dolomite possess a distinctive fetid odor, likely due to sapropel residue formed by the decay of organic matter (Byerly, 1966). Edgewise conglomerate, stromatolitic chert, and microbial mats occasionally appear in both the upper and lower sections of the formation. One anomalous conglomeratic layer (~6 m [~20 ft] thick) was observed in the southwest

(A)

(B)

Figure 2-9. Upper Honaker Dolomite outcrops. (A) Closely spaced, silty, ribbon limestone. Outcrop is located directly east of the W. Allens Bridge Road/Old Newport Highway intersection. (Field book is 12 x 19 cm). (B) Typical exposure of massive Honaker Dolomite exhibiting classic stitching wax texture. Located along the Nolichucky River within Linebaugh Bend. (Brunton compass is ~8 cm in diameter).

corner of the Cedar Creek quadrangle near the Green-Cocke County line. It is notably calcareous, containing limestone, dolomite, and chert clasts. The upper contact with the Nolichucky Shale is typically gradational but is rarely exposed in the study area.

Rutledge Limestone

The Rutledge Limestone, named for exposures near Rutledge, Tennessee, by Campbell (1894) is the oldest formation (with the lower Honaker Dolomite) exposed in the Pulaski sheet in the study area, comprising a thickness of ~122 m (~400 ft). Like most lower Conasauga Group formations in general, the Rutledge Limestone, due to the transition from the undivided Conasauga Shale to the west, becomes increasingly calcareous southeast of the Copper Creek/Narrows fault (Fig. 1-2) and increasingly dolomitic southeast of the Saltville fault (Hasson and Hasse, 1988).

It consists of medium to dark bluish-gray, thin-bedded to massive dolomite and ribbon limestone interbedded with shaly dolomite. Most of the massive limestone (Fig. 2-10) is usually somewhat dolomitic and exhibits a thrombolitic texture. Several slightly calcareous shaly dolomite and silty limestone beds, occur near the upper, gradational contact with the Rogersville Shale. These beds are well-exposed at Meadow Creek Mill in the Cedar Creek quadrangle. The base of the Rutledge is not exposed in the study area, due to faulting.

Rogersville Shale

The Rogersville Shale was named by Campbell (1894) for exposures near Rogersville, Tennessee. It has a wide range of thicknesses before an easterly thinning

Figure 2-10. Rutledge Limestone exposure near the intersection of Long Creek Road and Sane Road exhibiting thick-bedded to massive, dolomitic and somewhat mottled limestone. (Hammer is ~30 cm long).

and eventual disappearance, ranging from 122 m (400 ft) in the Hunter Valley thrust sheet, to 61 m (200 ft) in the Dumplin Valley sheet, to 14 m (46 ft) in the Saltville sheet near the Tennessee-Virginia border (Hatcher, 1965; Oder and Milici, 1965; Neuman, 1960; Helton, 1967; Bridge and Hatcher, 1973; Hasson and Haase, 1988). Although thin to non-existent in the study area with a thickness of 0-26 m (0-85 ft) in places, the very presence of this formation in parts of the Pulaski thrust sheet allows subdivision of the Honaker possible. However, the Rogersville Shale is not observed (exposed?) northwest of the Dunham Ridge fault in the Pulaski sheet, and equivalent southeastern facies that match the Maryville Limestone and Rutledge Limestone were mapped as Honaker Dolomite.

The Rogersville Shale is a light bluish-gray to greenish-gray, fissile, slightly calcareous to dolomitic shale and siltstone, interbedded with bluish-gray, thin-bedded, silty dolomite with characteristic blocky weathering (Fig. 2-11). A notably persistent middle member in the Rogersville of the central phase is the Craig Limestone Member (Rodgers and Kent, 1948). This ribbon limestone unit does not appear anywhere in the mapped Rogersville of the Pulaski sheet, although a few locations contain chert float that is typical of the limestone. The Craig Limestone Member may have pinched out before reaching here, or may have been included as the basal member of the overlying and lithologically similar Maryville Limestone, because of the absence of upper Rogersville shale exposures (Rankey, 1993).

Figure 2-11. Exposure of the Rogersville Shale consisting of dolomitic shale and siltstone with interbedded shaly dolomite. Note the fissile to blocky weathering. Located at Meadow Creek Mill along Birdwell Mill Rd. (Field book is 12 x 19 cm).

Maryville Limestone

Campbell (1894) named the Maryville Limestone for exposures in Maryville, Tennessee. The Maryville contains more limestone than any of the other middle Conasauga formations. Its thickness in the study area is 150 m (490 ft), whereas its maximum thickness in the neighboring Dumplin Valley sheet to the west (Fig. 1-2) is approximately 250 m (820 ft) (Neuman, 1960; Hatcher, 1965), reflecting an eastward thinning of the formation. The thickness of the Maryville Limestone in the Dumplin Valley thrust sheet can likely also be attributed to the inclusion of the similar Craig Limestone Member in the Rodgersville Shale (Hatcher, 1965; Bridge and Hatcher, 1973; Rankey, 1993).

The Maryville Limestone (Fig. 2-12) is a light to dark gray, thin- to thick-bedded, fine- to coarse-grained pelletic to micritic limestone containing layers of silty dolomite. Its evenly spaced "banded" appearance of medium to dark gray weathered limestone and light gray to brown weathered dolomite is a primary trait of this formation. Massive dolomite is generally confined to the lower half. Oölites and edgewise conglomerate are sparse, but common in areas to the northwest (Harris, 1965). The Maryville Limestone grades upward into thin-bedded limestone and siltstone near the base of the overlying Nolichucky Shale in the southwest corner of the Cedar Creek quadrangle. Due to lack of exposure, the nature of the contact with the Rogersville is uncertain, but appears to be abrupt.

Figure 2-12. Maryville Limestone consisting of closely spaced ribbon limestone (left) interbedded with silty brown-weathered dolomite (right). Located near the Greene-Cocke County line, south of Long Creek Road. (Hammer is ~30 cm long).

Nolichucky Shale

Originally described by Campbell (1894) after lithologies observed near the same Nolichucky River that transects the study area, the Nolichucky Shale is the most frequent Conasauga shale to appear throughout the area. Its thickness ranges from 45-61 m (150-200 ft) here, which, like most Conasauga shales, is drastically thinner than reported in the westernmost parts of the Saltville sheet: 427 m (1,400 ft) near Knoxville, Tennessee (Cattermole, 1958), and 274 m (890 ft) near Cleveland, Tennessee (Swingle, 1959). Feder (1963) and Little (1969), however, reported an average of 120-150 m (400-500 ft) within the Saltville/Dumplin Valley sheets in Jefferson County, Tennessee (west of Pulaski fault) and the Dunham Ridge block in Greene and Washington Counties, Tennessee (part of Pulaski sheet to the northeast), respectively.

The Nolichucky Shale consists of olive to light green, gray, and maroon argillaceous, fissile shale and siltstone that weathers bright yellow to yellowish-brown (Fig. 2-13). Thin-bedded to massive microbial and oölitic limestone is common in the middle to upper part of the section. At least three members [similar to those observed by Rodgers (1953b)] were recognized, although these were not mapped separately due to inconsistent thicknesses and exposure. The lower member, which appears the most frequently in the study area, contains non-calcareous shale and siltstone. The middle member, which is likely the equivalent to the Bradley Creek Member of Helton (1967), consists of massive microbial and oölitic limestone, similar in appearance to the Maynardville Limestone. The upper member is more or less identical to the lower member, except for the increased abundance of thin-bedded calcareous siltstone with thickly laminated interbedded limestone (Fig. 2-14). The best section of the upper

Figure 2-13. Typical exposure of the Nolichucky Shale with thin-bedded limestone interbedded (limestone is obscured by shale chips—note the reddish-brown soil, which is characteristic of carbonates in the region). Located along St. James Rd., just south of Meadow Creek. (Brunton compass is ~8 cm in diameter).

(A)

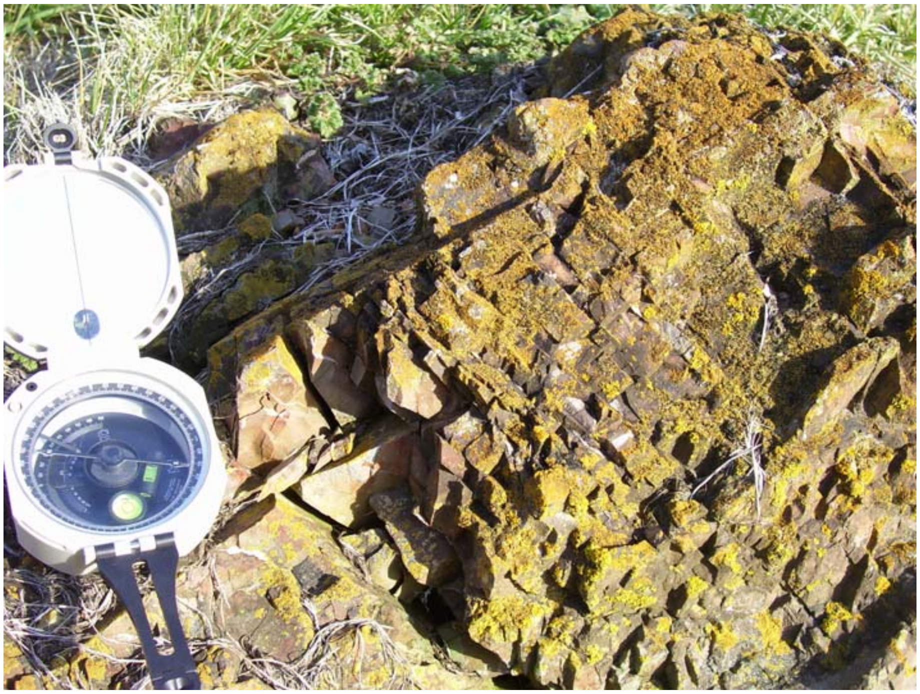

(B)

Figure 2-14. Exposure of the Nolichucky Shale located along Old Newport Highway, just off U.S. 321. (A) Well-cleaved, slightly calcareous, thin-bedded siltstone of the upper Nolichucky Shale. (Brunton compass is ~8 cm in diameter). (B) Tight fold with axial planar cleavage in the same rock type as (A). (Hammer handle is ~14 cm).

member is found just off U.S. 321 along Old Newport Highway in the Cedar Creek quadrangle. A good site to see the separate members in the same quadrangle is located along S. Allen Bridge Rd, just south of Meadow Creek. Although many contacts are not exposed, the Nolichucky Shale generally shows gradational contacts with both the underlying Maryville Limestone and overlying Maynardville Limestone.

Soils of the Nolichucky Shale contain abundant shale chips and have a dark yellow-brown color. The Nolichucky has been noted to be fossiliferous in parts of the Greeneville quadrangle (Byerly, 1966), but fossils are rarely observed in the study area. This may be due to the development of strong cleavage and lack of well-exposed bedrock in the area, as well as in other parts of the Pulaski sheet to the northeast (Little, 1969; Harlow, 1987). A single fragment of an agnostid trilobite was found along Shady Road, just off Old Newport Highway in the Cedar Creek quadrangle. Even with the lack of fossil indicators here, the base of the Nolichucky Shale is still considered to be the Middle-Upper Cambrian boundary and marks a distinct shift in the pattern of sedimentation (Rodgers, 1953a; Srinivasan, 1993).

Maynardville Limestone

Oder (1934), who named the Maynardville Limestone after Maynardville, Tennessee, originally placed the unit in the basal (Cambrian) part of the Knox Group, based on its lithologic similarities to the Copper Ridge Dolomite and Conococheague Limestone. Similarities in paleontological data to the Conasauga Group, first noted by Resser (1938), led Rodgers (1953a) to conclude that the Maynardville is a distinct unit in the upper Conasauga Group. Its thickness in the study area averages 93 m (~300 ft). The

Maynardville is mostly a light to medium bluish-gray, thick-bedded to massive, fine- to medium-grained limestone with interbedded silty dolomite that is more common in the upper part (Fig. 2-15). Ribbon limestone with thin (1-3 cm) clay seams is common. The formation contains sporadic edgewise conglomerate consisting of limestone and dolomite clasts, and it is also locally oölitic. Characteristic microbial mats associated with the massive limestone dominate the lower portion of the Maynardville.

The base of the Maynardville Limestone is usually gradational with the underlying Nolichucky Shale, yet some contacts, like the one in the hinge of the syncline just off U.S. 321 along Old Newport Highway in the Cedar Creek quadrangle, reveal a sharp contact. Maynardville Limestone becomes very thin-bedded, silty limestone or dolomite at the top of the formation near the transition with the basal sandstone layer (when present) of the Conococheague Limestone/Copper Ridge Dolomite. With the exception of microbial mats, fossils in the Maynardville Limestone are rare, although a mold of the trilobite *Blountia* was identified by Byerly (1966) in the Greeneville quadrangle, northwest of Walkertown.

Knox Group

Safford (1869) named the Knox Group for Knoxville and Knox County, Tennessee, and its type locality is along Second Creek near downtown Knoxville. The Knox Group carbonates make up the majority of the sedimentary rock units in East Tennessee. The entire group is 700-1,000 m (2,300-3,300 ft) thick in East Tennessee (Hardeman et al., 1966) and approximately 900 m thick (~3,000 ft) in the study area (Whitmer, 2005; this study). Extensive mapping and subdivision of the group has been

Figure 2-15. Maynardville Limestone exposure showing typical massive, microbial limestone. Located along Old Newport Highway, just off U.S. 321 in the hinge of an overturned syncline. (Hammer is ~30 cm).

done over the years, because of its importance in the exploration/development of zinc ore (Rodgers, 1953a). Its karst-dominated landscape and variably cherty units create the characteristic broad rolling hills and undulating topography across the Valley and Ridge. Fossils are rare in the Knox and are generally only found as molds in chert float (Rodgers, 1953a). Both dolomite and limestone generally dominate the Knox in the northwestern phase, while mostly limestone dominates the southeastern phase, including this sector of the Pulaski thrust sheet.

Five formations are mapped where the Knox is more easily divisible in the northwestern phase (in ascending order): the Copper Ridge Dolomite, Chepultepec Dolomite, Longview Dolomite, Kingsport Formation, and Mascot Dolomite. Aside from lithologies, subdivision of these formations in the field is based on certain characteristic chert and/or sandstone stratigraphic markers (Fig. 2-16). In the southeastern phase, where the Knox Group is generally dominated by limestone and contains equally abundant yet not easily identifiable stratigraphic markers, only two formations are mapped: the Conococheague Limestone and Jonesboro Limestone. The Upper Cambrian Conococheague Limestone of the southeastern phase is the calcareous equivalent of the Copper Ridge Dolomite and is the only Knox Group formation not deposited during the Ordovician. The Jonesboro Limestone accounts for the Ordovician Knox Group in the southeastern phase.

Interestingly, the study area contains some of the southeastern-most exposures of the northwest phase of Knox Group, and many similarities exist between the two phases here. The abundance of limestone in the Knox Group just to the northwest of the Pulaski fault may imply that these footwall units rest at or near the transition with the more

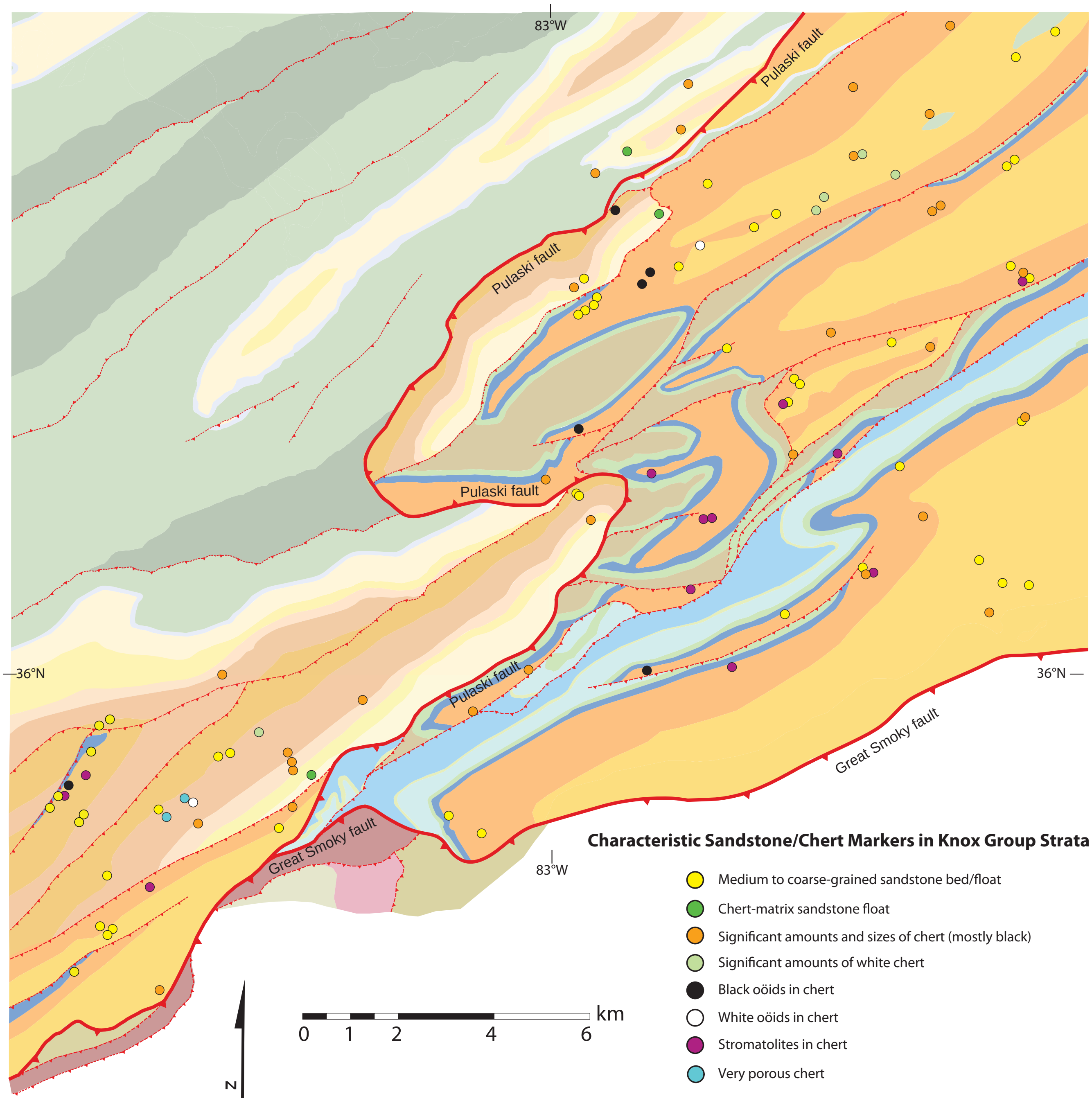

Figure 2-16. Map location of characteristic sandstone and/or chert stratigraphic markers in the Knox Group of both the northwest and southeast facies. Data from Whitmer (2005) are excluded. Colors of map units correspond to those in Plate I and Figures 2-1 and 2-2.

limestone-dominant southeastern phase. In the Mosheim anticline, Rodgers (1953b) and Lemiszki (2003) mapped Copper Ridge Dolomite stratigraphically and conformably below the Conococheague Limestone based on the amount of limestone present. This further implies that the two facies are likely near laterally widespread transition.

Conococheague Limestone

The Upper Cambrian Conococheague Limestone, named by Stose (1908) for exposures near Conococheague Creek in Franklin County, Pennsylvania, is one of the most extensive formations exposed in the Pulaski thrust sheet of the study area. It is the southeastern equivalent of the Copper Ridge Dolomite, and thus shares many similarities in lithology, stratigraphic markers, and topography with the Copper Ridge Dolomite in the area. The Conococheague Limestone is approximately 300 m (1,000 ft) thick in the study area, but deceptively produces a wider outcrop appearance because of several tight folds within the formation. It consists of mostly medium- to thick-bedded, light to dark bluish-gray, silty, ribbon limestone and interbedded dark bluish-gray dolomite (Fig. 2-17). Ribbons consist of lightly colored dolomite and are 2-5 cm thick. Typically, fresh samples of the darker gray saccharoidal dolomite exhibit a fetid (asphaltic) odor.

The lower half of the Conococheague Limestone contains more dolomite, as well as sporadic quartz arenite beds near the base. Oöids, matrix-supported rip-up clasts, and abundant chert of all colors, but mostly black (*in situ* and float), are common in places. One diagnostic feature of the Conococheague is the presence of black, ellipsoidal to spherical oöids found in chert (Rodgers, 1953a), particularly near the base of the formation. Stromatolitic chert is abundant in the Conococheague, and is useful for

(A)

(B)

Figure 2-17. Conococheague Limestone featuring (A) ribbon limestone located northwest of Ebenezer Church (hammer is ~30 cm) and (B) thinly ribboned (1 cm thick) limestone (light gray) interbedded with massive silty dolomite with a stitching-wax weathered surface texture. (Field book is 12 x 19 cm).

identifying the formation where no bedrock is exposed. Fractured and banded chert is also common. Soils are bright reddish orange and particularly fertile.

Copper Ridge Dolomite

The Upper Cambrian Copper Ridge Dolomite was named by Ulrich (1911) for exposures on Copper Ridge in Grainger County, Tennessee. Although a moderate quantity is contained near its upper boundary, limestone in this formation is rare in many parts of the eastern Tennessee Valley and Ridge, except at or near the southeast boundary of the central phase (i.e., the Pulaski fault of this study area) (Rodgers, 1953a). Thickness is estimated to be approximately 300 m (1,000 ft). Keeping true to its name, the formation produces many of the tallest knobs and ridges within the study area.

The Copper Ridge Dolomite (Fig. 2-18) consists of light to medium gray, medium-bedded to massive, coarse-grained, ribbon limestone with massive dark grayish-blue dolomite interbedded and occasional quartz arenite beds, commonly located near the Chepultepec Dolomite contact. Fresh samples of darker gray saccharoidal dolomite exhibit a fetid (asphaltic) odor. Oöids, matrix-supported rip-up clasts, and abundant dark-colored chert (*in situ* and float), are common in places. One diagnostic feature of the Copper Ridge Dolomite is the black ellipsoidal to spherical oöids in beds replaced by chert (Lemiszki, 1994), which are consistently located near the lower half of the formation in the Parrottsville quadrangle (Whitmer, 2005). Stromatolitic chert is another diagnostic feature of the Copper Ridge, as well as the Conococheague Limestone, which is used in identifying both formations where no bedrock is exposed.

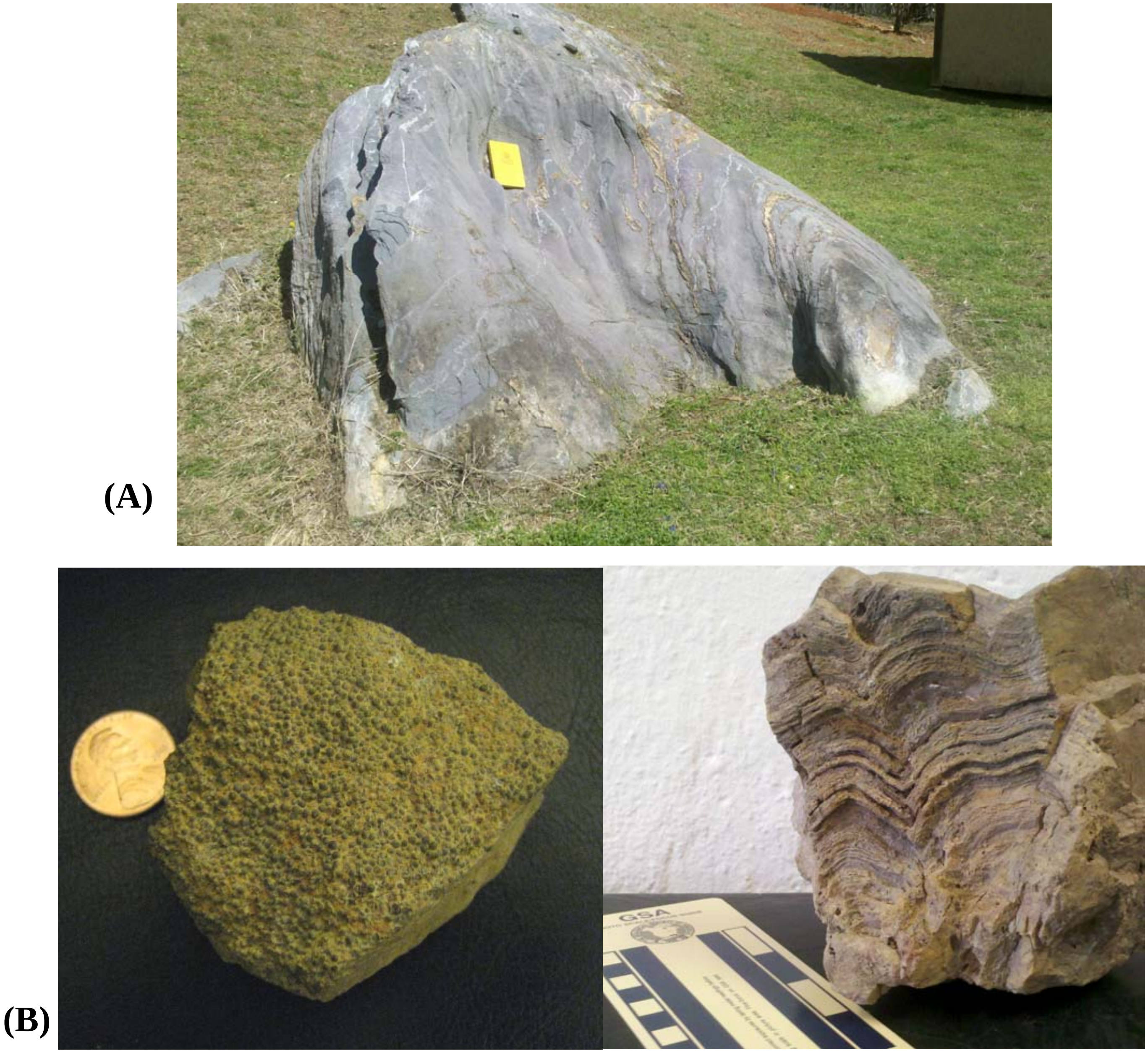

Figure 2-18. (A) Typical exposure of Copper Ridge Dolomite in the study area consisting of thick-bedded limestone with thick (2-7 cm) dolomite ribbons located northeast of Manning's Chapel Road near Bridgeport, TN. (Field book is 12 x 19 cm). (B) Characteristic chert markers of both Copper Ridge Dolomite and Conococheague Limestone showing black oöids in chert (left) and stromatolitic chert (right).

Jonesboro Limestone

Ulrich (1911) named the Jonesboro Limestone for the city of Jonesboro in Washington County, Tennessee. Unlike the Ordovician Knox Group of the northwest phase, the Jonesboro Limestone does not generally exhibit identifiable stratigraphic markers used in subdividing the group, such as chert matrix sandstone at the base of the Mascot. Some markers, such as the coarse-grained sandstone (Fig. 2-19A) occasionally found exposed near its base, however, are likely equivalent to the sandstone at the base of the Chepultepec Dolomite.

The Jonesboro Limestone (Fig. 2-19B) is approximately 580 m (1,900 ft) thick, and consists of light to dark bluish-gray, medium- to thick-bedded and massive, medium- to coarse-grained limestone, which is commonly ribboned and thrombolitic. Interbedded medium- to dark-blue dolomite is found sporadically. Light colored chert is seemingly confined to the lower portion of the Jonesboro, some of which contain white oöids. Some cherty beds do occur, along with scattered quartz arenite, but these are less abundant than those found in the Conococheague Limestone.

Chepultepec Dolomite

The Lower Ordovician Chepultepec Dolomite was named by Ulrich (1911) for the town of Chepultepec (now called Allgood) in Blount County, Alabama. The formation, which ranges in thickness from 230-245 m (750-800 ft), conformably overlies the Copper Ridge Dolomite, and its base is roughly the Cambrian-Ordovician boundary. It is the oldest formation exposed in the Oven Creek anticline, and most exposures in the study area occur in the Parrottsville quadrangle (Whitmer, 2005). Although valleys are

(A)

(B)

Figure 2-19. (A) Thin-bedded, coarse-grained sandstone, a characteristic of the base of the Jonesboro Limestone/Chepultepec Dolomite. Location is northeast of Manning's Chapel Road near Bridgeport, Tennessee. (Field book is 12 x 19 cm). (B) Jonesboro Limestone outcrop located ~2 km southeast of Susong Memorial Church featuring medium-bedded thrombolitic limestone and interbedded dolomite (beneath hammer). (Hammer is ~30 cm long).

most typical, ridges characterize Chepultepec topography in particular areas in the Neddy Mountain quadrangle, where the unit contains notably more abundant chert.

The Chepultepec Dolomite (Fig. 2-20) is medium to dark bluish-gray, medium-coarse grained, thin- to thick-bedded, cherty limestone with interbedded, massive light to medium gray dolomite and scattered carbonate-cemented quartz sandstone. The base of the Chepultepec Dolomite is marked by several sandstone beds up to 0.5-1.5 m (1-5 ft) thick. Chert here can be very porous and is typically light tan to white, contrasting the darker chert of the Copper Ridge Dolomite. Oöids in the chert, if visible, are generally white and have been observed mostly in the middle of the unit (Whitmer, 2005). Soils are light orange to tan and are clay rich.

Longview Dolomite

The Longview Dolomite was named by Butts (1926) for Longview in Shelby County, Alabama. It is a little over 90 m (300 ft) thick and resembles the lithology of underlying Chepultepec Dolomite, but is more siliceous. The Longview (Fig. 2-21) consists of light to medium gray, fine- to coarse-grained, medium- to thick-bedded, thrombolitic and ribbon limestone with interbedded massive silty dolomite. In the Parrottsville quadrangle, Whitmer (2005) noted a dominance of dolomite in the formation when compared to the Chepultepec Dolomite.

The Longview contains abundant massive chert, usually light gray to tan, as well as scattered 1-3 cm thick quartz arenite beds. The upper third of the Longview has been reported to contain occasional matrix-supported dolomite rip-up clasts (Whitmer, 2005).

Figure 2-20. Bluish-gray limestone and ribbon dolomite of the Chepultepec Dolomite located near Manning Chapel School. (Field book is 12 x 19 cm).

Figure 2-21. Slightly dolomitic limestone of the Longview Dolomite with a thrombolitic texture and interbedded silty dolomite. Exposure is located southwest of Cochran Bend. (Hammer is ~30 cm long).

Fossils are rare, but the gastropod *Lecanospira* was observed in the nearby Greeneville quadrangle (Byerly, 1966).

Kingsport Formation

The type locality for the Kingsport Formation is located near Kingsport, Tennessee, and was first described by Oder and Miller (1945). It contains more limestone than other Knox Group formations in the study area, which contrasts with the overlying and very dolomite-abundant Mascot Dolomite. The Kingsport (Fig. 2-22) reaches a thickness of about 80 m (~265 ft) and consists of light to dark bluish-gray, medium-bedded to massive, mostly fine-grained, ribbon limestone with sporadic chert nodules. Many of the massive limestones exhibit a thrombolitic texture, common in Ordovician Knox and equivalent Jonesboro formations. Most of the massive dolomite within the Kingsport Formation is confined to the upper portion and can be oölitic.

A few varieties of gastropods have been found in Kingsport chert in the Parrottsville quadrangle (Whitmer, 2005), among other northwestern belts (Lemiszki, 1994). Clay-rich soils here generally weather light orange to light brown. Solubility differences between the Kingsport limestone and the dense overlying dolomite of the Mascot are thought to be a major factor in the regional dolomitization and collapse features at the contact (Harris, 1971).

Mascot Dolomite

The Mascot Dolomite, first named after exposures in Mascot, Tennessee, and described by Oder and Miller (1945), is the youngest formation in the Knox Group. Its thickness in the study area is approximately 230 m (750 ft), but it can vary dramatically from 120-245 m (400-800 ft), because of the regional Knox unconformity at the top of the formation (Rodgers, 1953a).

The Mascot Dolomite (Fig. 2-23) is a light to medium gray, mostly thick-bedded to massive, fine-grained dolomite with light gray, interbedded and ribbon limestone. The massive dolomite, which appears mainly in the lower half of the formation, tends to weather a very light gray to tan and may display a light pink color from a higher manganese content (Scholle and Ulmer-Scholle, 2003). Chert is not abundant, but some cherty limestones were observed in the Parrottsville quadrangle, where ridges dominate the topography (Whitmer, 2005). The base of the Mascot Dolomite is characteristically marked by a chert matrix sandstone or other sandstone (quartz arenite) bed, mostly observed as float in the study area. Although no fossils were observed here, the gastropod *Ceratopea* has been reported near the top of the formation (Bridge, 1955). Soils are generally light reddish-orange.

Chickamauga Group

The Chickamauga Limestone was named by Hayes (1891) for Chickamauga Creek in southeastern Tennessee and northwestern Georgia, and was later elevated to group status by Swingle (1964); the stratigraphy of the Chickamauga Group has historically been debated concerning its divisions and correlations throughout Tennessee (Ulrich, 1911; Butts, 1933; Keith, 1895; Rodgers, 1953a). It represents a package of shallow-water carbonate-platform deposits formed during a transgression of the extensive Middle Ordovician sea (Ruppel and Walker, 1995). These carbonates grade into a

Figure 2-22. Exposure of Kingsport Formation showing bluish-gray fine-grained limestone with thinly ribboned (0.5-1 cm) dolomite. Location is east of Bethel Church near the Pulaski fault trace. (Field book is ~12 x 19 cm).

Figure 2-23. Mascot Dolomite near the Pulaski fault contact along Bright Hope Road. Exposure consists of typical massive light gray and fresh, fine-grained dolomite. (Hammer is ~30 cm long).

detrital wedge eastward in the Appalachian basin (McLaughlin, 1973). The Sevier Shale, in particular, had a southeast clastic source during the Blountian phase of the Taconic orogeny (Drake et al., 1989). The Lenoir Limestone, deposited along the forelandward stable carbonate bank of the Middle Ordovician Sevier basin, comprises the oldest formation of the Chickamauga in this area.

Lenoir Limestone

Safford and Killebrew (1876) named the Lenoir Limestone for Lenoir City, Tennessee, to describe the basal Chickamauga limestone. The Lenoir rests disconformably on the underlying Mascot Dolomite and is approximately 45-60 m (150-200 ft) thick, with variations in thickness attributed to the erosional nature of its contact. One of the best places to observe this contact in the study area is along Bright Hope Road, near the intersection with Poplar Springs Road in the Cedar Creek quadrangle. The formation (Fig. 2-24A) consists of a dark bluish-gray, medium-bedded to massive, nodular limestone with several 0.5-2 cm-thick clay seams.

A distinctive facies of the Lenoir in the study area, the Mosheim Member (Fig. 2-24B), consists of a massive, light gray, fine-grained limestone. The Mosheim Member, named by Ulrich (1911) for Mosheim in Greene County, Tennessee, does not contain the characteristic nodular texture of the Lenoir facies. Rip-up clasts of Mascot chert and dolomite from the Knox unconformity have been documented near the base of the Mosheim facies, along with bird's-eye structures. (Whitmer, 2005). The gastropod *Maclurites magnus* was identified in the study area and has also been reported in both

(A)

(B)

Figure 2-24. Exposures of Lenoir Limestone showing (A) wavy-bedded to fine-nodular limestone with several 0.5-2 cm thick clay seams located northwest of the Poplar Springs Road/Bright Hope Road intersection, and (B) the Mosheim Member consisting of massive fine-grained limestone near the Pulaski fault contact along Bright Hope Road. (Hammer is ~30 cm long).

Lenoir and Mosheim facies in the Pulaski sheet in the adjacent Davy Crockett Lake quadrangle (Robertson et al., 2011).

Sevier Shale

The Sevier Shale was named by Campbell (1894), likely after Sevier County, Tennessee. This formation was recently subdivided by Lemiszki (2003), Bultman (2005), and Whitmer (2005) into lower, middle, and upper Sevier Shale. Only the lower and middle units are exposed in the mapped area, forming much of the knobby topography to the northwest along U.S. 321. Total thickness (Upper Sevier included) has been estimated to approach over 2,100 m (7,000 ft) here, based on work in the neighboring Mosheim and Parrottsville quadrangles (Lemiszki, 2003; Whitmer, 2005). The Sevier Shale is a structurally weak unit and exhibits well-developed cleavage in most places.

The lower Sevier Shale (~760 m [~2,500 ft] thick) is a dark gray to black, slightly calcareous, fissile and silty shale with thin lenses of medium-coarse-grained limestone (Fig. 2-25). Its contact with the underlying Lenoir Limestone ranges from gradational to abrupt (Bultman, 2005; Whitmer, 2005; Robertson et al., 2011). The lower Sevier is graptolite-rich and has been determined to be within the upper part of the *Nemagraptus gracilis* graptolite zone (Whitmer, 2005). The shale weathers yellowish-brown to olive-brown, which contrasts with the brighter yellow to yellowish-brown of the Upper Cambrian Nolichucky Shale. A distinct eastward-directed facies change of the lower Sevier to a coarser-grained, calcareous sandstone occurs in the adjacent Davy Crockett Lake quadrangle (Robertson et al., 2011).

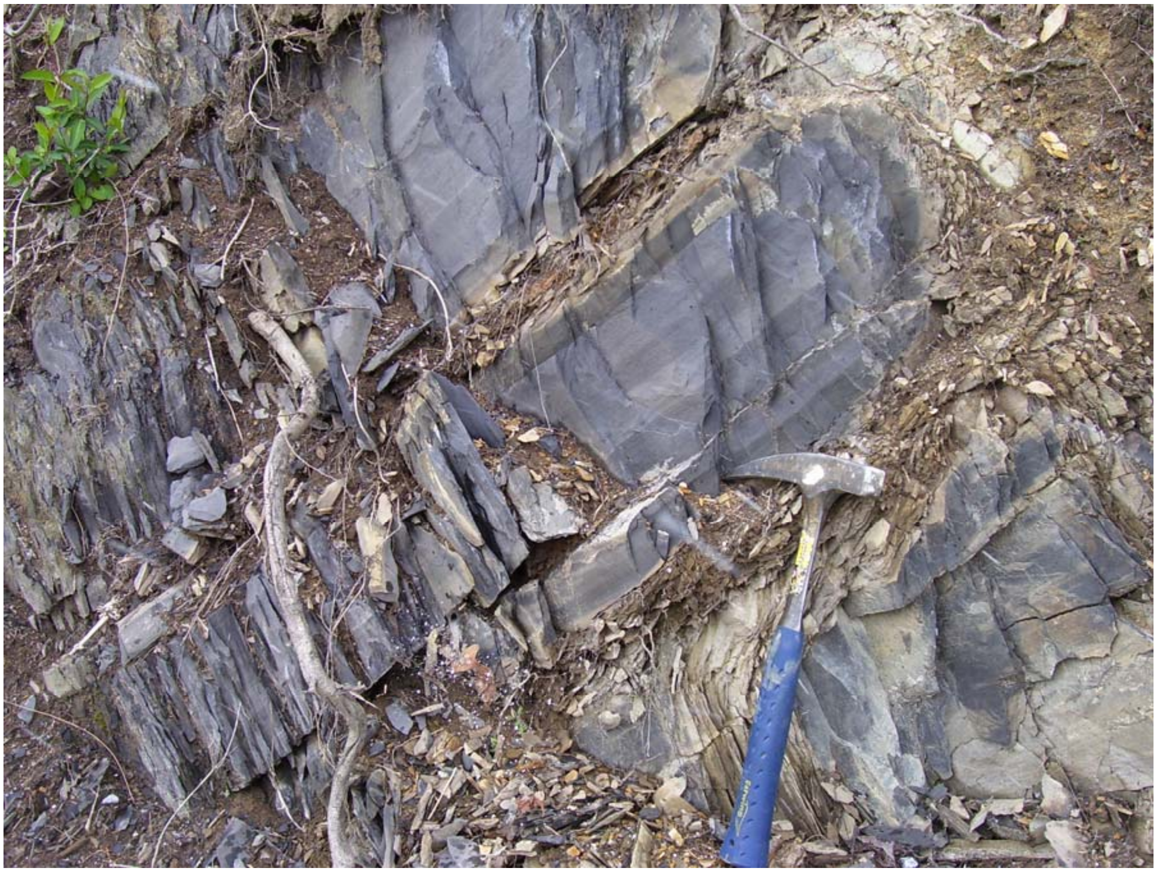

Figure 2-25. Dark bluish-gray, silty lower Sevier Shale, showing a great example of bedding/cleavage relationships (section is upright). Located northeast of Pigeon Creek along Gibson Rd. (Hammer is ~30 cm long).

With the assistance of Dr. Gary Gill Bible, samples of the darkest lower Sevier Shale were collected and sent to Humble Geochemical to test for its thermal maturity. The Sevier Shale in the study area is in the upper condensate/lower peak gas phase. One sample, collected just northeast of Pigeon Creek along Gibson Road, contains ~0.82 percent organic matter, just below the 1 percent minimum considered for good source material.

The middle Sevier Shale (Fig. 2-26) contains more sandstone than the lower Sevier Shale, and thus becomes coarser-grained, especially in the Mosheim quadrangle (Lemiszki, 2003). Its thickness is approximately 760 m (2,500 ft), and consists of thin- to thick-bedded, calcareous sandstone with interbedded calcareous shale. No graptolites were observed here.

Quaternary Deposits

Alluvial, terrace, and colluvial deposits make up the Quaternary units that were mapped. Alluvium consists of mostly poorly sorted and unconsolidated clay, silt, sand, and gravel found along floodplains of the Nolichucky and French Broad Rivers and their branching channels. Terrace deposits consist of rounded pebbles and cobbles composed of mostly quartzite or gneiss of non-local origin. Extensive colluvium is found primarily in the high topography of the Blue Ridge, consisting of large chunks of mostly quartzite.

Stratigraphy Discussion

The different facies of Knox and Conasauga Groups observed on each side of the Pulaski fault imply that the fault is a tectonic boundary that separates distinct and major

Figure 2-26. Middle Sevier shale-sandstone outcrop along Union Hill Road in the Parrottsville quadrangle consisting of calcareous fine-grained sandstone and interbedded limestone. (Hammer is ~30 cm long).

facies. Successful subdivision of Honaker Dolomite in parts of the Pulaski thrust sheet indicates that the Maryville Limestone, Rogersville Shale, and Rutledge Limestone, all originally exclusive to the central phase of the Conasauga Group, do not completely pinch out in this area of the southeastern phase as previously thought.

The abundance of limestone in the typically dolomite-dominant northwest facies Knox Group in the Pulaski fault footwall may indicate its close lateral proximity to the southeastern phase (Conococheague Limestone and Jonesboro Limestone). This implies that there is a relatively widespread facies transition in this portion of the Saltville thrust sheet. The Pulaski fault, therefore, was emplaced over this transition, carrying farther southeastern phase Knox and Conasauga Group facies.

CHAPTER III

STRUCTURE

Overview of Fold-Thrust Belts

In the southern Appalachian Valley and Ridge foreland fold-thrust belt, the source of Mississippian to Permian Alleghanian deformation and the master décollement can be attributed to the emplacement of the Blue Ridge-Piedmont megathrust sheet and ultimately derived from the collision of Gondwana with Laurentia (Hatcher et al., 2007a). This event involved: 1) initiation by the propagation of a master detachment fault in the ductile-brittle transition zone in crystalline crust; 2) ramping of the fault from basement into the Neoproterozoic-Early Cambrian rift succession; and 3) propagating into a mechanically weak Early Cambrian clastic unit (i.e., Rome/Waynesboro Formation) beneath the carbonate platform (Hatcher, 1989).

Foreland fold-thrust belts occur between the undeformed craton (platform) and the metamorphic cores of mountain chains. Chapple (1978) characterized these thrust belts as: (1) being thin-skinned, or involving no basement; (2) possessing a weak basal layer for the detachment to traverse; (3) having a wedge (Coulomb wedge) geometry that is maintained throughout deformation; and (4) exhibiting plastic behavior for the entire thrust belt. The thin-skinned concept was applied to the Pine Mountain thrust sheet by Rich (1934), when he correctly interpreted the structure as one involving the thrust ramping from a lower (Rome Formation) to a higher (Chattanooga Shale) detachment. His interpretation was made well before the concept was proved in the Canadian Rockies and Foothills by Bally et al. (1966). Bounding surfaces for the fold-thrust belt in the

Valley and Ridge province include the basement detachment, base of the indenter (Blue Ridge-Piedmont thrust sheet), and surface topography (Hatcher et al., 2007a). Wedge geometry was recognized by Elliott (1976) as a major factor in the deformation of thrust belts and is preserved in foreland fold-thrust belts by accretion, basal layer weakening, out-of-sequence thrusting, and normal faulting/extension (Suppe, 1981; Davis et al., 1983; Woodward, 1987).

Thrust development in the Appalachian Valley and Ridge is generally considered to be older closer to the interior of the mountain chain, propagating toward the foreland (Perry, 1978). Major faults contained in the belt generally rise from the décollement near the basement contact. These faults will consequently ramp at higher angles through strong units (e.g., limestones, dolomites, and sandstones) versus flattening that occurs along weak units (e.g., shales, evaporites). Therefore, the ramp-flat structures observed in the Valley and Ridge can be partially attributed to the varying rock type.

Understanding the relationship of structure to stratigraphy is especially relevant in fold-thrust belts (Rodgers, 1970b). Although not scale dependent, stratigraphic variations in this part of the Valley and Ridge may help explain deformation styles and structures evident in a given region or thrust sheet (Woodward et al., 1988). Thrust development and folding styles, in particular, can be characterized by the notion of structural lithic units (Currie et al., 1962), which are mechanically similar stratigraphic sequences of contrasting mechanical properties (strong vs. weak). Three sequences that are considered structural lithic units have been recognized in the study area: the Rome-Conasauga interval, Knox Group interval, and the Middle Ordovician (Chickamauga Group) interval (Harris, 1976; Woodward et al., 1988). The relatively low mechanical strength of the

Rome-Conasauga and Middle Ordovician intervals, when compared to the more competent Knox Group, typically controls thrust geometry and detachment location and also generates tighter and more complex folds under compression.

Mesoscopic Structures

Bedding

In the study area, the average strike of bedding is N57E, typical of this part of the Valley and Ridge (Figs. 3-1A, 3-1B). Although deformation style contrasts on both sides of the Pulaski fault, no distinct differences in bedding orientation could be recognized between the Pulaski and Saltville sheets here (Figs. 3-1C, 3-1D). Because bedding is a primary planar structure, it may not have been substantially affected by the timing or complexity of deformation in the region. Furthermore, horizontal compaction of strata from an early stage of Alleghanian deformation could have increased the overall strength of both thrust sheets, thus reducing the extent of subsequent deformation observed in bedding.

Variation in bed thickness throughout the area plays an important role in influencing mesoscopic structures, including the presence of cleavage, spacing of joints, and displacement of faults. More competent rocks generally have thick to massive bedding, but mechanically weaker rocks (e.g., Nolichucky and Sevier shales) commonly exhibit with very thin to thin beds. Frequently, beds observed in the Honaker Dolomite and its central phase equivalent formations have several thickness fluctuations. This variation in thickness affects mesoscale fold geometry, most notably during the processes of flexural-slip and strain partitioning.

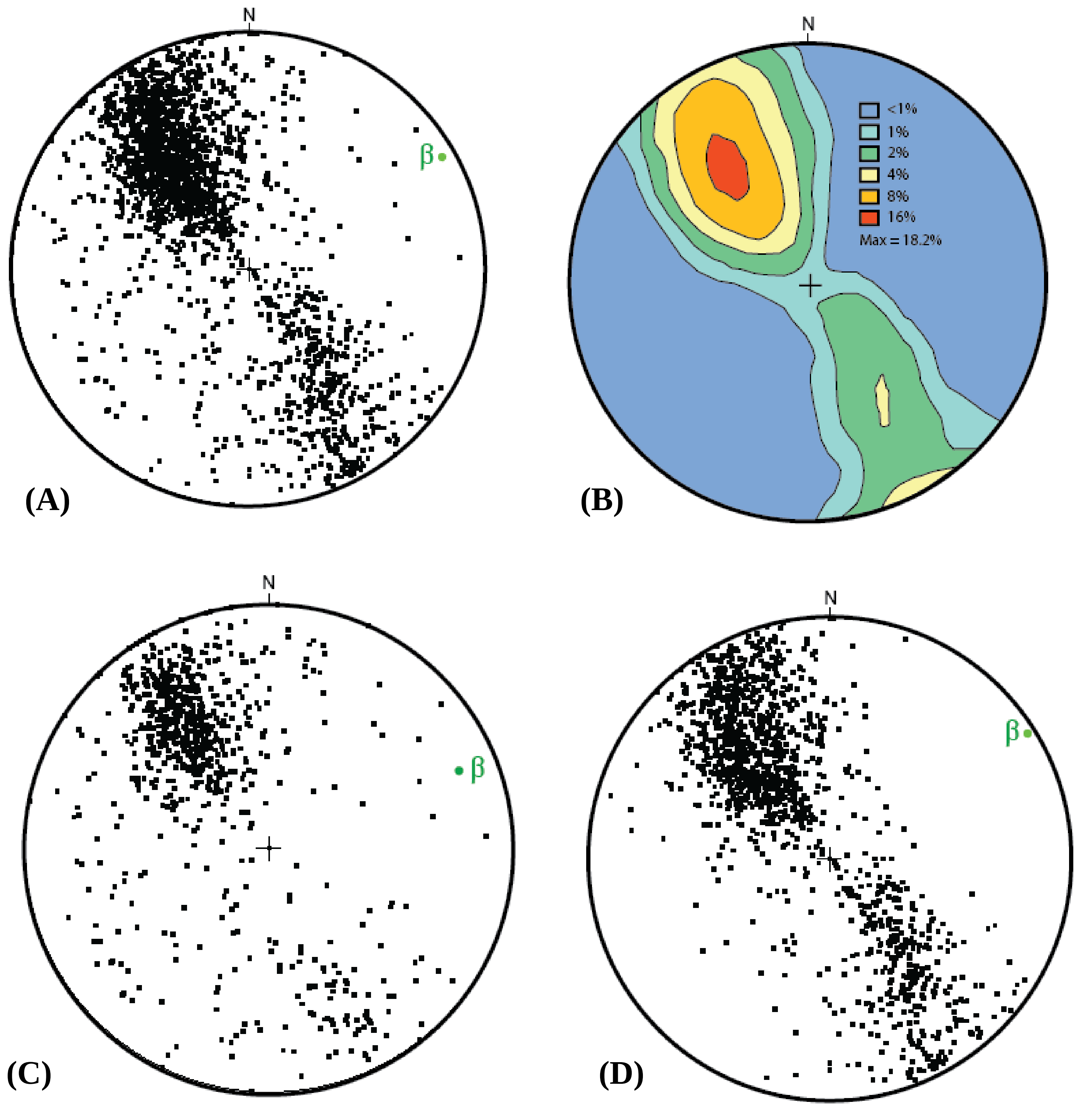

Figure 3-1. Lower hemisphere, equal-area projection of (A) 2,166 poles to bedding in the study area. Bedding data include measurements made by Whitmer (2005). (B) Contoured data from (A). (C) Only data points in the Pulaski thrust sheet (n=806) from (A). (D) Only data points from the Saltville thrust sheet (n=1,360) in (A). Fold axis orientations in the study area is not accurately represented from the beta angles (green) on these bedding plots, since many of the macroscopic folds are highly noncylindrical. Plots made using GEOrient v. 9.2 by Rod Holcombe (University of Queensland).

Faults

Few mesoscopic thrust faults with considerable displacement, ranging from 0.5 m in the Jonesboro Limestone near the Great Smoky fault and up to 3 m in parts of the Sevier Shale (Whitmer, 2005), were observed in the study area. Several thrust and normal faults with minor displacement (< 0.5 m) were observed in the cores of folds, generally anticlines, which are probably accommodation structures. The best location to see mesoscale faults in outcrop is along U.S. 70 near where the Great Smoky fault crosses the French Broad River (Fig. 3-2). This array of thrust and normal faults, drag folds, and fault gouge is interpreted as footwall deformation from the adjacent overriding Blue Ridge-Piedmont megathrust sheet.

Folds

Buckle folds make up the majority of folds in the study area, largely in part related to the large amount of shortening that accompanied fold-thrust belt formation in close proximity to the megathrust sheet indentor. Both flexural-slip and flexural-flow mechanisms are prevalent, depending on layer thickness and contrast in internal ductility. Flexural-slip folds here are commonly seen in the Sevier sandstones in the Parrottsville quadrangle and the thin- to medium-bedded carbonates of the Conasauga Group in the Pulaski sheet (Fig. 3-3). Examples of fault-propagation folds were observed in the Sevier Shale (Whitmer, 2005).

Fold types consist of both cylindrical and noncylindrical geometry, with the bulk of noncylindrical folds contained in the Pulaski sheet nearest to the map trace of the Pulaski fault. Most folds are gently plunging and are characterized by axial surfaces,

Figure 3-2. Outcrop is along U.S. 70 near the Great Smoky fault-French Broad River intersection containing footwall deformation in Jonesboro Limestone. (A)—uninterpreted. (B)—interpreted. Fault gouge, which is not clearly seen in the photo, is confined to the fault zone (yellow shaded polygon) in (B). Hammer is ~30 cm. (Photo by Robert D. Hatcher, Jr.)

Figure 3-3. Tight fold in the Rutledge Formation showing flexural-slip and flexural-flow, indicated by slickensides on the bedding planes (slip mechanism) and a thickened hinge (flow mechanism). Plunge is into photo. This outcrop is located along Long Creek Road, just southwest of Peanut Road in the Neddy Mountain quadrangle. Field book is 12 x 19 cm.

planar to cleavage, that are generally steep to near vertical (Fig. 3-4).

Numerous disharmonic folds also formed here because of the rheological and/or thickness differences between layers. This is most notably evident in the middle and upper Conasauga Group rocks that commonly comprise interbedded shaly units between more competent carbonates (Fig. 3-5A). A relatively high concentration of strongly disharmonic folds can be observed ~1.6 km (~1 mile) northeast of the Long Creek/Kenyon Road intersection, adjacent to both the Pulaski and Dunham Ridge faults (Fig. 3-5B). Here, the gradational and interfingering contact of Nolichucky Shale and thin-bedded Maryville Limestone in the core of an overturned syncline provides a weak and highly anisotropic zone for strain to accumulate.

Mesoscopic fold hinges frequently display similar trends to map-scale folds (Fig. 3-4; Plate I), echoing Pumpelly's rule, which states that small-scale structures are generally congruent with large-scale structures that were formed at the same time (Pumpelly et al., 1894). The discrepancies in orientations that exist between mesoscopic and macroscopic orientations may reflect multiple deformation phases, but the relatively few mesoscopic fold measurements collected in the Pulaski sheet cannot confirm this.

Cleavage

Slaty and fracture cleavage are non-pervasive throughout the study area and are generally associated with meso- and macroscopic folds and faults in weaker units of the region (Yust, 1975; Whitmer, 2005). Because of the abundance of calcareous units and their relative solubility, pressure solution is the dominant cleavage-forming mechanism in the Pulaski and Saltville thrust sheets. The majority of cleavage in both sheets has an

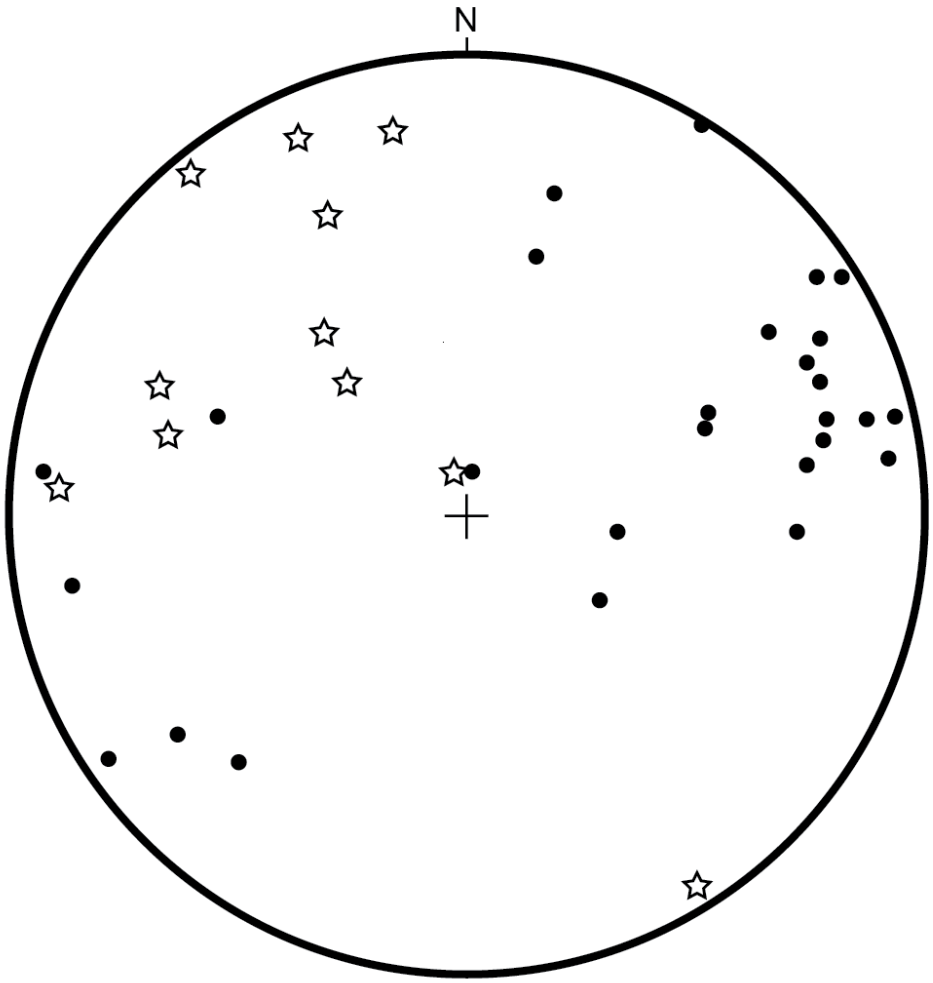

Figure 3-4. Lower hemisphere, equal-area projection of 38 poles to axial surfaces (stars) and hinge lines (black dots). The mean principal orientation for axial surfaces is 048/61SE and 067/17NE (trend and plunge) for hinge lines.

(A)

(B)

Figure 3-5. (A) Disharmonic folding, with a component of flexural slip (and flexural flow?) in Nolichucky Shale. (Hammer head is ~18.5 cm). (B) Strongly disharmonic folds in thin-bedded Maryville Limestone. (Brunton compass is ~8 cm in diameter). Both (A) and (B) are located in the southwest corner of the Cedar Creek quadrangle.

axial planar orientation (058/89SE; Fig. 3-6) and typically found well-developed near fold hinges in fine-grained rocks (e.g., lower Sevier Shale and Nolichucky Shale) and less frequently found in the thick carbonate units of the Knox Group.

Figure 3-6 shows a distribution of cleavage that is fanned and spread over the study area. This implies that cleavage was developing during folding here. A second distribution of steeply dipping (northeast and southwest) cleavage sets may represent a later folding stage, supporting the argument for polyphase deformation in the Pulaski thrust sheet. Troensegaard (1965) also interpreted cleavage in this area to have formed during or in late stages of folding, since cleavage is commonly not displaced by slip along bedding. Aside from overturned stratigraphic sequences, the angular relationships between cleavage and bedding were used in determining whether a fold limb is upright or overturned (Fig. 3-7). Bedding is often obscured in the lower Sevier Shale and Nolichucky Shale where cleavage is dominant. However, pencil cleavage from bedding-cleavage intersections is common in both formations and parallels adjacent fold axial traces (Fig. 3-8).

Lemiszki (2008) noted that cleavage in the Knox Group is rare to nonexistent in the Valley and Ridge of Tennessee, except within the Pulaski thrust sheet. The abundance of limestone in the southeastern Knox facies of the Pulaski sheet, versus more dolomite in thrust sheets to the west, could have contributed to the higher frequency of cleavage formation, since dolomite is more resistant than calcite at shallow crustal levels (Hugman and Friedman, 1979). Cleavage development in the Knox Group in the Newport quadrangle contributed to Lemiszki's suggestion for the continuation of the Pulaski fault farther southwest than the terminus shown in Hardeman et al. (1966).

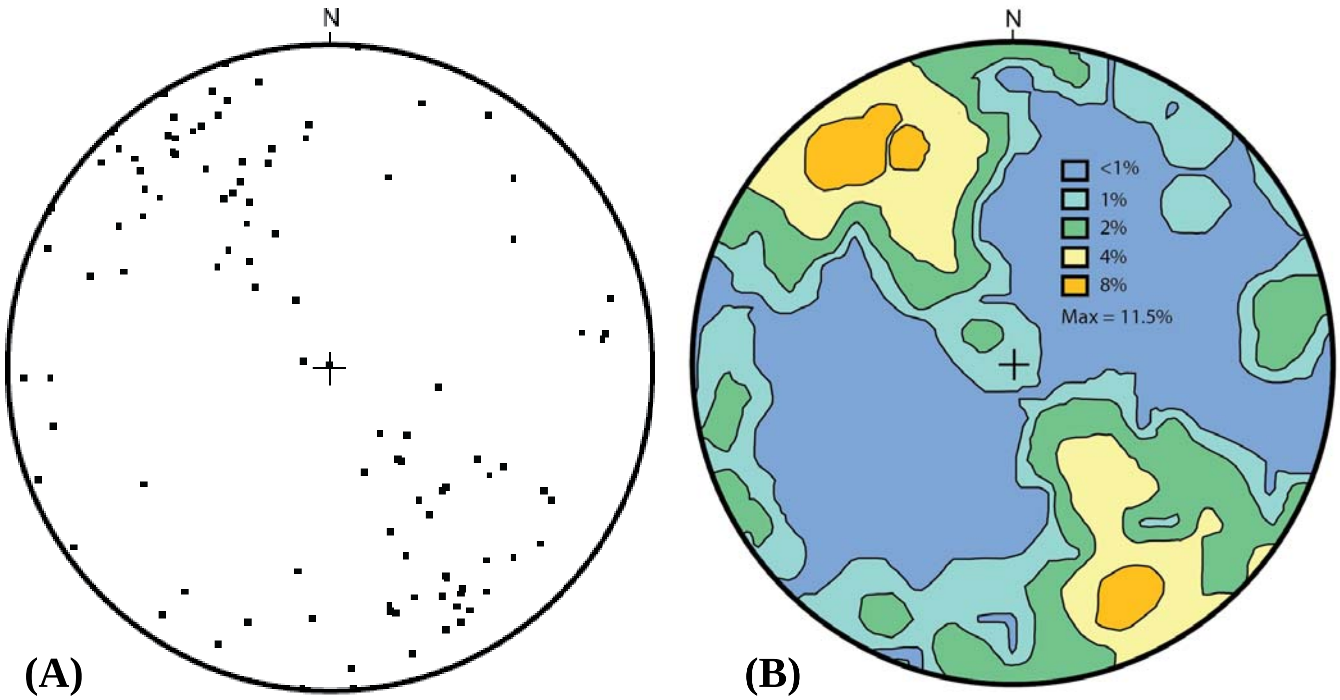

Figure 3-6. (A) Lower hemisphere, equal-area projection of 113 poles to cleavage planes. (B) Contoured data from (A). Mean principal direction is 058/89SE. Data include measurements from Whitmer (2005). Plots made using GEOrient v. 9.2 by Rod Holcombe (University of Queensland).

Figure 3-7. Outcrop of middle Sevier Shale near Trentham Hollow Road in the Parrottsville quadrangle showing cleavage (green lines) and bedding (orange lines) relationships. The dip of cleavage is steeper (~80º) than bedding (~55º), indicating that this section is upright. Field book is 12 x 19 cm.

Figure 3-8. Outcrop of lower Sevier Shale southeast of Whittenburg Church in the Cedar Creek quadrangle exhibiting pencil cleavage. Brunton compass is ~8 cm in diameter.

However, he acknowledged that Knox Group cleavage is also present in the footwall of his projected Pulaski fault, and therefore the presence of cleavage could not be a deciding factor for the location of the fault.

Joints

Although not a major focus of this study, joints are well-developed in all rock units and most exhibit irregular surfaces; they can be filled with calcite. As noted by Byerly (1966) in the Greeneville quadrangle, jointing, like cleavage, is most evident in both Nolichucky Shale and Sevier Shale where closely spaced joint sets produce blocky shale chips. Joint spacing of many of the carbonate rock units is relatively wide and more difficult to accurately determine in the field than in less competent units.

Stylolites

Diagenetic and tectonic stylolites are sparingly present in all carbonate units of the study area and are most frequently seen in the Knox Group (Fig. 3-9). Diagenetic stylolites are generally bedding-parallel, indicating that σ_1 was vertical, while tectonic stylolites are generally transverse or at a high angle to bedding (Hatcher, 1995). Andrews and Railsback (1997) analyzed both types of stylolites in the southern Appalachians and determined that bedding-parallel stylolites could have formed in both pre-tectonic and post-tectonic settings, with the latter reflecting loading by overthrust burden and/or the shedding of sediment from the hinterland.

Figure 3-9. Possible tectonic stylolite located northwest of Cottage Road in the Neddy Mountain quadrangle. Stylolite is dipping at a higher angle (~65º) than bedding here (50º; not shown in photo). Amplitudes of teeth (normal to σ_1) average 0.5-1.5 cm. Diameter of formerly lost golf ball is ~4 cm.

Regional Structures

Pulaski Fault

The Pulaski fault (i.e., thrust system) stands out among other faults in the Valley and Ridge. One aspect is its overall large extent, some 563 km (350 miles) from Rockingham County, Virginia, to its southwestern terminus in this study area south of Parrottsville, Tennessee (Fig. 1-2). Here the Pulaski is overridden by the thin-skinned Great Smoky fault in the Neddy Mountain quadrangle. Strangely, this is the only southern Appalachian Valley and Ridge fault to continue into the central Appalachians around the 30º bend of the Roanoke recess in southwestern Virginia (Rodgers, 1970b). Southern Appalachian faults, including the Saltville, Copper Creek/Narrows, and St. Clair faults terminate as anticlines in the Roanoke bend (Butts, 1933; Rodgers, 1970b; Couzens and Dunne, 1994). Near the recess, dominant folding trends change upwards of 55º from the central to the southern Appalachians (Bartholomew, 1987; Evans and Dunne, 1991). The Pulaski fault becomes a series of thrusts here, including the Catawba, Salem, and Christiansburg faults (Fig. 3-10). At its northern terminus near Staunton and Harrisonburg, Virginia, the Pulaski fault dies into a northeast-plunging anticline, similar to other southern Valley and Ridge faults (Rodgers, 1970b). This occurs adjacent to the northeast terminations of the Blue Ridge thrust system and Rockfish Valley fault near Front Royal, Virginia (Bartholomew and Lewis, 2010).

As indicated by its sinuous trace in the study area, the Pulaski fault has a very low dip, ranging from subhorizontal to 20º near the surface and becomes steeper near its junction with the Dunham Ridge fault (Fig. 3-11). The "S"-curve trace of the Pulaski

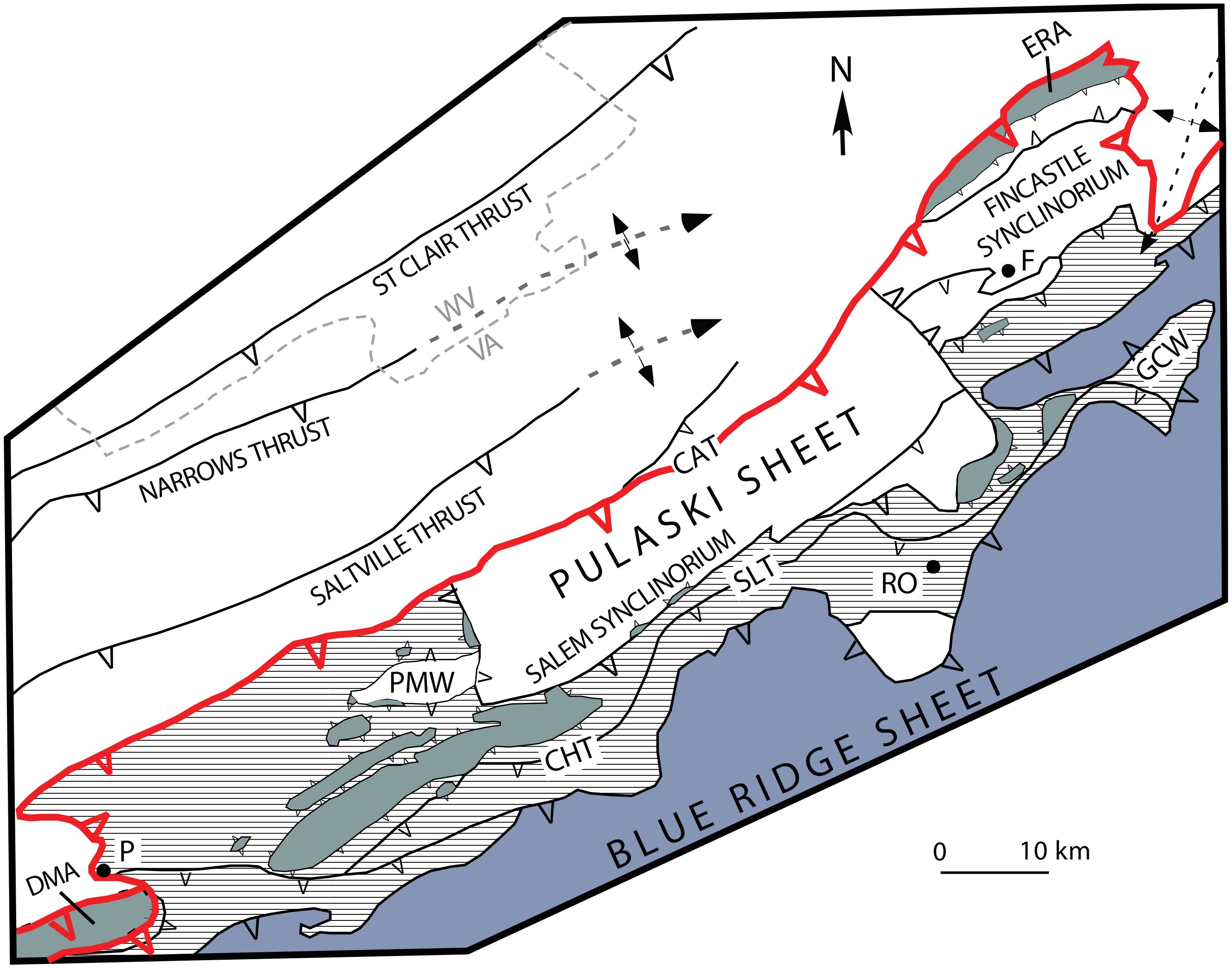

Figure 3-10. Generalized tectonic map of the Pulaski thrust sheet and adjacent structures near the Roanoke recess. Lined area is the complexly folded and faulted plate that contains the "broken formation" of Schultz (1986) to which the Max Meadows breccia is confined. Bluish-green polygons are orphans and horses within the Pulaski sheet. Royal blue-Blue Ridge province; bold red line-Pulaski fault; CAT-Catawba fault; CHT-Christiansburg fault; DMA-Draper Mountain allochthon; ERA-Eagle Rock allochthon; GCW-Goose Creek window; PMW-Price Mountain window; SLT-Salem thrust; F-Fincastle; P-Pulaski; RO-Roanoke/Roanoke recess. Modified from Bartholomew (1987) and Bartholomew and Lewis (2010).

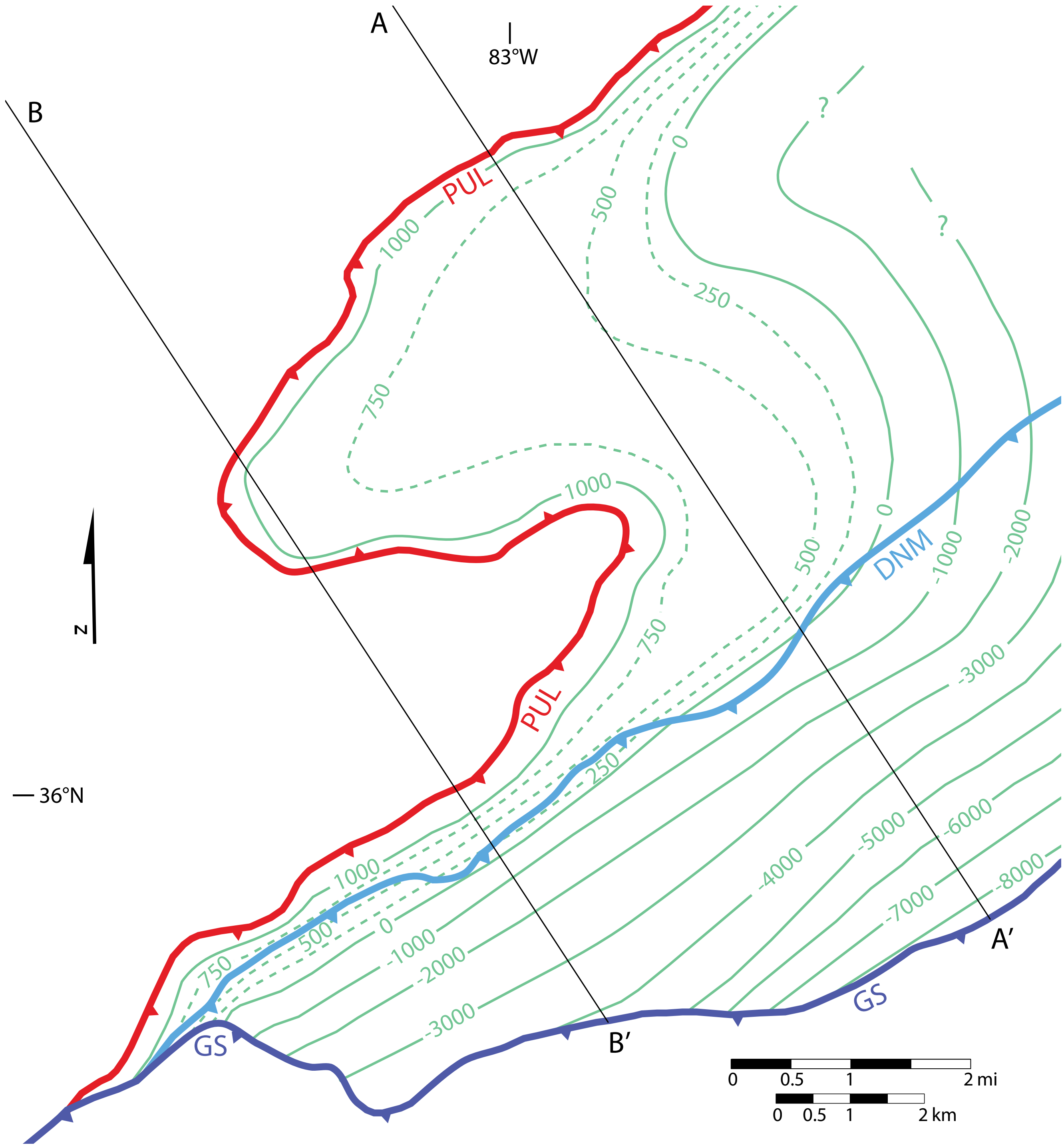

Figure 3-11. Structure contour map of the main Pulaski fault (PUL) near its terminus in the study area. Contour lines (green) are expressed in feet above and below sea-level. Contour interval for solid contours is 1,000 ft. Dashed contours (C.I. = 250 feet) are added to provide more detail in the flattest area. Note steeper dips in proximity to the Dunham Ridge (DNM) and Great Smoky (GS) faults. Cross sections from lines A-A′ and B-B′ are found on Plate II.

here is also prevalent in other areas along the fault, such as the Babbs Knobs flap near Greeneville, Tennessee, which exhibits a similar but more complex "S" and "Z" pattern (Keith, 1905a; Rodgers, 1953b; Byerly, 1966; Roper, 1977; Bultman, 2005), and near Marion and Staunton, Virginia (Butts, 1933). Byerly not only attributed the irregularity of the fault trace in the Babbs Knobs flap and the rest of northeast Tennessee to a shallow dip (10º to 20º), but also to post-emplacement folding. His interpretation of the flap is based on its strong similarities to geometry and drill data of the Rocky Valley fault near New Market, Tennessee (Bumgarner et al., 1964). As shown in Figure 3-11, the Pulaski fault in the study area has also been folded.

Stratigraphic displacement changes considerably in the study area, with relatively progressive displacement increasing southward along the Pulaski trace. Approximately 853 m (2,800 ft) of vertical displacement exists near the core of the Bright Hope anticline. Stratigraphic displacement is at least 1.4 km (4,500 ft) where the Rutledge Limestone and Mascot Dolomite are contiguous adjacent to the Pulaski fault terminus. However, this extreme and southwesterly progressive vertical displacement change is mostly likely apparent and not true displacement, caused by the sinuous trace/low dip of the Pulaski fault and the lateral change in lithofacies (e.g., Knox Group) between thrust sheets (Fig. 3-12).

Based on restored and balanced cross sections through the study area, horizontal displacement of the Pulaski fault (not factoring in structurally lower thrust sheets) is at least 23.8 km (14.8 mi) with approximately 30% shortening within the enclosed Pulaski thrust sheet. Near Roanoke, Virginia, the Draper half window exposes the Pulaski sheet, indicating horizontal displacement of the fault to be at least 15 km (9.3 miles) (Hatcher et

Figure 3-12. Pulaski fault along Whittenburg Road in the northern Cedar Creek quadrangle, shown thrusting the southeastern phase Jonesboro Limestone over lower Sevier Shale. Northwestern phase Knox Group is immediately northwest of the fault.

al., 1989). Palinspastic restoration of the entire Pulaski thrust sheet in the Roanoke recess places the origin of the leading edge of the thrust sheet 100-110 km to the southeast (Bartholomew, 1987). This is roughly 5-6 times greater than the combined displacement along the Saltville, Copper Creek/Narrows, and St. Clair faults near the recess (Bartholomew and Whitaker, 2010).

Based on the presence of Shady Dolomite and Chilhowee Group rocks in the Pulaski thrust sheet (Glade Mountain and Lick Mountain anticlinoria) between Pulaski and Marion, Virginia, the Pulaski fault most likely originated in a structurally lower detachment than the Rome Formation at this latitude (Butts, 1933; Rankin et al., 1972; Bartholomew et al., 1980). This aspect is surprisingly similar to faults of the Blue Ridge, such as the Miller Cove fault, which carries pre-deformed strata unlike the thin-skinned Great Smoky fault (Hatcher et al., 2007b). That raises questions as to whether or not the Pulaski fault represents a dismembered thin-skinned segment of the Blue Ridge frontal thrust complex or is a true Valley and Ridge thrust that happens to contain Lower Cambrian rocks from a more easterly drift basin (Hatcher et al., 1989). However, the fact that the Pulaski sheet contains relatively unmetamorphosed rocks in stratigraphic continuity with ages as young as Middle Ordovician in northeastern Tennessee (Rodgers, 1953a) and lower Mississippian in southwestern Virginia (Butts, 1933) suggests Valley and Ridge affinity.

Interestingly, Middle Cambrian formations (i.e., Honaker Dolomite and equivalent central facies; Fig. 2-8) are the oldest rocks exposed in the Pulaski fault hanging wall in this study area and all of northeast Tennessee (Rodgers, 1953b; Hardeman et al., 1966). Based on this relationship and lack of the Lower Cambrian

Rome Formation in the thrust sheet, Rodgers (1953a) and Byerly (1966) suggested that a weak lower shaly unit in the Honaker Dolomite, or probably the Rutledge Limestone/Pumpkin Valley Shale transition, served as a local detachment for the Pulaski fault here. In the footwall, the structurally weak basal part of the lower Sevier Shale likely acted as a glide zone for the Pulaski fault, subsequent to ramping from its lower detachment. Although Knox Group rocks adjacent to the fault trace are most prevalent toward the southwest portion of the study area, the Sevier Shale comprises most of the adjacent footwall to the northern region, and to most of the nearly 48 km (30 mile) segment of the Pulaski fault in the Mosheim and Greeneville quadrangles (Byerly, 1966; Lemiszki, 2003).

Another diagnostic feature of the Pulaski fault system is its association with the massive Max Meadows tectonic breccia, named for Max Meadows, Virginia. It occurs most frequently near the Max Meadows fault, sequentially located a few hundred meters above the basal Pulaski fault in southwestern Virginia (Cooper, 1938; Cooper and Haff, 1940). This breccia was first concluded to have a tectonic origin by Cooper (1938), but was previously thought to be a sedimentary conglomerate or cave breccia (Campbell, 1925). Rodgers (1970a) further postulated that the Max Meadows breccia was derived from a tectonically deformed Cambrian evaporite sequence. Specific occurrences of the breccia are along faults, in the cores of folds, and as breccia “dikes” in an undeformed wall rock (Cooper, 1939; Cooper and Haff, 1940; Bartholomew and Schultz, 1980; Bartholomew, 1987).

Unfortunately, no tectonic breccia observed in the study area matches the thickness or character of the Max Meadows breccia, but a few contained in the Pulaski thrust sheet may be correlative. An isolated tectonic breccia "dike" with large clasts up to 5 cm in diameter was observed near the Long Creek Road/Peanut Road intersection in the Neddy Mountain quadrangle (Fig. 3-13A). This and other tectonic breccias in the study area (Figs. 3-13B, 3-13C) are positioned close to major faults, although none are directly associated with the main Pulaski trace. Only one of these breccias, located immediately southwest of St. James Church in the Cedar Creek quadrangle, is positioned in a major fault zone of the area (i.e., the Dunham Ridge fault).

Pulaski Thrust Sheet Characteristics

The Pulaski thrust sheet is bounded in the study area by two major faults, the Pulaski and Great Smoky (Plate I), and is positioned on the easternmost boundary of the Tennessee Valley and Ridge province, underlying the adjacent Great Smoky and Holston-Iron Mountain thrust sheets. Bartholomew (1987) defined the Pulaski thrust sheet as a complex, composite sheet in which various "plates" were juxtaposed during different stages of Alleghanian thrusting. The Pulaski sheet has been interpreted to be part of an extensive duplex thrust system, with the Pulaski fault serving as the floor thrust in most cases and the Great Smoky-Holston Mountain fault being the roof thrust (Boyer and Elliott, 1982; Woodward and Gray, 1985; Bartholomew, 1987; Harlow, 1987).

The style of folding between the Pulaski and adjacent Saltville thrust sheets differs in both geometry and complexity. Several macroscopic folds in the Pulaski sheet are tight to isoclinal and overturned. At least four major folds, some highly noncylindrical, shallow their axial surfaces and change from upright to overturned along strike (Fig. 3-14). Therefore, I interpret a majority of these folds to exhibit a type 3

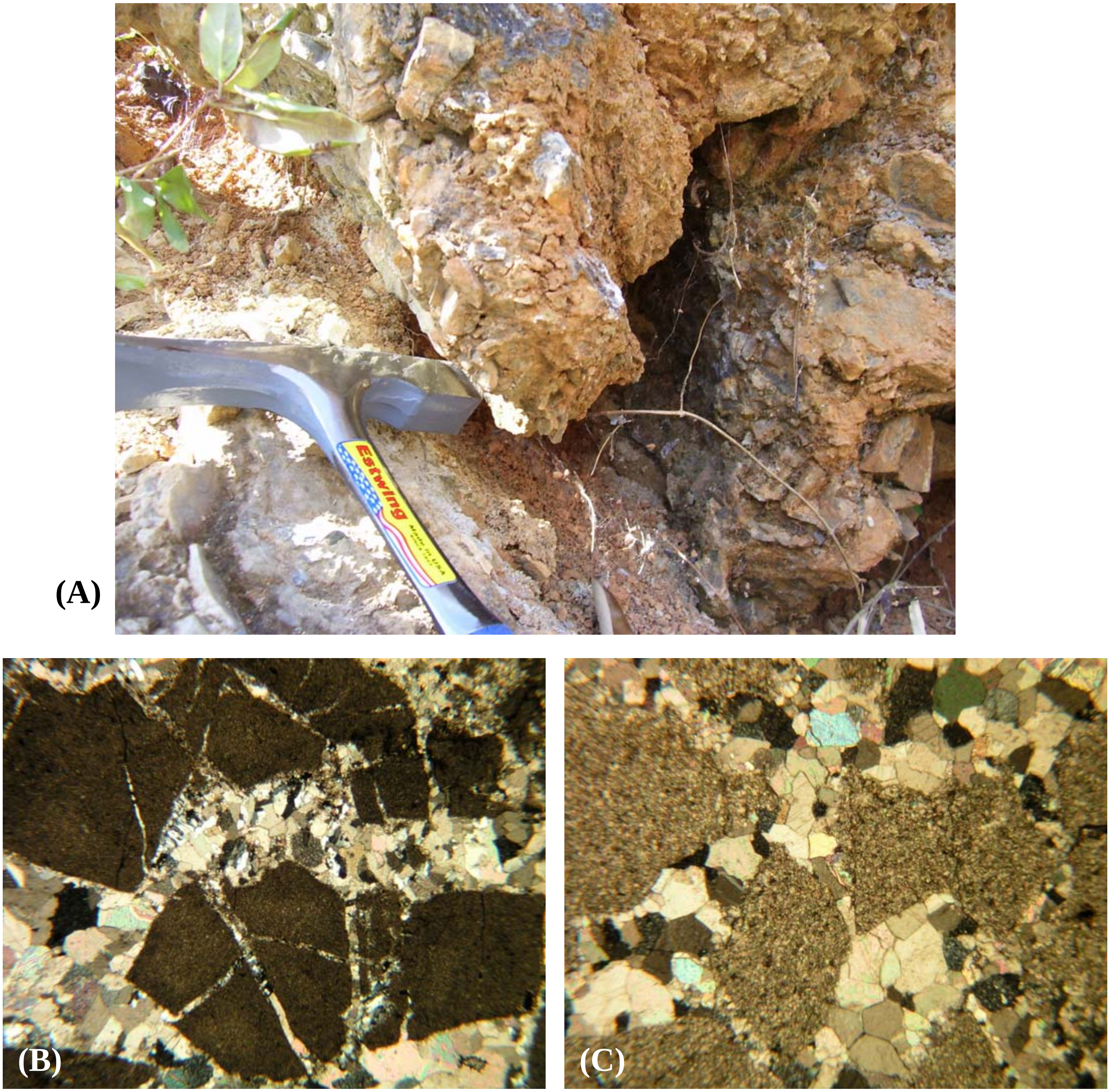

Figure 3-13. (A) Tectonic breccia "dike" with clasts as large as 5 cm in diameter, located just north of the Long Creek Road/Peanut Road intersection. Hammer head is ~18.5 cm. (B) Photomicrograph (crossed nicols) of breccia found in the Dunham Ridge fault zone near St. James Church. Large clasts are mostly dolomite and siltstone in a calcite-cemented matrix. (C) Photomicrograph (crossed nicols) of breccia found near the Great Smoky fault along Happy Hollow Road in the Neddy Mountain quadrangle. This breccia is more matrix-supported than (B), and contains mostly limestone and some dolomite clasts in a sparry calcite-cemented matrix. Field of view for (B) and (C) is ~10 mm.

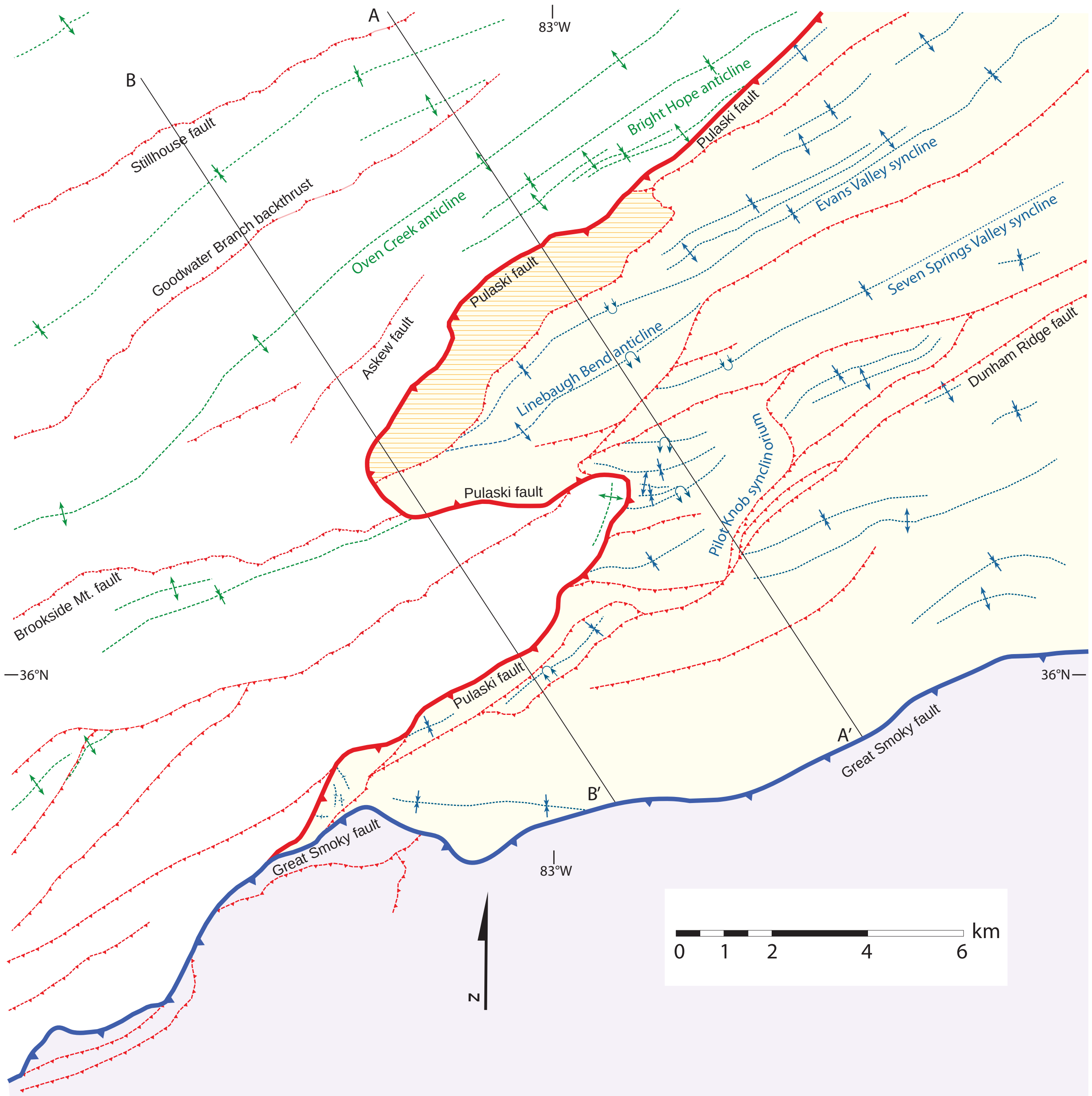

Figure 3-14. Structural trend map of the northeast Tennessee study area, which includes data from Whitmer (2005). Light tan—Pulaski thrust sheet; light purple—Blue Ridge province. Note the several tightly spaced and overturned folds within the Pulaski thrust sheet (shown in blue), versus the broad open folds of the Saltville sheet (shown in green). The horse at the leading edge of the Pulaski sheet is designated by the orange lined area. Fault and fold symbols correspond to those in Plate I. Cross sections for lines A-A′ and B-B′ are found on Plate II.

interference pattern, caused by a minor reorientation of shortening direction as a continuation of the same folding process that affected the rocks previously (Ramsay, 1962; Hatcher, 1995). The change of Knox Group facies in the Pulaski hanging wall, including more limestone and thinner beds, also likely played an important role in the style and degree of deformation observed.

Macroscopically, the only types of faults observed in the Pulaski thrust sheet are thrusts, which are more abundant than in the adjacent Saltville sheet (Fig. 3-14). These faults, which tend to vary in orientation, exhibit much steeper dips than the Pulaski floor fault and emerge along the northwest limbs of several folds. The Nolichucky Shale and Honaker Dolomite act as the weak detachment layer for many faults in the Pulaski thrust sheet. Aside from the Dunham Ridge fault, most possess relatively small displacements.

In the north-central portion of the study area, a horse of northwestern facies Knox Group is contained in the Pulaski thrust sheet. As the Pulaski fault propagated through the massive Knox carbonates of the underlying Saltville thrust sheet, this slice of the footwall was transported within the Pulaski thrust sheet at its leading edge. The horse may be part of a cutoff syncline. Bartholomew and Lewis (2010) worked out fold and fault geometry in the Pulaski thrust sheet of southwestern Virginia by suggesting the term orphan, which is a variety of horse. Orphans are commonly considered far-traveled (upwards of 100 km) horses or duplexes and consist of strata that are unrelated to nearby rocks of the hanging wall or footwall (Bartholomew and Lewis, 2010). Based on cross sections, the horse in the study area could have originated from Knox Group strata at the Pulaski fault transition of ramp-to-flat geometry, which is approximately located beneath the Dunham Ridge fault. Transport distance of the horse, and thus the thrust sheet from this point, would be ~2.9 km (1.8 mi). Therefore, I do not consider this structure in the study area to qualify as an orphan, and the sequential ramping history of the Pulaski fault derived from reconfiguration of orphans in the southwestern Virginia area cannot be reproduced here.

Crosscutting relationships in the study area suggest that the Pulaski fault may be an out-of-sequence thrust, emplaced after many of the underlying thrusts in the footwall (Plate II). In contrast, the occurrence of higher conodont alteration index (CAI) values in the Pulaski thrust sheet than those in the Saltville thrust sheet, suggests that the Pulaski sheet was emplaced first (Epstein et al., 1977; Harris, 1979; Lewis and Hower, 1990). Based on these data and the Pulaski's large transport distance, Lewis and Hower (1990) speculated that the "thermal event" affecting the Pulaski thrust sheet could be a different phase than other sheets in the Valley and Ridge.

Major Footwall Structures

One major regional structure in the Pulaski footwall is the doubly plunging Bays Mountain synclinorium (Fig. 3-15), which occupies ~1,425 km^2 (550 mi^2) of the Valley and Ridge province and extends ~145 km from Kingsport, Tennessee, southwest to Etowah, Tennessee (Cummings, 1962, 1965; Bultman, 2005; Whisner, 2005). The area is characterized by relatively large and open, doubly plunging folds, which are typical in the thick Cambro-Ordovician carbonate sequence. These map-scale folds are outlined by the Bays Formation (not seen in the study area) and the Sevier Shale (Rodgers, 1953a, 1953b; Cummings, 1962). At this latitude, the Bays Mountain synclinorium is ~26 km wide (perpendicular to strike) and is flanked by the Saltville and Dumplin Valley faults to

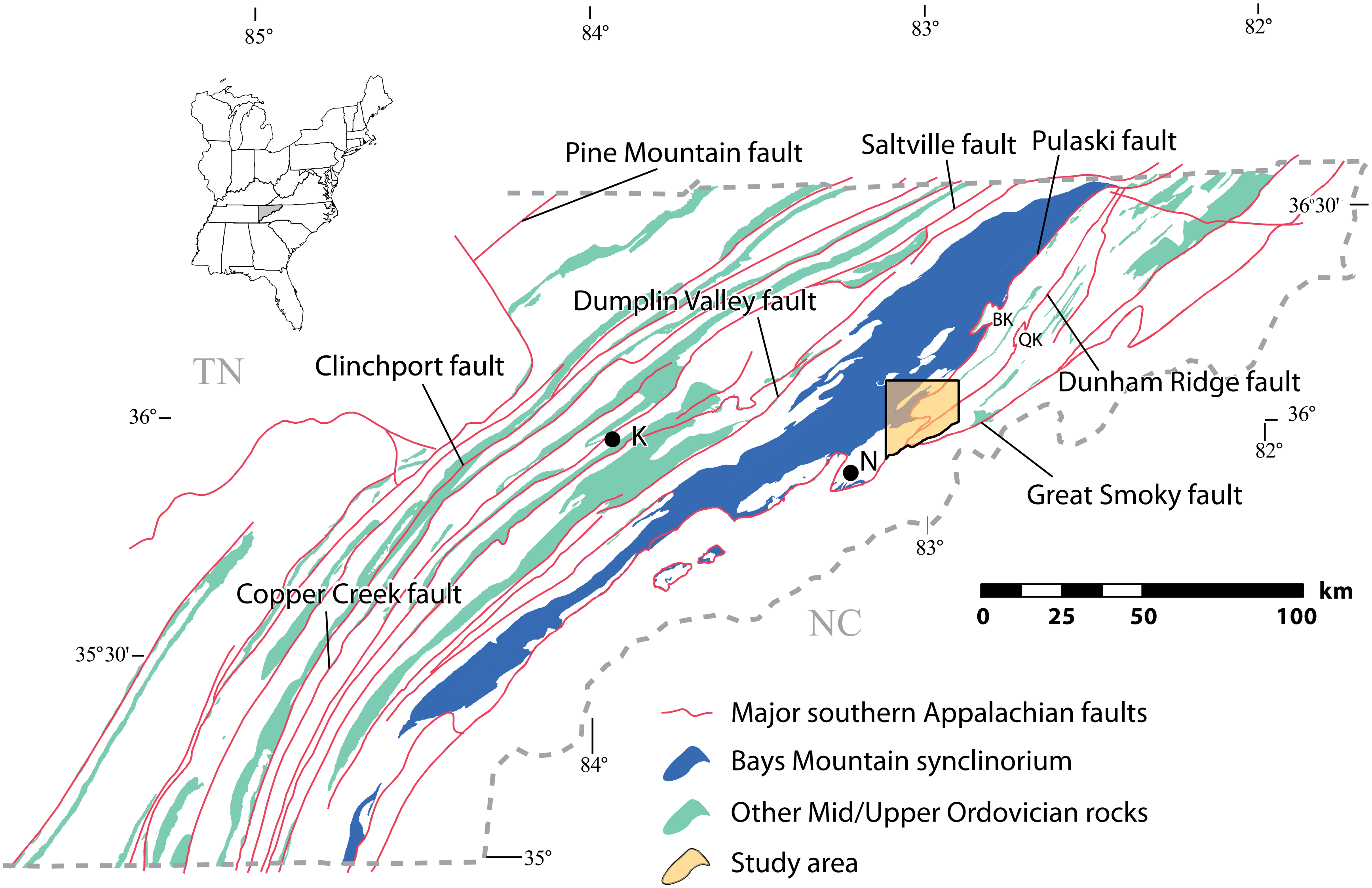

Figure 3-15. Extent of the Bays Mountain synclinorium in relation to the study area and the rest of the Tennessee Valley and Ridge province. Study area includes mapped Parrottsville and portion of the Cedar Creek quadrangles from Whitmer (2005). K-Knoxville; N-Newport; BK-Babbs Knobs flap; QK-Quaker Knobs flap. Modified from Hatcher et al. (1990) and Whitmer (2005).

the northwest and the Pulaski and Great Smoky faults to the southeast (Rodgers, 1953b, Whitmer, 2005). On a regional scale, the majority of the mesoscopic folds are generally disharmonic from the varying mechanical strengths of units (Bultman, 2005). The Sevier Shale absorbed most of the deformation/strain, based on the majority of observed mesoscopic structures being confined to this formation (Troensegaard, 1965).

In the study area, the footwall block of the Pulaski fault is the Saltville thrust sheet. The Saltville fault, named by Stevenson (1885) for exposures near Saltville, Virginia, is the largest fault system in the Appalachian Valley and Ridge. It extends from south of Dalton, Georgia, where it is interpreted to transfer displacement to the Rome fault (Munyan, 1951; Rodgers, 1953b), to its northeastern terminus near the central-southern Appalachian transition northwest of Roanoke, Virginia (Fig. 1-2). Locally, the most dominant macroscale structures in the Saltville thrust sheet are the Oven Creek anticline and the Stillhouse fault (Plate I). Fold geometry is characteristically broad and open here (Fig. 3-14), typical of folding in the thick and competent Knox Group contained in the Bays Mountain synclinorium. While Sevier Shale dominates the northern portion of the Saltville sheet, both facies of Knox Group rocks, along with Maynardville Limestone, make up the southern half. This area is highly faulted and perhaps associated with its proximity to the Pulaski fault terminus and/or the overriding Great Smoky fault.

<u>Great Smoky Fault</u>

The thin-skinned Great Smoky fault, previously referred to as the Meadow Creek Mountain-Holston Mountain thrust fault in the study area (Rodgers, 1953b; Hardeman et al., 1966), serves as the local boundary between the Valley and Ridge and Blue Ridge provinces. The entire Great Smoky fault system (including the Miller Cove fault to the southwest) is the only thrust system of the Blue Ridge to exhibit thin-skinned behavior (Hatcher et al., 2007b). Its upper detachment is likely in the weak, subchlorite-grade Walden Creek shales (Sandsuck Formation), while its lowest detachment is along the ductile-brittle transition in Paleozoic basement to the southeast (Hatcher et al., 2007b).

The Great Smoky is not well exposed in most of the study area, because of the abundance of colluvial/alluvial cover obscuring its trace. Mostly unmetamorphosed Lower Cambrian rocks are exposed in its hanging wall, including the Rome Formation, Shady Dolomite, and Chilhowee Group. Although not depicted in cross sections constructed in the study area, the Great Smoky is likely a shallow-dipping fault, based on nearby seismic reflection lines (Hatcher et al., 2007b).

Map-Scale Structures

Several of the most prominent map-scale structures delineated from detailed mapping in this study have been assigned locally relevant names for referral purposes. Names for most of the macroscopic faults that transect the Parrottsville quadrangle were suggested by Lemiszki (2003) and Whitmer (2005). Although some of the same structures of this study area were previously mapped by Rodgers (1953b), no names were assigned to any of the major folds in the Pulaski sheet. For additional information regarding map-scale structures in the Parrottsville quadrangle portion of the study area, see Whitmer (2005).

Oven Creek anticline

The Oven Creek anticline (~18 km in length), which crosses parts of three quadrangles (Parrottsville, Cedar Creek, and Mosheim), trends northeast-southwest and is doubly plunging. A complete section of the Ordovician Knox Group, with Chepultepec Dolomite exposed in its core, can be observed via a transect in the northwestern corner of the Cedar Creek quadrangle. On the southeast limb, dip measurements average 55ºSE, whereas dips average 60ºNW on the northwestern limb with numerous steeply overturned (~70º) southeast dips. Based on bedding data collected in the portion of the Oven Creek anticline in the study area, its axial trend is N58ºE with a plunge of 3ºSW (Whitmer, 2005). The Pulaski and Brookside Mill faults serve as the southernmost margin of the southeast limb. Industry seismic reflection data (Fig. 3-16) from a profile in the Parrottsville quadrangle were used to assist in interpreting depths and geometry of the anticline. Imbricates from the Stillhouse fault were placed in the core of the Oven Creek anticline based on the seismic data and room problems.

Bright Hope anticline

Immediately southeast of the Oven Creek anticline in the Cedar Creek quadrangle lies the Bright Hope anticline, named in this study for a main road transecting the fold (Plate I; Fig. 3-14). It is located just to the northwest of the Pulaski fault trace. On average, the anticline (at least 6.4 km in length) trends 058 and possesses steeper dips on its southeastern limb (~72º) than its northwestern limb (~59º). It appears that the Pulaski fault may have obliquely truncated part of the Bright Hope anticline. However, the occurrence of different Knox Group facies on each side of the Pulaski fault here implies

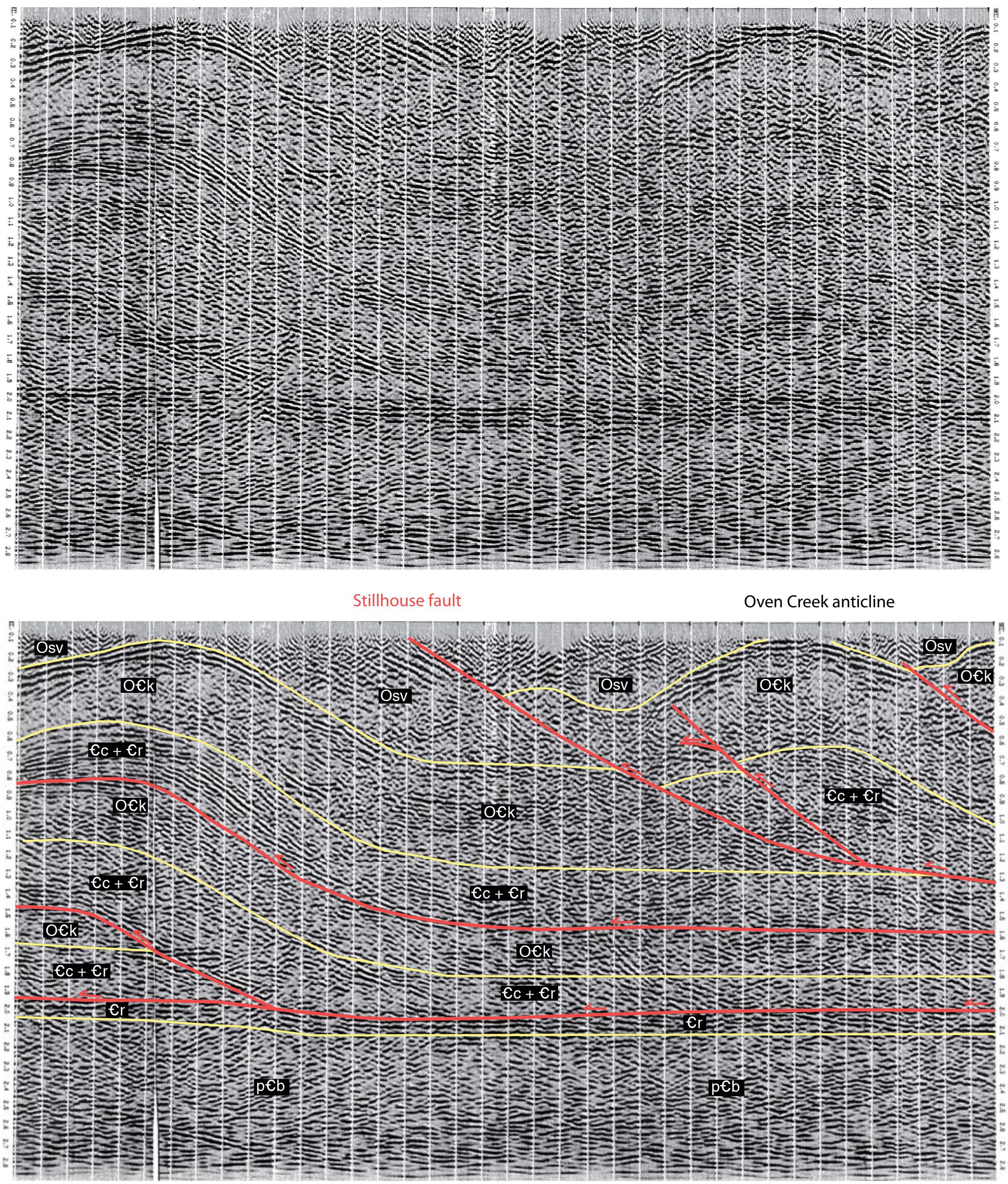

Figure 3-16. Seismic profile from the Amoco 5CM-1 line in the Parrottsville quadrangle (Plate I) showing uninterpreted (A) and interpreted (B) data. Red—faults; Yellow—unit bedding contacts. One second in T.W.T. equals ~2.85 km. For explanation of abbreviations, see Plate I. Interpretations modified from Whitmer (2005).

an unusually large displacement within the anticline. Therefore, I interpret that the adjacent rocks on the southeastern side of the Pulaski fault are likely not a cutoff part of the Bright Hope anticline, but instead are associated with other hanging wall structures.

Stillhouse fault

The northwest-verging Stillhouse fault is located northwest of the Oven Creek anticline and serves as the main detachment for the Goodwater Branch and Askew faults. This fault was originally recognized by Hatcher (unpublished data) in several seismic reflection profiles (Fig. 3-16) and was subsequently mapped on the surface by Whitmer (2005). In cross section view, it is the only fault present that is exposed on the surface and also joins the underlying Saltville fault. Its horizontal displacement is up to 4.7 km (2.9 miles). Like the Pulaski fault, displacement increases progressively southwestward along strike, where lower Sevier Shale is thrust over middle Sevier Shale.

Askew fault and Goodwater Branch backthrust

The two major imbricates of the Stillhouse fault that crop out at the surface are the Askew and Goodwater Branch faults located on the southeast and northwest flanks of the Oven Creek anticline, respectively. Both have very small displacements, with only the Askew fault clearly showing displacement in map view (Mascot Dolomite over lower Sevier Shale). The Goodwater Branch backthrust is a southeast-verging fault and may continue to the northeast for up to 7 km in the Mosheim quadrangle (Lemiszki, 2003). Both faults have been interpreted to form via accommodation during emplacement of the Stillhouse fault (Whitmer, 2005). Remapping of these faults in this study (Plate I) was based on changes in topography, bedding data, and locations in the seismic reflection profile (Fig. 3-16).

Brookside Mill fault

The northwest-verging Brookside Mill fault is positioned in the southernmost part of the Parrottsville quadrangle and appears to be truncated by the shallow-dipping Pulaski fault. Unlike the Pulaski and Stillhouse faults, it increases stratigraphic displacement to the northeast. Projection of the Brookside Mill fault and apparent deformation in its hanging wall observed beneath the Pulaski fault in cross section might suggest deformation in the Pulaski footwall prior to its emplacement. However, I agree with both Bartholomew (1987) and Woodward and Beets (1988) that regionally speaking, the Pulaski fault ramped across a relatively undeformed footwall.

Evans Valley and Seven Springs Valley synclines

The two longest macroscopic folds in the study area are the Evans Valley syncline (14.5 km, trending 059) and the Seven Springs Valley syncline (10.5 km, trending 062), both of which are named for prominent topographic lows. They are gently northeast-plunging and noncylindrical along their axes. Both contain at least one overturned limb and are gradually positioned upright down plunge. The Seven Springs Valley syncline contains rocks as young as Jonesboro Limestone, whereas the Evans Valley syncline exposes units as young as lower Sevier Shale in its core. Several tight folds are positioned along the northwest limb of the Evans Valley syncline, denoting the large amount of shortening that occurred in the Pulaski sheet, especially near the leading edge.

Linebaugh Bend anticline

The Linebaugh Bend anticline, named for the nearby bend in the Nolichucky River, trends 058 and is positioned within the interior of the Pulaski's "S"-curve trace. It shares the northwest limb with the Evans Valley syncline, and like its neighbor, the Linebaugh Bend anticline changes from upright to overturned northeastward along strike. Dips on the overturned northwest limb of the fold average 74º SE and average 46º SE on the southeastern limb. Honaker Dolomite is the oldest unit exposed in the core, which is abruptly cut off by the Pulaski fault. A splay from the underlying Pulaski fault also truncates the southeastern limb.

Pilot Knob synclinorium

Located in the Pulaski thrust sheet and adjacent to the sinuous leading edge, the Pilot Knob synclinorium, named for a prominent ridge at the core, contains at least four major fold axial traces (two of them being nearly isoclinal with overturned northwest limbs) and is bounded on all sides by faults. The oldest unit exposed here is the Honaker Dolomite, while the youngest unit is the Conococheague Limestone, exposed in the synclinorium core. Previous mapping by Rodgers (1953b) did not recognize this structure, likely because of poor stratigraphic and structural control in this area (Fig. 3-17). The Pilot Knob synclinorium may be considered a type 3 hook pattern (Ramsay, 1962), resulting from continued folding during the same event.

I further interpret these folds in the synclinorium were likely not folded coeval with the propagating Pulaski fault, based on geometric and crosscutting relationships between the synclinorium and the Pulaski fault trace. The Pulaski's trace is oblique to

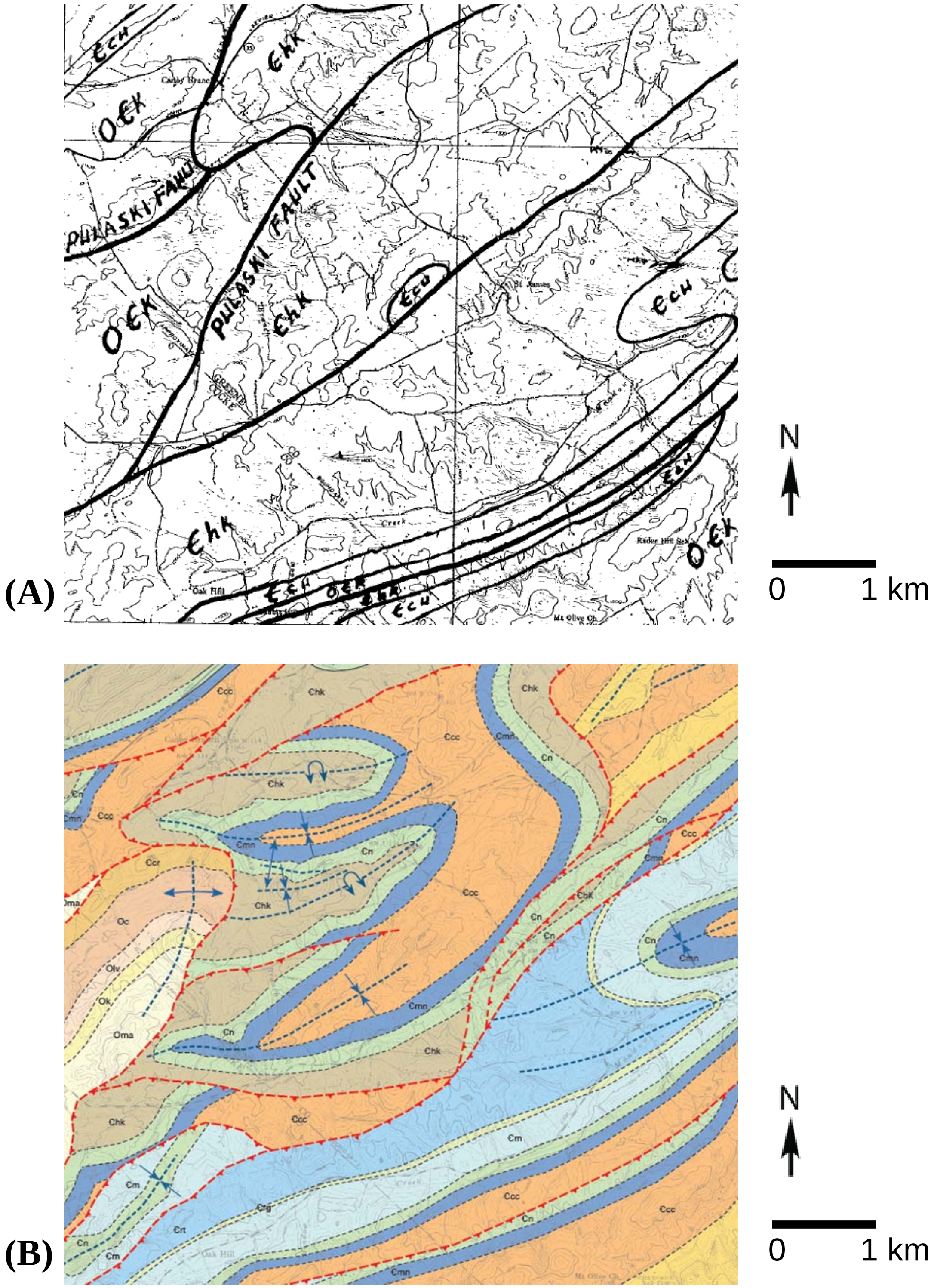

Figure 3-17. Comparison of work in (A) by Rodgers (1953b) with the results of this study (B) related to the Pilot Knob synclinorium in the Cedar Creek quadrangle. Note that Rodgers mainly mapped roadside outcrops here and was not focused on mapping to the level of detail shown in this study.

the cores of each overturned anticline and even truncates the limb of an upright syncline. These relationships suggest that the synclinorium, and perhaps other folds in the Pulaski thrust sheet, were not directly shortened by the emplacement of the Pulaski and may have been formed earlier and later passively transported.

Dunham Ridge fault

The Dunham Ridge fault, one of the major thrusts in the Pulaski thrust system, is traceable ~75 km from its northeastern terminus near the Tennessee/Virginia border to its southwestern terminus in the Neddy Mountain quadrangle (Figs. 1-2, 3-15) (Rodgers, 1953b; Hardeman et al., 1966). Like the Pulaski fault, it too is truncated by the Great Smoky fault, likely merging with the Pulaski immediately beneath the Blue Ridge sheet. Perhaps coincidentally, the majority of subdivided Honaker Dolomite is located in its hanging wall. A relatively large fault zone localized in Nolichucky Shale exists along the Dunham Ridge fault near St. James Church. This is an intensely brecciated zone with calcite-cemented tectonic breccias containing mostly dolomite/siltstone clasts (Fig. 3-13B).

Little (1969) estimated the minimum horizontal displacement of the Dunham Ridge fault to be at least 2.6 km (8,500 ft), with stratigraphic displacement averaging 1.7 km (5,500 ft). Horizontal displacement could not be determined in the study area, but it likely represents a large portion of the overall displacement in the Pulaski thrust sheet here. This is probably due to the shallow exposure and eroded portions of the frontal Pulaski thrust sheet. The Dunham Ridge fault contains the Quaker Knobs flap, similar to the Babbs Knobs flap along the main Pulaski fault, which is also attributed to post-fault folding and shallow dips of 10-20º (Little, 1969). Tight folds were observed in the Dunham Ridge thrust sheet in Little's study area, as well as in mine.

Cross Sections

Two balanced cross sections with no vertical exaggeration were created at 1:24,000 scale perpendicular to the average strike in the study area (Figs. 3-18, 3-19). Some of the basic principles that should be assumed when constructing cross sections in a foreland fold-thrust belt include: (1) no significant change in volume can occur during deformation; (2) plane strain (all deformation is parallel to the section line); (3) thickness of the units must remain constant throughout the cross section; and (4) no internal strain is involved in the units. Room problems, which exist when a void is created between units during the construction of a section, mainly arose in the cores of anticlines (e.g., Oven Creek anticline) at depth. These were resolved by the use of specific fault geometries, most of which occur as listric splays from larger floor thrusts.

Faults in the study area tend to propagate at higher angles through Knox Group formations and occasionally the Sevier Shale, although flats are also recognized at the base of the Sevier. The thinly bedded Lenoir Limestone and Rome Formation constitute the other units where flattening occurs in the cross sections. Reflecting its peculiarity, the Pulaski fault ramps through Knox carbonates, flattens across a footwall syncline and anticline of the same upper Knox units, and then ramps through mechanically weaker middle and lower Sevier Shale. The footwall here exhibits a duplex-like geometry with possible floor and roof (Pulaski fault) thrusts, and was drawn as such in A-A′ to project the exposed footwall beneath the Pulaski thrust sheet.

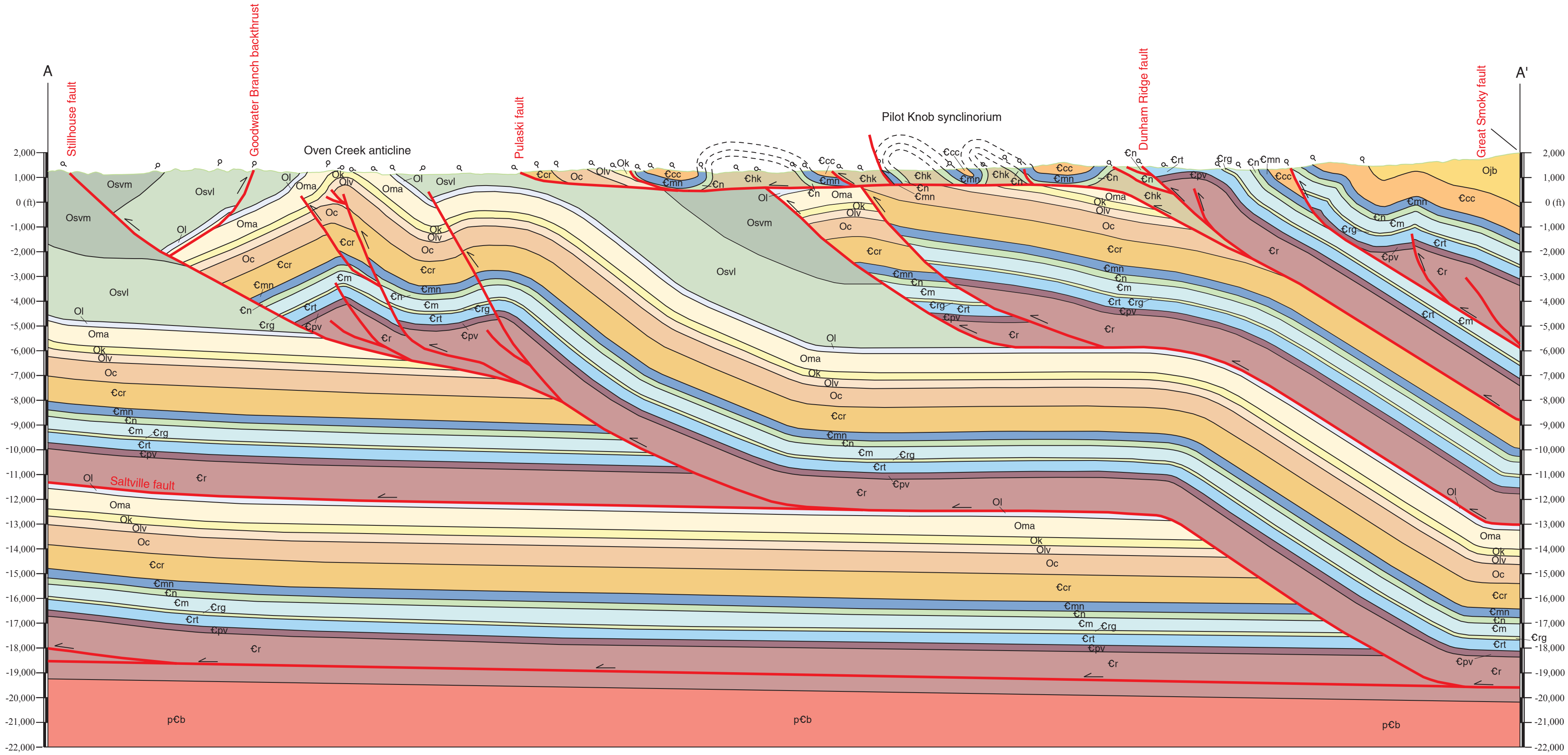

Figure 3-18. Balanced cross section along A-A′ in the study area with no vertical exaggeration (in feet). See Plate I for explanation of unit colors and abbreviations. See Plate II to view the retrodeformed section.

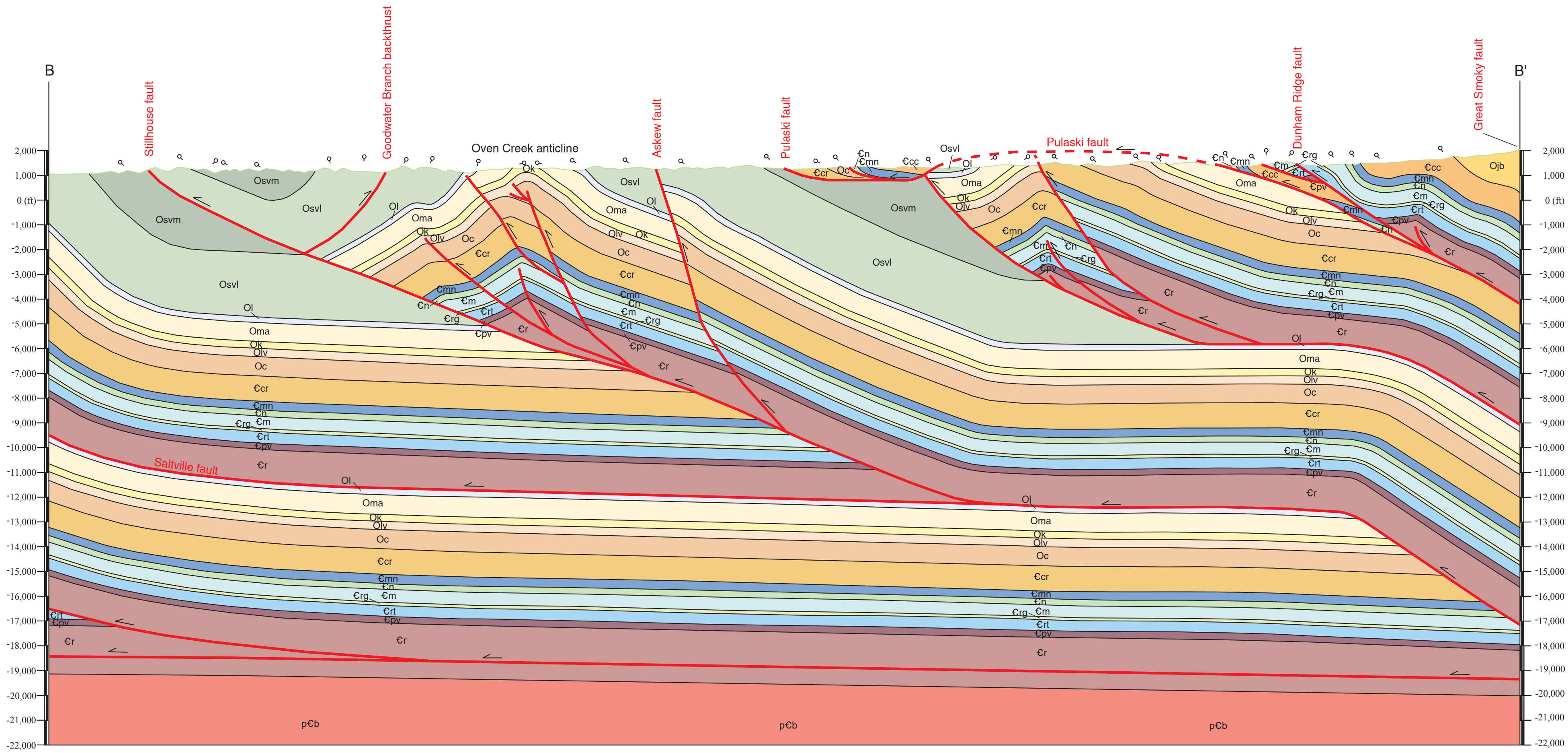

Figure 3-19. Balanced cross section along B-B′ in the study area with no vertical exaggeration (in feet). See Plate I for explanation of unit colors and abbreviations. See Plate II to view the retrodeformed section.

Cross sections were drawn in Adobe Illustrator™ CS3 and CS4. The topographic surface for each section was extracted from the four 7.5-minute topographic quadrangles of the study area using the 3D analyst tool in ArcMap™. Stratigraphic/fault contacts, fold axial traces, and bedding dips were then added from the detailed geologic map (Plate I) to interpret subsurface structures and interpolate contacts at depth. The circle or "bubble" method was utilized during construction, which aids in maintaining consistent thickness of units throughout the cross section, especially in folds. It involves drawing a perfect circle in Illustrator™ for each unit contained in the section with a diameter that equals to the unit thickness. These circles are then distributed in correct stratigraphic sequence and contacts are drawn between them. Depth to basement for the cross sections was extracted from Hatcher et al. (2007a), and refined using seismic reflection data from the Amoco 5CM-1 line in the Parrottsville quadrangle (Fig. 3-16).

Balancing cross sections was accomplished through line-length and area methods by measuring the length of the deformed layers and restoring this length to an undeformed state. The original area of the section should not have changed during deformation. The telegraphics filter tool in Illustrator™, which measures the path length of a curved line and/or the total area of a polygon, was used to maintain consistency in the original deformed section. A balanced cross section can be a useful device for obtaining accurate results, although it has been well stated that if the cross section does not balance then it cannot be acceptable, yet if the cross section does balance, then the section could possibly be correct (Dahlstrom, 1969).

Calculated minimum percent shortening from the retrodeformed sections is 74% for A-A′ and 72% for B-B′. The slightly lower value for B-B′ can be attributed to the eroded portion of the Pulaski thrust sheet not factored into the restorations. Total shortening includes both the foreshortened and retrodeformed Pulaski sheet to account for shortening prior to the emplacement of the Pulaski fault. The retrodeformed section for Stillhouse thrust sheet does not appear to balance since displacement along the Stillhouse fault increases downdip. However, the Oven Creek anticline likely accounts for much of its missing displacement.

For a comparison of regional shortening and the nature of faults at depth, a cross section was constructed across the entire Valley and Ridge (Fig. 3-20), from the southeastern edge of the Cumberland Plateau in the Pine Mountain block to the Great Smoky fault and westernmost portion of the Blue Ridge. Like the study area, major faults have ramp/flat geometries and originate from a basal décollement in the Rome Formation. Shortening of the entire section is close to 50%, which is typical in the Valley and Ridge foreland fold-thrust belt (compare with sections in Hatcher, 1989; Hatcher et al., 2007a; and Hatcher and Geiser, 2010).

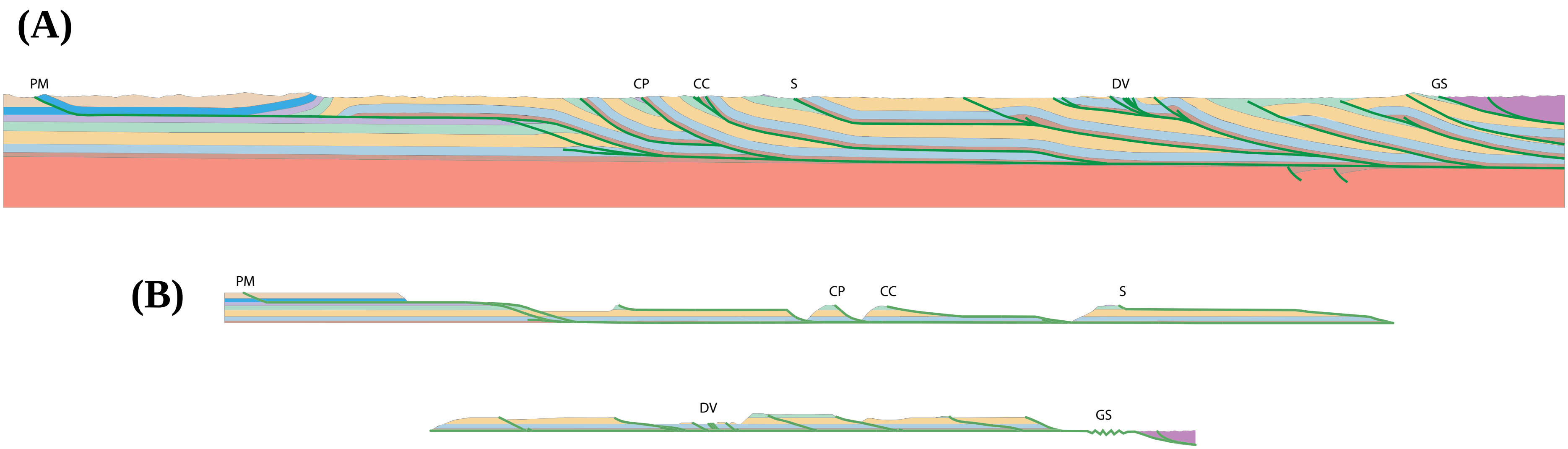

Figure 3-20. (A) Balanced cross section through the southern Appalachian Valley and Ridge from the Pine Mountain block to the Great Smoky fault and westernmost portion of the Blue Ridge province. Section does not include the Pulaski fault. (B) Retrodeformation of (A), split into three segments. Light tan-Pennsylvanian sandstones; Dark blue-Mississippian carbonates and Pennington formation; Light purple-Silurian, Devonian, and Mississippian undivided; Light green-Chickamauga Group and Upper Ordovician undivided; Yellow-Knox Group; Light blue-Conasauga Group; Reddish brown-Rome Formation; Dark green-Ocoee Supergroup; Salmon-Middle Proterozoic basement. Faults (green lines) are labeled: PM-Pine Mountain thrust; CP-Clinchport fault; CC-Copper Creek fault; S-Saltville fault; DV-Dumplin Valley fault; GS-Great Smoky fault.

CHAPTER IV

INTERPRETATION OF DEFORMATIONAL HISTORY

Overview of Pulaski Thrust Sheet Deformation

Several unique characteristics of the Pulaski thrust sheet in northeastern Tennessee and southwestern Virginia promote interpretations of deformational history that are atypical to other Valley and Ridge thrust sheets. Because of the great extent and displacement of the Pulaski sheet, these interpretations are significant regarding the timing and emplacement of large thrust sheets in the central and southern Appalachian fold-thrust belt. When comparing the Pulaski thrust sheet at its southwestern terminus with other areas to the immediate northeast and into Virginia, a common argument for distinct phases of deformation exist within a single Alleghanian event. Stratigraphic relationships, especially in the study area, may play an important role in recording these different phases.

In particular, a change in the nature and orientation of folds on both sides of the Pulaski fault in the study area may indicate at least two phases of deformation/folding. One of the best methods in determining multiple folding phases involves examining the fold geometry of outcrop patterns on geologic maps and/or at the mesoscopic scale (Hatcher, 1995). Because superposed folds in the field are rarely observed in this study area, separate and distinct fold orientations and folding styles can be used to suggest, but not confirm, multiple deformation episodes. Roeder and Witherspoon (1978) observed and interpreted uncommonly “warped,” or refolded thrust sheets and folded fault structures near the Cumberland Escarpment in the western Valley and Ridge. They defined this specific type of polyphase deformation, which strongly parallels deformation observed in the Pulaski thrust sheet, as movement during kinematically and/or geologically distinct time intervals with westward advancing tectonic activity.

Deformation in the Study Area and Northeast Tennessee

Major folds in the study area, specifically the Evans Valley syncline, Seven Springs syncline, and Linebaugh Bend anticline, exhibit a highly asymmetrical and shallowing axial surface along strike (Fig. 3-14), comparable to observations by Roeder and Witherspoon (1978). The most noteworthy structure in the area however, regarding interpretations for Pulaski deformation, is the Pilot Knob synclinorium in the Cedar Creek quadrangle (Fig. 3-17; Plate I). As discussed in Chapter III, this structure is interpreted as a refold and possibly a type 3 hook pattern, based on map patterns and cross sections (Fig. 3-17).

In map view, the shallow Pulaski fault trace transects the Pilot Knob synclinorium, oblique to the core of each overturned anticline, and also truncates the limb of an upright syncline. Qualitatively, these occurrences imply that folding, at least in my area, was not generated during propagation of the Pulaski fault. Thus, earlier stages of folding were likely overprinted by another stage, creating the numerous asymmetrical tight and overturned folds, complex folding patterns, thrust faults that misleadingly display younger strata on older strata, and axial-planar cleavage documented in the study area. The geometric relationships of the Pulaski fault and the characteristics of the Pilot Knob synclinorium may suggest evidence for a lateral/oblique ramp in the southwestern portion of the Cedar Creek quadrangle. At fault-related fold terminations, lateral/oblique ramps are exemplified by steeply plunging folds and hanging wall cutoff lines trending at high angles to fault strike (Wilkerson et al., 2002).

Both Byerly (1966) and Little (1969) also noted the contrast in folding styles on each side of the Pulaski fault, which was originally documented by Rodgers (1953b) and Hardeman et al. (1966) in the study area. Byerly interpreted the discrepancy to represent foreshortening by the Pulaski fault, with the folds in the hanging wall having been palinspastically closer to the stress source. Little (1969) mapped several very tight to isoclinal folds in the Dunham Ridge (Pulaski) thrust sheet, most averaging only ~1-2 km in width. He interpreted some of these folds to represent pre-fault folding. Most folds, he concluded, occurred contemporaneously with faulting and were later tightened by post-fault folding. The shallow-dipping Babbs Knobs flap near Greeneville, Tennessee, and the Quaker Knobs flap, near Rheatown, Tennessee, are both interpreted to have formed by post-emplacement folding of the Pulaski fault. Likewise, irregularities of the Pulaski fault trace in the study area are clearly attributed to low dip and post-emplacement folding.

Footwall deformation beneath the Pulaski thrust sheet is most evident near the "S"-curve trace. In cross sections through the area (Figs. 3-18, 3-19), a portion of the footwall, with the Brookside Mill fault serving as a local detachment, exhibits a duplex-like geometry with possible floor and roof (Pulaski fault) thrusts. Woodward and Gray (1985) constructed cross sections that showed the Pulaski fault being folded by footwall duplex horses. Although eroded, the Pulaski fault shown in B-B′ (Fig. 3-19) may exhibit a slight but similar behavior. Whether or not some of the deformation observed in the footwall formed prior to emplacement of the Pulaski cannot be determined here and has been debated in other parts of the thrust sheet as well (Bartholomew et al., 1989).

Comparisons with Southwestern Virginia

Although no chronology of multiple deformation episodes has been established thus far in the Pulaski thrust sheet in northeastern Tennessee, this process has been recognized in parts of southwestern Virginia, particularly in the Roanoke recess. Bartholomew (1987) recognized at least five distinctive stages of the Pulaski thrust sheet deformation here based on crosscutting relationships: (1) deformation occurring before ramping out of the Rome Formation and lower detachments; (2) deformation as the Pulaski thrust sheet ramped across Cambrian-Ordovician strata to décollements in Mid-to-Upper Ordovician shales; (3) deformation as the sheet ramped to flats in the Devonian shales; (4) deformation as the sheet ramped across uppermost Devonian to Mississippian rocks to reach flats in the Price Formation (along the Catawba fault in the fault system) and Maccrady Formation (along the main Pulaski fault); and (5) deformation of the coupled Pulaski/Saltville sheet. The ramp zone had to cut across the entire stratigraphic section to expose older units, such as in the Price Mountain window (Fig. 3-10).

Bartholomew (1987) referred to a large region of the Pulaski sheet that displays highly deformed folds and tectonic breccias as the "complexly deformed plate" (Fig. 3-10). This region is more or less equivalent to the complex folds and faults of the Pulaski sheet observed in the study area. High values of percent shortening (85-90%) were calculated by Bartholomew (1987) for the Pulaski thrust sheet in the recess, similar to high values (~73%) from northeast Tennessee (Roeder and Witherspoon, 1978; this study). This value from the study area, although identical to that of Roeder and Witherspoon, encompasses parts of the Saltville thrust sheet, because the Pulaski sheet is less extensive near the terminus.

One useful means by which Bartholomew's deformation sequence was established involves the 300-500 m-thick "broken formation" of Schultz (1983), a zone of intense deformation in the complexly deformed plate that contains the Max Meadows tectonic breccia. Broken formations frequently develop beneath a detachment, possibly under high pore fluid pressure (Hatcher, 1995). The complexly deformed folds, faults, and breccias observed in the formation were interpreted by Schultz (1983, 1986) and Gibson and Gray (1985) to have developed continuously along with ramping of the Pulaski fault. This was supported by similar fold orientations measured in both footwall and hanging-wall carbonates, as well as the incorporated broken formation (Schultz, 1983). In contrast, Bartholomew (1987) interpreted the broken formation as a lower-level décollement zone that largely formed during an earlier Alleghanian stage, prior to ramping of the Pulaski fault. It was then passively transported and affected by subsequent Alleghanian deformation, similar to other stratigraphic units carried in the thrust sheet. Bartholomew further asserted that footwall deformation took place after the Pulaski reached upper detachments/flats in Mississippian strata, insinuating that similar fold orientations in footwall/hanging wall rocks and the broken formation (Schultz, 1983) reflect later Alleghanian deformation post-ramping of the Pulaski.

Prior to work by Bartholomew and Schultz (1980) and Bartholomew (1987), Reks and Gray (1983) determined a deformation sequence for folds and cleavage in the Pulaski sheet near Abingdon and Marion, Virginia, by calculating the amount of time and strain needed to form these structures. They concluded that cleavage and folding here must have formed at different stages of the same event. Like the Pulaski thrust sheet in northeastern Tennessee, Reks and Gray noted that the most well-developed cleavage occurs adjacent to thrust faults and the cores of regional folds. Curiously, a portion of the Pulaski sheet contains relatively lower average strains, although compared to other parts of the thrust sheet, its folds are tighter and many are overturned. Pronounced tightness of folds, anomalously low strain values, and dissimilar mechanical behavior of rocks suggest that this portion of the thrust sheet formed earlier and possibly deeper. Conditions of high pore fluid pressure could have reduced frictional strength and caused these early stages of shortening (Davis et al., 1983; Reks and Gray, 1983). Reks and Gray also stated that cleavage must have been superposed onto the axial surfaces of previously formed Class 3 buckle folds. Timing of fault propagation, along with cleavage/penetrative strain development, would therefore be later than folding in certain parts of the Pulaski thrust sheet.

Bartholomew and Whitaker (2010) developed a model for the Alleghanian deformational sequence in the Roanoke recess and projected the orientation of the Pulaski thrust sheet at different stages on a regional scale (Fig. 4-1). Five distinct orientations were determined by structural measurements in southwestern Virginia from joint sets, clastic dikes, and layer-parallel shortening (LPS)/total strain. Timing of each stage was supported by relating the fracture sets to specific southern and central Appalachian macroscopic structures, with the general assumption that central Appalachian structures formed prior to southern Appalachian structures (Whitaker and Bartholomew, 1999; Bartholomew and Whitaker, 2010). The Appalachian-wide stress field is presented in

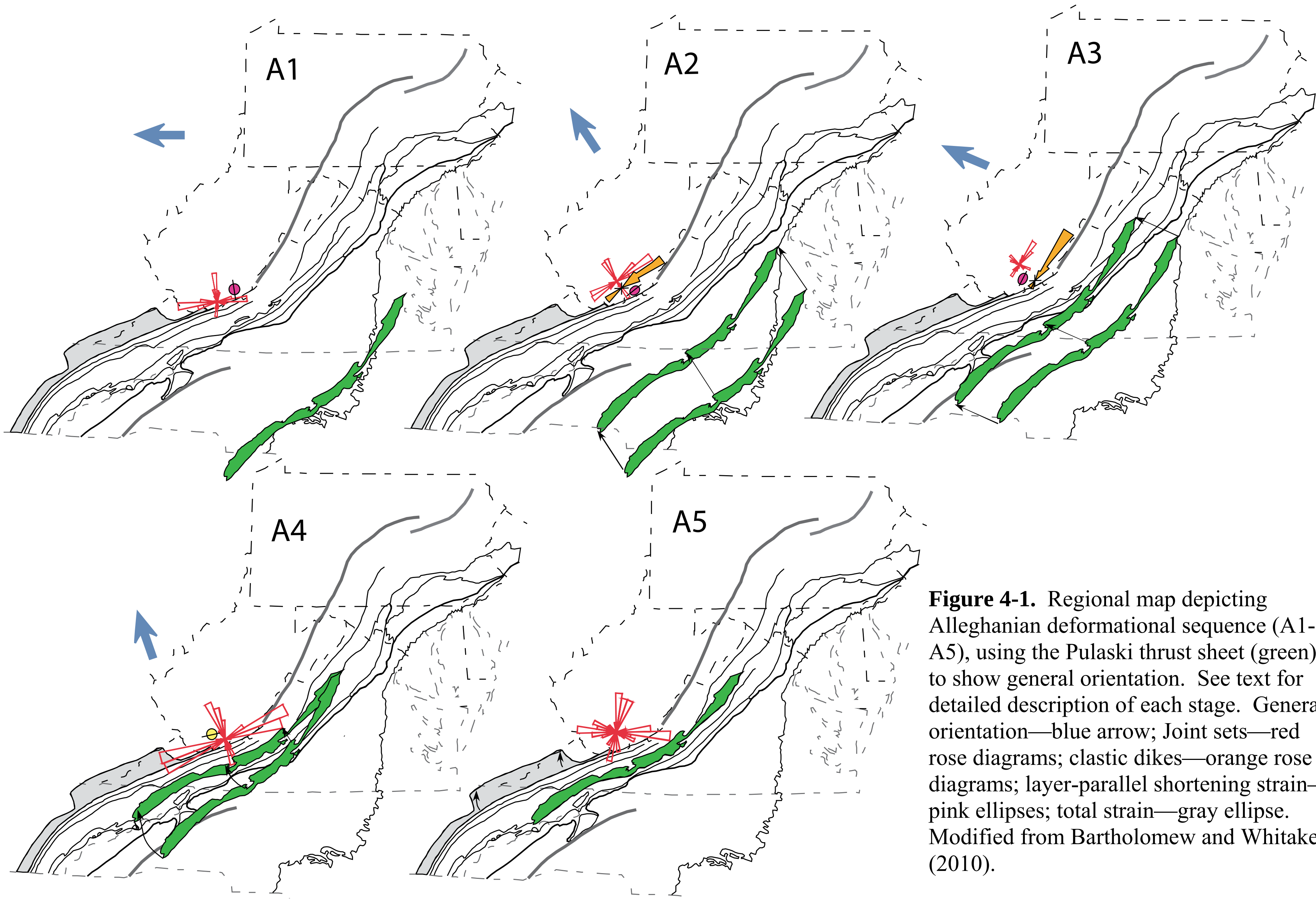

Figure 4-1. Regional map depicting Alleghanian deformational sequence (A1-A5), using the Pulaski thrust sheet (green) to show general orientation. See text for detailed description of each stage. General orientation—blue arrow; Joint sets—red rose diagrams; clastic dikes—orange rose diagrams; layer-parallel shortening strain—pink ellipses; total strain—gray ellipse. Modified from Bartholomew and Whitaker (2010).

the A1 stage, shown by early east-west-directed shortening, probably during the late Mississippian or early Pennsylvanian (Bartholomew and Whitaker, 2010). At this time, movement of the Pulaski thrust sheet had not yet begun. A2 exhibits a dominant northwest-southeast trend and began the movement of the Pulaski thrust sheet. Bartholomew and Whitaker assigned this set of orientations to the "Princeton event" (similar to ages of A1 and A2), which preceded both the central and southern Appalachian structural trends in the Valley and Ridge. The more easterly directed shortening in A3 formed most central Appalachian structures, while the clockwise rotation of shortening in A4 (now north-northwest) produced most southern Appalachian structures. The Princeton event in A2, and possibly part of A3, may be correlative with the late Mississippian to Pennsylvanian Lackawanna phase of Geiser and Engelder (1983). A4 then signifies the final emplacement of the Pulaski thrust sheet. Both this stage and A2/A3 (Lackawanna phase equivalent) also coincides with the zipper tectonic model (Hatcher, 2002), in which clockwise rotation and head-on collision of Gondwana with Laurentia occurred in the southern Appalachians. The last set of orientations, A5, may be related to deformation during emplacement of the Pine Mountain thrust sheet and is not expressed in the Pulaski thrust sheet (Bartholomew and Whitaker, 2010).

Lackawanna and Main Phases

In part of the central and New England Appalachian foreland, Geiser and Engelder (1983) recognized two discrete, but likely diachronous, non-coaxial phases (or pulses) of Alleghanian deformation—the late Mississippian to Pennsylvanian Lackawanna phase and the late Pennsylvanian to Early Permian main phase (Fig. 4-2).

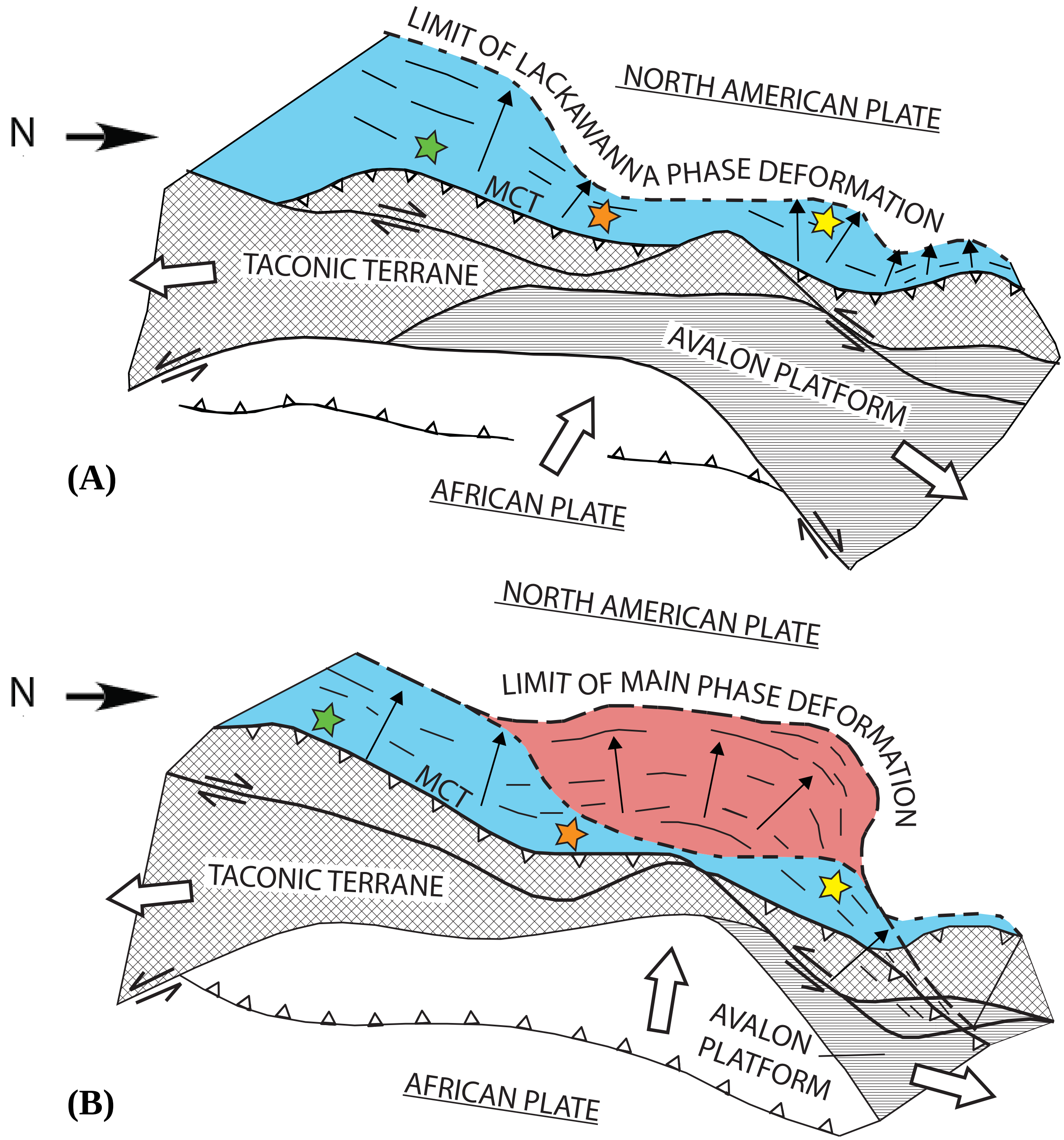

Figure 4-2. Generalized tectonic sketch of the (A) Lackawanna (Pennsylvanian) and (B) Main (Permian) phases of the Alleghanian orogeny showing relative displacement directions (white arrows) for the African plate and Taconic/Avalon terranes. Foreland shortening directions (black arrows) were derived from fold/fault data and LPS fabrics. Green star-NE TN study area; Orange star-Roanoke recess; Yellow star-Lackawanna synclinorium; MCT-main crystalline thrust. Early left-lateral motion depicted on the western margin of the Avalon platform was derived from McMaster et al. (1980). Modified from Geiser and Engelder (1983).

The Lackawanna phase is considered to have involved a significant strike-slip component, while the main phase, which caused the bulk of southern Appalachian foreland deformation, represents the final collision of Gondwanan terranes with Laurentia. Geiser and Engelder documented these phases with evidence for tectonic overprinting in the Lackawanna synclinorium of the Pennsylvania Valley and Ridge and Plateau. A distinct set of structural trends from mostly LPS fabrics (detachment faults, pressure solution cleavage, joints), interpreted as the Lackawanna phase, are crossed by a later (main) phase of the Alleghanian orogeny.

Early deformation recorded by the Pulaski thrust sheet in the study area and other parts in northeast Tennessee and southwestern Virginia may be a manifestation the Lackawanna phase. Several folds in the thrust sheet (e.g., Pilot Knob synclinorium) could have been initially deformed prior to emplacement of the Pulaski fault during this phase. Later propagation of the fault and dominant northwestward-directed folding of the thrust sheet during the main phase could have produced the tight to overturned and highly noncylindrical folding observed here. Although these phases were recognized a considerable distance away, the deformational history of the study area seems to coincide with the timeframe documented by Geiser and Engelder (1983).

A similar succession of deformation phases was documented by Dean et al. (1988) in southeastern West Virginia, where an early “structural event” with distinct orientations was superposed by a later set of orientations. This led them to agree with Rodgers’ (1970b) assessment that, generally speaking, central Appalachian structures postdate southern Appalachian structures. However, this view was countered by Whitaker and Bartholomew (1999) and Bartholomew and Whitaker (2010) from work in the Glen Lyn syncline, a southern Appalachian fold, near the central/southern Appalachian transition. From overprinting LPS fabric data, they concluded that the more likely scenario was the initiation of central Appalachian deformation prior to formation of the Glen Lyn syncline. This scenario agrees with the zipper tectonic model for the Alleghanian orogeny (Hatcher, 2002), which involves progressively southward Alleghanian deformation.

In contrast to Geiser and Engelder's (1983) conclusions about the Lackawanna synclinorium and the phases observed, Harrison et al. (2004) interpreted part of the synclinorium to be a collapse structure, nullifying any crosscutting relationships of structural trends there. This implies that at least the northwestern trend of the upper half of the synclinorium (the collapse structure) does not represent a discrete east-west shortening event observed by Geiser and Engelder (1983). However, the matching symmetry of the upper portion to other structures outside of the synclinorium seems to still suggest an earlier deformation episode.

Nevertheless, the Lackawanna synclinorium was likely not affected by discrete phases, but rather by pulses of deformation combined with overburden collapse during a continuous event (Harrison, 2006). All deformation in the fold-thrust belt of the Valley and Ridge should still be attributed to a single event (Hatcher, 1989). I agree with the conclusion by Harrison (2006) that the Lackawanna and main phases are simply pulses of shortening during the Alleghanian orogeny with a change in shortening direction through time. Although this conclusion does not fully contradict previous work from Geiser and Engelder (1983), shortening caused by distinct changes in orientation during a continuous event is more probable.

Deformation Discussion

Perhaps the most logical explanation for the style of folding in the Pulaski thrust sheet of northeast Tennessee, also considered by Byerly (1966), is that these folds, formed prior to faulting, were palinspastically closer to the stress source (i.e., Blue Ridge-Piedmont megathrust sheet) than folds of the adjacent Saltville thrust sheet. Thus, the tight folds observed here are expected in strata positioned nearest to the source. However, geometric and crosscutting relationships along parts of the Pulaski thrust sheet in this area and in southwestern Virginia suggest some hanging wall, and possibly footwall, deformation prior to emplacement of the thrust sheet. The relatively high values of the percent shortening in the Roanoke recess (85-90%) and the study area (74%) reflect this first stage deformation, and both values are strongly similar when evaluated against the entire Valley and Ridge (~50%). This implies that the shortening/deformation affecting the Pulaski sheet in my study area in northeast Tennessee is reasonably comparable to the Pulaski sheet of the Roanoke recess.

Deformation observed in the Pulaski thrust sheet in my study area, particularly type 3 interference patterns, likely represent small changes in orientation of continued shortening, similar to those in Figure 4-1. The initial deformation may be a manifestation of the late Mississippian to Pennsylvanian Lackawanna phase. Stages A2 and possibly A3 correspond well with this phase, while A4 likely represents the late Pennsylvanian to Early Permian main phase of the Alleghanian orogeny. Even if the Lackawanna phase, as suggested by Harrison (2006), is not considered a discrete episode of Alleghanian orogenesis, early deformation in my study area could still be a manifestation of this phase. However, orientations at different stages of deformation from work done in the

Roanoke recess and northern Pennsylvania/New York may not have a direct correlation to the Pulaski thrust sheet in my study area, since shortening direction and location of continental margins were probably a factor over the duration of the Alleghanian orogeny. Multistage deformation observed in one portion of the Pulaski thrust sheet cannot be assumed to be applicable to the entire thrust sheet.

Stratigraphic relationships in my study area may have aided in the recording for much of the alleged early deformation in the Pulaski sheet, because the thrust sheet here contains predominantly weak Conasauga shales and carbonates sandwiched between more competent Knox carbonates. As discussed in Chapter III, structural styles can be largely controlled by stratigraphic variations (Woodward et al., 1988). This concoction of rheologically different rocks made it possible to more clearly view and interpret the complex folding. Had the entire thrust sheet consisted of entirely thick carbonates or incompetent shales, folding styles and/or polyphase deformation would not be as readily distinguished. In a similar fashion, stratigraphy largely aided interpretations of the deformational history of the complexly deformed plate in the Roanoke recess (Schultz, personal comm.).

A complete picture of the displacement and hanging wall/footwall deformation are obscured by the shallow dip of the Pulaski fault and the proximity to its terminus. Although polyphase deformation occurring here is very likely, a large amount of folding that occurred coevally with the emplacement of the Pulaski fault clearly took place, as indicated by mesoscopic bedding, cleavage, and available folding measurements from the study area.

CHAPTER V

CONCLUSIONS

1) At its southwestern terminus, the Pulaski fault is overridden by the thin-skinned Great Smoky fault in the Neddy Mountain 7.5-minute quadrangle, ~5 km (3 miles) south of Parrottsville, Tennessee. The location of the terminus delineated in this study is close to the terminus mapped by Rodgers (1953b; 1970a) and compiled by Hardeman et al. (1966).

2) The Pulaski thrust sheet acts as a stratigraphic break and contains distinct facies of Conasauga and Knox Groups that contrast with the same units in other Valley and Ridge thrust sheets to the northwest (Rodgers, 1953a). Limestone dominates the Knox Group in the Pulaski sheet, whereas dolomite and more clearly identifiable chert and sandstone stratigraphic markers are more abundant in the Saltville sheet. In contrast, Conasauga Group rocks consist of more dolomite in the Pulaski sheet versus more limestone and shale in the Saltville sheet. An abundance of limestone in the Knox Group immediately northwest of the Pulaski fault may imply that these units in the footwall rest on or near the transition between northwestern and southeastern facies.

3) Honaker Dolomite was successfully subdivided in parts of the Pulaski thrust sheet in the study area. This is based on identification of the thin to a featheredge of Rogersville Shale, which varies from 0-26 m (0-85 ft) in the study area. Where no Rogersville was observed, the unit was mapped as Honaker Dolomite.

4) The Pulaski fault has a very low dip, ranging from subhorizontal to 20° near the surface, and steepens near its junction with the Dunham Ridge fault. Stratigraphic displacement progressively increases southward along the Pulaski trace and reaches up to at least 1.4 km (4,500 ft) in the study area. Horizontal displacement is at least 23.8 km (14.8 mi) with approximately 30% shortening within the Pulaski thrust sheet. When comparing percent shortening to the entire Valley and Ridge (~50%), the relatively high values calculated in the study area (72-74%) and the Roanoke recess (85-90%; Bartholomew, 1987) are very similar.

5) The nature and orientation of macroscopic folds in the Pulaski thrust sheet strongly contrast with those in the adjacent Saltville thrust sheet. Complex tight to overturned and highly noncylindrical folds are present in the Pulaski sheet, many of them exhibiting a type 3 interference pattern. The Saltville sheet contains broad and mostly open folds, typical of buckle folding in thick Knox Group carbonates. These folds formed prior to faulting and palinspastically closer to the source of deformation (i.e., Blue Ridge-Piedmont megathrust sheet). The close proximity could have created several of the tight folds observed here.

6) At least two phases of Alleghanian deformation/folding may have been recorded here in the Pulaski thrust sheet, similar to interpretations of the Pulaski sheet in southwestern Virginia (Bartholomew and Schultz, 1980; Bartholomew, 1987; Reks and Gray, 1983; Bartholomew and Lewis, 2010; Bartholomew and Whitaker, 2010). In the study area, geometric and crosscutting relationships of certain structures (e.g., Pilot Knob synclinorium) imply that folding was not generated during propagation of the Pulaski fault. An earlier stage of folding, possibly equivalent to the late Mississippian to Pennsylvanian Lackawanna phase (Geiser and Engelder, 1983), was likely overprinted by the main phase of Alleghanian deformation, creating the complex fold patterns seen in the study area. Parallel comparisons to the "complexly deformed plate" in the Roanoke recess further support an argument for at least two distinct phases of deformation within a single Alleghanian event.

Outstanding Issues

Complex fold patterns and fault-fold relationships near the Pilot Knob synclinorium in the Cedar Creek quadrangle could be attributed to a lateral/oblique ramp underlying this area. This type of ramp is briefly discussed in Chapter IV, but may be significant towards the kinematic interpretation and deformational history of the Pulaski fault in the study area. Cross sections from this study show the Pulaski fault cutting downsection in the Knox Group and Sevier Shale, violating conventional rules for cross section construction in fold-thrust belts. Out-of-sequence thrusting of the Pulaski fault or the possibility of a lateral/oblique ramp in the study area may have contributed to its atypical geometry.

REFERENCES CITED

Andrews, L.M., and Railsback, L.B., 1997, Controls on stylolite development: morphologic, lithologic, and temporal evidence from bedding-parallel and transverse stylolites from the U.S. Appalachians: The Journal of Geology, v. 105, p. 59-73.

Bally, A.W., Gordy, P.L., and Stewart, G.A., 1966, Structure, seismic data, and orogenic evolution of southern Canadian Rocky Mountains: Bulletin of Canadian Petroleum Geology, v. 14, p. 337-381.

Barnaby, R.J., and Read, J.F., 1990, Carbonate ramp to rimmed shelf evolution: Lower to Middle Cambrian continental margin, Virginia Appalachians: Geological Society of America Bulletin, v. 102, p. 391-404.

Bartholomew, M.J., 1987, Structural evolution of the Pulaski thrust system, southwestern Virginia: Geological Society of America Bulletin, v. 99, p. 491-510.

Bartholomew, M.J., and Lewis, S.E., 2010, Orphans of the far-traveled Pulaski thrust sheet: Exotic detached duplexes and their implications for original fold-and-thrust geometry, *in* Tollo, R.P., Bartholomew, M.J., Hibbard, J.P., and Karabinos, P.M., eds., From Rodinia to Pangea: the lithotectonic record of the Appalachian region: Geological Society of America Memoir 206, p. 417-430.

Bartholomew, M.J., and Schultz, A.P., 1980, Deformation in the hanging wall of the Pulaski thrust sheet near Ironto, Montgomery County, Virginia, *in* Geologic structure and hydrocarbon potential along the Saltville and Pulaski thrusts in southwestern Virginia and northeastern Tennessee: Virginia Division of Mineral Resources Publication 23, part B, sheet 3.

Bartholomew, M.J., and Whitaker, A.E., 2010, The Alleghanian deformational sequence at the foreland junction of the central and southern Appalachians, *in* Tollo, R.P., Bartholomew, M.J., Hibbard, J.P., and Karabinos, P.M., eds., From Rodinia to Pangea: the lithotectonic record of the Appalachian region: Geological Society of America Memoir 206, p. 431-454.

Bartholomew, M.J., Milici, R.C., and Schultz, A.P., 1980, Regional structure and hydrocarbon potential, *in* Geologic structure and hydrocarbon potential along the Saltville and Pulaski thrusts in southwestern Virginia and northeastern Tennessee: Virginia Division of Mineral Resources Publication 23, part A, sheet 1.

Bartholomew, M.J., Schultz, A.P., Woodward, N.B., and Beets, J.W., 1989, Critical evidence for southern Appalachian Valley and Ridge thrust sequence: Discussion and reply: Geological Society of America Bulletin, v. 101, p. 1103-1104.

Boyer, S.E., and Elliott, D., 1982, Thrust systems: American Association of Petroleum Geologists Bulletin, v. 66, p. 1196-1230.

Bridge, J., 1955, Disconformity between the Lower and Middle Ordovician series at Douglas Lake, Tennessee: Geological Society of America Bulletin, v. 66, p. 725-730.

Bridge, J., and Hatcher, R.D., Jr., 1973, Geologic map of the New Market quadrangle, Tennessee: Tennessee Division of Geology Geologic Map GM-155-SE, scale 1:24,000.

Brokaw, A.L., Dunlap, J.C., and Rodgers, J., 1966, Geology and mineral deposits of the Mosheim and Johnson anticlines, Greene County, Tennessee: U.S. Geological Survey Bulletin v. 1222-A, p. A1-A21.

Bucher, W.H., 1956, Role of gravity in orogenesis: Geological Society of America Bulletin, v. 67, p. 1295-1318.

Bultman, J.G., 2005, Stratigraphic, structural, and tectonic analysis of a portion of the Sevier-Blountian and Martinsburg basins, Bays Mountain synclinorium, northeast Tennessee [M.S. thesis]: Knoxville, University of Tennessee, 176 p.

Bumgarner, J.G., Houston, P.K., Ricketts, J.E., and Wedow, H., Jr., 1964, Habit of the Rocky Valley thrust fault in the west New Market area, Mascot-Jefferson City zinc district, Tennessee: U.S. Geological Survey Professional Paper 501-B, p. 112-115.

Butts, C., 1926, The Paleozoic rocks, *in* Adams, G.I., Butts, C., Stephenson, L.W., and Cooke, W., eds., Geology of Alabama: Alabama Geological Survey Special Report No. 14, p. 41-230.

Butts, C., 1940, Geology of the Appalachian Valley in Virginia, part 1, Geologic text and illustrations: Virginia Geological Survey Bulletin 52, part 1, 568 p.

Butts, C.W., 1933, Geologic map of the Appalachian Valley of Virginia with explanatory text: Virginia Geological Survey Bulletin, v. 42, scale 1:62,500.

Byerly, D.W., 1966, Structural geology along a segment of the Pulaski fault, Greene County, Tennessee [Ph.D. dissert.]: Knoxville, University of Tennessee, 94 p.

Byrd, W.J., Weinberg, E.L., and Yochelson, E.L., 1973, Salterella in the Lower Cambrian Shady Dolomite of southwestern Virginia: American Journal of Science, v. 273A, p. 252-260.

Campbell, M. R., 1925, The Valley coal fields of Virginia: Virginia Geological Survey Bulletin 25, 322 p.

Campbell, M.R., 1894, Estillville folio: U.S. Geological Survey Geologic Atlas, no. 12, scale 1:125,000.

Campbell, M.R., 1897, Tazewell folio: U.S. Geological Survey Geologic Atlas, no. 44, scale 1:125,000.

Campbell, M.R., 1899, Bristol folio: U.S. Geological Survey Geologic Atlas, no. 59, scale 1:125,000.

Cattermole, J.M., 1958, Geologic map of the Knoxville quadrangle, Tennessee: U.S. Geological Survey Geological Quadrangle Map GQ-115.

Chapple, W. M., 1978, Mechanics of thin-skinned fold-and-thrust belts: Geological Society of America Bulletin, v. 89, p. 1189-1198.

Cooper, B. N., 1938, Duality of the Pulaski fault in the type locality (abs.): Proceedings of the Geological Society of America for 1938, p. 74.

Cooper, B.N., 1936, Stratigraphy and structure of the Marion area, Virginia: Virginia Geological Survey Bulletin, v. 46, p. 133-163.

Cooper, B.N., 1939, Geology of the Draper Mountain area, Virginia: Virginia Division of Mineral Resources Bulletin, v. 25, 98 p.

Cooper, B.N., 1970, The Max Meadows breccias: A reply, *in* Fisher, G.W., Pettijohn, F.J., Reed, J.C., Jr., and Weaver, K.N., eds., Studies of Appalachian geology: Central and southern: New York, Interscience Publishers, p. 179-191.

Cooper, B.N., and Cashion, W.W., 1970, Relation of the Pulaski and Seven Springs faults in southwestern Virginia: American Journal of Science, v. 268, p. 385-396.

Cooper, B.N., and Haff, J.C., 1940, Max Meadows fault breccia: Journal of Geology, v. 48, p. 945-974.

Couzens, B.A., and Dunne, W.M., 1994, Displacement transfer at thrust terminations: the Saltville thrust and Sinking Creek anticline, Virginia, U.S.A.: Journal of Structural Geology, v. 16, p. 781-793.

Cummings, D., 1962, Geology of the Bays Mountain synclinorium, northeast Tennessee [Ph.D. dissert.]: East Lansing, Michigan State University, 152 p.

Cummings, D., 1965, Stratigraphy and heavy minerals of the Bays Formation, Bays Mountain synclinorium, northeast Tennessee: Geological Society of America Bulletin, v. 76, p. 591-600.

Currie, J. B., Patnode, H. W., and Trump, R. P., 1962, Development of folds in sedimentary strata: Geological Society of America Bulletin, v. 73, p. 655-674.

Dahlstrom, C.D.A., 1969, Balanced cross sections: Canadian Journal of Earth Sciences, v. 6, p. 743-757.

Davis, D., Suppe, J., and Dahlen, F.A., 1983, Mechanics of fold-and-thrust belts and accretionary wedges: Journal of Geophysical Research, v. 88, p. 1153-1172.

Dean, S.L., Kulander, B.R., and Skinner, J.M., 1988, Structural chronology of the Alleghanian orogeny in southeastern West Virginia: Geological Society of America Bulletin, v. 100, p. 299-310.

Drake, A.A., Jr., Sinha, A.K., Laird, J., and Guy, R.E., 1989, The Taconic orogen, *in* Hatcher, R.D., Jr., Thomas, W.A., and Viele, G.W., eds., The Appalachian-Ouachita Orogen in the United States: Boulder, Colorado, Geological Society of America, The Geology of North America, v. F-2, p. 107-177.

Elliott, D., 1976, The motion of thrust sheets: Journal of Geophysical Research, v. 81, p. 949-963.

Epstein, A.G., Epstein, J.B., and Harris, L.D., 1977, Conodont color alteration: an index to organic metamorphism: U.S. Geologic Survey Professional Paper 995, 27 p.

Evans, M.A., and Dunne, W.M., 1991, Strain factorization and partitioning in the North Mountain thrust sheet, central Appalachians, U.S.A.: Journal of Structural Geology, v. 13, p. 21-35.

Feder, G., 1963, The geology of the Oak Grove area, Jefferson County, Tennessee [M.S. thesis]: Knoxville, University of Tennessee, 30 p.

Foreman, J.L., 1991, Petrologic and geochemical evidence for water-rock interaction in the mixed carbonate-siliciclastic Nolichucky Shale (Upper Cambrian) in East Tennessee [Ph.D. dissert.]: Knoxville, University of Tennessee, 228 p.

Geiser, P.A., and Engelder, T., 1983, The distribution of layer parallel shortening fabrics in the Appalachian foreland of New York and Pennsylvania: Evidence for two non-coaxial phases of the Alleghanian orogeny: Geological Society of America Memoir 158, p. 161-175.

Gibson, R.G., and Gray, D.R., 1985, Ductile-to-brittle transition in shear during thrust sheet emplacement, southern Appalachian thrust belt: Journal of Structural Geology, v. 7, p. 513-525.

Greene, R.C., 1959, The geology of English Mountain and vicinity, Cocke, Jefferson and Sevier Counties, Tennessee [M.S. thesis]: Knoxville, University of Tennessee, 54 p.

Gwinn, V.E., 1964, Thin-skinned tectonics in Plateau and northwestern Valley and Ridge provinces of the central Appalachians: Geological Society of America Bulletin, v. 75, p. 863-900.

Hardeman, W.D., Swingle, G.D., and Miller, R.A., 1966, Geologic map of Tennessee: Tennessee Division of Geology, scale 1:250,000.

Harlow, G.E., 1987, The structural geology of a part of the Pulaski thrust sheet near Boone Dam: Sullivan and Washington Counties, Tennessee [M.S. thesis]: Knoxville, University of Tennessee, 103 p.

Harris, L.D., 1965, Geologic map of the Tazewell quadrangle, Claiborne County, Tennessee: U.S. Geological Survey Geological Quadrangle Map GQ-465.

Harris, L.D., 1971, A lower Paleozoic paleoaquifer—the Kingsport Formation and Mascot Dolomite of Tennessee and southwest Virginia: Economic Geology, v. 66, p. 735-743.

Harris, L.D., 1976, Thin-skinned tectonics and potential hydrocarbon traps—Illustrated by a seismic profile in the Valley and Ridge province of Tennessee: U.S. Geological Survey Professional Paper 1018, 40 p.

Harris, L.D., 1979, Similarities between the thick-skinned Blue Ridge anticlinorium and the thin-skinned Powell Valley anticline: Geological Society of America Bulletin, v. 90, p. 525-539.

Harrison, M.J., 2006, Fold-thrust belt structures of the Lackawanna synclinorium, Pennsylvania: Insight into the tectonic evolution of the central Appalachians: Northeastern Geology & Environmental Sciences, v. 28, p. 358-367.

Harrison, M.J., Marshak, S., and McBride, J.H., 2004, The Lackawanna synclinorium, Pennsylvania: A salt-collapse structure, partially modified by thin-skinned folding: Geological Society of America Bulletin, v. 116, p. 1499-1514.

Hasson, K.O., and Haase, C.S., 1988, Lithofacies and paleogeography of the Conasauga Group (Middle and Late Cambrian) in the Valley and Ridge province of East Tennessee: Geological Society of America Bulletin, v. 100, p. 234-246.

Hatcher, R.D., Jr., 1965, Structure of the northern portion of the Dumplin Valley fault zone in east Tennessee [Ph.D. dissertation]: Knoxville, University of Tennessee, 168 p.

Hatcher, R.D., Jr., 1989, Tectonic synthesis of the U.S. Appalachians, *in* Hatcher, R.D., Jr., Thomas, W.A., and Viele, G.W., eds., The Appalachian-Ouachita orogen in the United States: Boulder, Colorado, Geological Society of America, The Geology of North America, v. F-2, p. 511-535.

Hatcher, R.D., Jr., 1995, Structural geology principles, concepts, and problems (second edition): Upper Saddle River, New Jersey, Prentice Hall, 525 p.

Hatcher, R.D., Jr., 2002, The Alleghanian (Appalachian) orogeny, a product of zipper tectonics: rotational transpressive continent-continent collision and closing of ancient oceans along irregular margins, *in* Martínez Catalán, J.R., Hatcher, R.D., Jr., Arenas, R., and Garcia, F.D., eds., Variscan-Appalachian dynamics: The building of the Late Paleozoic basement: Geological Society of America Special Paper 394, p. 199-208.

Hatcher, R.D., Jr., and Geiser, P.A., 2010, Toward a solution of the 3D balancing problem in curved segments of orogens *in* Law, R.D., Butler, R.W., Holdsworth, R.E., Krabbendam, M, and Strachan, R.A., eds., Continental tectonics and mountain building: The legacy of Peach and Horne: Geological Society of London Special Publication 335, p. 405-428.

Hatcher, R.D., Jr., Lemiszki, P.J., and Whisner, J.B., 2007a, Character of rigid boundaries and internal deformation of the southern Appalachian foreland fold-thrust belt, *in* Sears, J.W., Harms, T.A., and Evenchick, C.A., eds., Whence the Mountains? Inquiries into the Evolution of Orogenic Systems: A Volume in Honor of Raymond A. Price: Geological Society of America Special Paper 433, p. 243-276.

Hatcher, R.D., Jr., Bream, B.R., and Merschat, A.J., 2007b, Tectonic map of the southern and central Appalachians: A tale of three orogens and a complete Wilson cycle, *in* Hatcher, R.D., Jr., Carlson, M.P., McBride, J.H., and Martínez Catalán, J.R., eds., 4-D Framework of Continental Crust: Geological Society of America Memoir 200, p. 595-632.

Hatcher, R.D., Jr., Osberg, P.H., Drake, A.A., Jr., Robinson, P., and Thomas, W.A., 1990, Tectonic map of U.S. Appalachians, *in* Hatcher, R.D., Jr., Thomas, W.A., and Viele, G.W., eds., The Appalachian-Ouachita Orogen in the United States: Boulder, Geological Society of America, The Geology of North America, v. F-2, Plate 1, scale 1:2,500,000.

Hatcher, R.D., Jr., Thomas, W.A., Geiser, P.A., Snoke, A.W., Mosher, S., and Wiltschko, D.V., 1989, Alleghanian orogen, *in* Hatcher, R.D., Jr., Thomas, W.A., and Viele, G.W., eds., The Appalachian-Ouachita Orogen in the United States: Boulder, Colorado, Geological Society of America, The Geology of North America, v. F-2, p. 233-318.

Hayes, C.W., 1891, The overthrust faults of the southern Appalachians: Geological Society of America Bulletin, v. 2, p. 141-152.

Helton, W.L., 1967, Lithostratigraphy of the Conasauga Group between Rogersville and Kingsport, Tennessee [Ph.D. dissert.]: Knoxville, University of Tennessee, 96 p.

Hugman, R.H.H., III, and Friedman, M., 1979, Effects of texture and composition on mechanical behavior of experimentally deformed carbonate rocks: American Association of Petroleum Geologists Bulletin, v. 63, p. 1478-1489.

Keith, A., 1895, Description of the Knoxville folio (Tennessee-North Carolina): U.S. Geological Survey Geologic Atlas, Folio 16, 6 p.

Keith, A., 1903, Description of the Cranberry folio (Tennessee-North Carolina): U.S. Geological Survey Geologic Atlas, Folio 90, 9 p.

Keith, A., 1905a, Description of the Greeneville Folio (Tennessee-North Carolina): U.S. Geological Survey Geologic Atlas, Folio 118, 12 p.

Keith, A., 1905b, Description of the Morristown Folio (Tennessee-North Carolina): U.S. Geological Survey Geologic Atlas, Folio 27, 13 p.

King, P.B., Ferguson, H.W., Craig, L.C., and Rodgers, J., 1944, Geology and manganese deposits of northeastern Tennessee: Tennessee Division of Geology Bulletin 52, 275 p.

Lemiszki, P.J., 1994, Geological mapping of the Oak Ridge K-25 Site, Oak Ridge, Tennessee: Environmental Sciences Division, Oak Ridge K-25 Site, Martin Marietta Energy Systems, Inc., Oak Ridge, Tennessee, 51 p.

Lemiszki, P.J., 2003, Geologic map of the Mosheim quadrangle, Tennessee: Tennessee Division of Geology, open file map scale 1:24,000.

Lemiszki, P.J., 2008, Geologic mapping of the Newport quadrangle, Tennessee: Making a case for the southwest continuation of the Pulaski fault: Geological Society of America Abstracts with Programs, v. 40, no. 4, p. 13.

Lewis, S.E., and Hower, J.C., 1990, Implications of thermal events on thrust emplacement sequence in the Appalachian fold and thrust belt: some new vitrinite reflectance data: The Journal of Geology, v. 98, p. 927-942.

Little, R.L., 1969, Lithostratigraphy and structural geology of a portion of the Dunham Ridge thrust block, Greene and Washington Counties, Tennessee [Ph.D. dissert.]: Knoxville, University of Tennessee, 130 p.

Mack, G.H., 1980, Stratigraphy and depositional environments of the Chilhowee Group (Cambrian) in Georgia and Alabama: American Journal of Science, v. 280, p. 497-517.

McLaughlin, R.E., 1973, Observations on the biostratigraphy and stratigraphy of Knox County, Tennessee and vicinity: Tennessee Division of Geology Bulletin 70, p. 25-62.

McMaster, R.L., de Boer, J., and Collins, B.P., 1980, Tectonic development of southern Narragansett Bay and offshore Rhode Island: Geology, v. 8, p. 496-500.

Milici, R.C., 1975, Structural patterns in the southern Appalachians—Evidence for a gravity slide mechanism for Alleghanian deformation: Geological Society of America Bulletin, v. 86, p. 1315-1320.

Munyan, A.C., 1951, Geology and mineral resources of the Dalton quadrangle, Georgia-Tennessee: Georgia Geological Survey Bulletin, v. 57, p. 100-101.

Neuman, R.B., 1955, Middle Ordovician rocks of the Tellico-Sevier belt, eastern Tennessee: U.S. Geological Survey Professional Paper 274-F, 178 p.

Neuman, R.B., 1960, Geologic map of the Wildwood quadrangle, Tennessee: U.S. Geological Survey, Geological Quadrangle Map GQ-130, scale 1:24,000.

Oder, C.R.L., 1934, Preliminary subdivision of the Knox Dolomite in East Tennessee: Journal of Geology, v. 42, p. 469-497.

Oder, C.R.L., and Milici, R.C., 1965, Geologic map of the Morristown quadrangle, Tennessee: Tennessee Division of Geology Geologic Map GM-163-NE, scale 1:24,000.

Oder, C.R.L., and Miller, H.W., 1945, Stratigraphy of the Mascot-Jefferson City zinc district: American Institute of Mining, Metallurgical, and Petroleum Engineers Institute Publication 1818, p. 223-231.

Perry, W.J., Jr., 1978, Sequential deformation in the central Appalachians: American Journal of Science, v. 278, p. 518-542.

Pfeil, R.W., and Read, J.F., 1980, Cambrian carbonate platform margin facies, Shady Dolomite, southwestern Virginia, U.S.A: Journal of Sedimentary Petrology, v. 50, p. 91-116.

Pumpelly, R., Wolff, J.E., and Dale, T.N., 1894, Geology of the Green Mountains Part III, Mount Greylock: its areal and structural geology: U.S. Geologic Survey Monograph 23, p. 1-206.

Ramsay, J.G., 1962, The geometry and mechanics of formation of “similar” type folds: The Journal of Geology, v. 70, p. 309-327.

Rankey, E.C., 1993, Carbonate platform response to tectonism and eustasy: The Middle Cambrian carbonates of the lower and middle Conasauga Group, east Tennessee [M.S. thesis]: Knoxville, University of Tennessee, 191 p.

Rankin, D.W., 1975, The continental margin of eastern North America in the southern Appalachians: The opening and closing of the proto-Atlantic Ocean: American Journal of Science, v. 275, p. 298-336.

Rankin, D.W., Espenshade, G.H., and Neuman, R.B., 1972, Geologic map of the west half of the Winston-Salem quadrangle, North Carolina, Virginia, and Tennessee: U.S. Geological Survey Miscellaneous Geologic Investigations Map 1-709-A, scale 1:250,000.

Reks, I.J., and Gray, D.R., 1983, Strain patterns and shortening in a folded thrust sheet: an example from the southern Appalachians: Tectonophysics, v. 93, p. 99-128.

Resser, C.E., 1938, Cambrian system (restricted) of the southern Appalachians: Geological Society of America Special Paper 15, 140 p.

Rich, J. L., 1934, Mechanics of low-angle overthrust faulting illustrated by the Cumberland thrust block, Virginia, Kentucky, and Tennessee: American Association of Petroleum Geologists Bulletin, v. 18, p. 1584-1596.

Robertson, P.B., Hatcher, R.D., Jr., and Derryberry, P.M., 2011, Structural and stratigraphic/sedimentological analysis of part of the Middle Ordovician Sevier foredeep basin, southeastern Greene County, Tennessee: Geological Society of America Abstracts with Programs, v. 42, no. 2, p. 54.

Rodgers, J., 1953a, Geologic map of East Tennessee with explanatory text: Tennessee Division of Geology Bulletin 58, part 2, 168 p.

Rodgers, J., 1953b, Geologic map of East Tennessee with explanatory text: Tennessee Division of Geology Bulletin 58, part 2, scale 1:125,000.

Rodgers, J., 1970a, The Pulaski fault, and the extent of Cambrian evaporites in the central and southern Appalachians, *in* Fisher, G.W., Pettijohn, F.J., Reed, J.C., Jr., and Weaver, K.N., eds., Studies of Appalachian geology: Central and southern: New York, Interscience Publishers, p. 175-178.

Rodgers, J., 1970b, The tectonics of the Appalachians: New York, Interscience Publishers, 271 p.

Rodgers, J., and Kent, D.F., 1948, Stratigraphic section at Lee Valley, Hawkins County, Tennessee: Tennessee Division of Geology Bulletin 55, 47 p.

Roeder, D., and Witherspoon, W.D., 1978, Palinspastic map of east Tennessee: American Journal of Science, v. 278, p. 543-550.

Roper, D.C., 1977, Mesoscopic fabric of Babbs Knobs area: (Pulaski thrust, East Tennessee) [M.S. thesis]: Knoxville, University of Tennessee, 83 p.

Ruppel, S.C., and Walker, K.R., 1995, Petrology and depositional history of a Middle Ordovician carbonate platform: Chickamauga Group, northeastern Tennessee: Geological Society of America Bulletin, v. 95, p. 568-583.

Safford, J.M., 1869, Geology of Tennessee, State of Tennessee: Nashville, Mercer, 550 p.

Safford, J.M., and Killebrew, J.B., 1876, The elementary geology of Tennessee, Nashville, 550 p.

Samman, N.F., 1975, Sedimentation and stratigraphy of the Rome Formation in East Tennessee [Ph.D. dissert.]: Knoxville, University of Tennessee, 337 p.

Scholle, P.A., and Ulmer-Scholle, D.S., 2003, A color guide to the petrology of carbonate rocks: Grains, textures, porosity, diagenesis: American Association of Petroleum Geologists Memoir 77, 474 p.

Schultz, A.P., 1983, Broken formations of the Pulaski thrust sheet near Pulaski, Virginia [Ph.D. dissert.]: Blacksburg, Virginia Polytechnic Institute and State University, 99 p.

Schultz, A.P., 1986, Broken formations of the Pulaski thrust sheet near Pulaski, Virginia, *in* McDowell, R.C., and Glover, L., III, eds., the Lowry Volume: Studies in Appalachian geology: Virginia Polytechnic Institute and State University Dept. of Geological Sciences Memoir 3, p. 13-26.

Schwab, F.L., 1970, Origin of the Antietam Formation (Late Precambrian?—Lower Cambrian), central Virginia: Journal of Sedimentary Petrology, v. 40, p. 354-366.

Simpson, E.L., and Eriksson, K.A., 1989, Sedimentology of the Unicoi Formation in southern and central Virginia: Evidence for Late Proterozoic to Early Cambrian rift-to-passive margin transition: Geological Society of America Bulletin, v. 101, p.42-54.

Spigai, J.J., 1963, A study of the Rome Formation in the Valley and Ridge Province of East Tennessee [M.S. thesis]: Knoxville, University of Tennessee, 179 p.

Srinivasan, K., 1993, Depositional history, sequence stratigraphy and diagenesis of Maryville Limestone (Middle Cambrian), southern Appalachians [Ph.D. dissert.]: Knoxville, University of Tennessee, 166 p.

Srinivasan, K., and Walker, K.R., 1993, Sequence stratigraphy of an intrashelf basin carbonate ramp to rimmed platform transition: Maryville Limestone (Middle

Cambrian), southern Appalachians: Geological Society of America Bulletin, v. 105, p. 883-896.

Stevenson, J.J., 1885, Notes on the geological structure of Tazewell, Russell, Wise, Smyth, and Washington Counties, Virginia: Proceedings of the American Philosophical Society, v. 22., p. 114-161.

Stose, G.W., 1908, The Cambro-Ordovician limestones of the Appalachian Valley in southern Pennsylvania: Journal of Geology, v. 16, p. 698-714.

Suppe, J., 1981, Mechanics of mountain building and metamorphism in Taiwan: Geologic Society of China Memoir 4, p. 67-89.

Swingle, G.D., 1959, Geology, mineral resources, and groundwater of the Cleveland area, Tennessee: Tennessee Division of Geology Bulletin 61, 125 p.

Swingle, G.D., 1964, Elevation of the Chickamauga Limestone to group status in East Tennessee [abs]: Tennessee Academy of Science Journal, v. 39, no. 2, p. 66.

Troensegaard, K.W., II, 1965, Development of cleavage in a portion of the Bays Mountain synclinorium, Greene, Cocke, Hamblen, and Jefferson Counties, Tennessee [M.S. thesis]: Knoxville, University of Tennessee, 39 p.

Ulrich, E.O., 1911, Revision of the Paleozoic systems: Geological Society of America Bulletin, v. 22, p. 281-681.

Whisner, C.W., 2005, The Middle Ordovician Tellico-Sevier syncline: A stratigraphic, structural, and paleoseismic investigation [Ph.D. dissert.]: Knoxville, University of Tennessee, 230 p.

Whitaker, A.E., and Bartholomew, M.J., 1999, Layer parallel shortening: A mechanism for determining deformation timing at the junction of the central and southern Appalachians: American Journal of Science, v. 299, p. 238-254.

Whitmer, N.E., 2005, Structural and stratigraphic investigations of the Bays Mountain synclinorium, Parrottsville and a portion of Cedar Creek 7.5-minute quadrangles, east Tennessee [M.S. thesis]: Knoxville, University of Tennessee, 129 p.

Wilkerson, M.S., Apotria, T., and Farid, T., 2002, Interpreting the geologic map expression of contractional fault-related fold terminations: lateral/oblique ramps versus displacement gradients: Journal of Structural Geology, v. 24, p. 593-607.

Woodward, N.B., 1987, Geological applicability of critical-wedge thrust-belt models: Geological Society of America Bulletin, v. 99, p. 827-832.

Woodward, N.B., and Beets, J.W., 1988, Critical evidence for southern Appalachian Valley and Ridge thrust sequence, *in* Mitra, G., and Wojtal, S. eds., Geometries and mechanisms of thrusting with special reference to the Appalachians: Geological Society of America Special Paper 222, p. 165-178.

Woodward, N.B., and Gray, D.R., 1985, Four southwestern Virginia-northeast Tennessee balanced cross sections, *in* Woodward, N.B., ed., Valley and Ridge thrust belt; Balanced structural sections, Pennsylvania to Alabama: Knoxville, University of Tennessee, Department of Geological Sciences Studies in Geology, v. 12, p. 40-43.

Woodward, N.B., Walker, K.R., and Lutz, C.T., 1988, Relationships between early Paleozoic facies patterns and structural trends in the Saltville thrust family, Tennessee Valley and Ridge, southern Appalachians: Geological Society of America Bulletin, v. 100, p. 1758-1769.

Yust, W.W., 1975, A mesoscopic fabric analysis of a portion of the Tellico-Sevier belt of East Tennessee [M.S. thesis]: Knoxville, University of Tennessee, 106 p.

APPENDIX

Structure and Lithology Data for the Study Area
[Does not include data from Whitmer (2005)]

Explanation:

CC—Cedar Creek
NM—Neddy Mountain
PR—Paint Rock
PV—Parrottsville

Note: UTM coordinates (17N, North American Datum 1983) included only in data from Cedar Creek quadrangle

QUAD	UTM Easting	UTM Northing	STATION	STRIKE	DIP	FEATURE	DOMINANT LITHOLOGY/UNIT	DESCRIPTION 1	DESCRIPTION 2	OTHER LITHOLOGY/UNIT 1	OTHER LITHOLOGY/UNIT 2
CC	3996014E	322580N	1	55	67	bedding	Conococheague Limestone	Massive	Ribboned	Dolomite	
CC	3995974E	322562N	2	58	51	bedding	Conococheague Limestone	Massive			
CC	3992680E	323060N	3	40	50	bedding	Limestone				
CC	3998404E	323321N	4	59	81	bedding	Limestone	Ribboned		Dolomite	
CC	3995806E	321572N	5	61	65	bedding	Shale	Fissile	Shaly	Lower Sevier Shale	
CC	3995557E	322179N	6	60	39	bedding	Limestone	Massive			
CC	3997787E	322092N	7	0	0	float	Conococheague Limestone	Cherty			
CC	3998324E	325352N	8	59	82	bedding	Jonesboro Limestone	Massive	Thrombolitic		
CC	3998277E	325213N	9	58	70	bedding	Limestone	Cherty	Sandy	Sandstone	
CC	3994128E	323401N	10	67	79	bedding	Limestone			Sandstone	
CC	3994800E	322929N	11	248	79	bedding	Limestone			Sandstone	
CC	3994754E	322942N	13	245	83	bedding	Limestone	Massive		Dolomite	
CC	3994066E	322593N	14	58	47	bedding	Limestone	Cherty		Siltstone	
CC	3994017E	322605N	15	0	0	float		Cherty			
CC	3994075E	322513N	16	58	25	bedding	Limestone				
CC	3994163E	322433N	17	252	63	bedding	Limestone	Ribboned		Dolomite	
CC	3994337E	323100N	18	65	69	bedding	Limestone	Sandy	Ribboned	Dolomite	Jonesboro Limestone?
CC	3998628E	325557N	19	55	55	bedding	Limestone	Shaly	Sandy	Dolomite	Conococheague Limestone
CC	3995300E	322358N	20	79	26	bedding	Limestone				
CC	3992391E	323336N	21	60	72	bedding	Limestone				
CC	3992378E	323260N	22	55	50	bedding	Dolomite				
CC	3994475E	320477N	23	80	47	bedding	Limestone	Massive	Ribboned	Dolomite	Conococheague Limestone
CC	3994828E	320381N	24	0	0	float	Dolomite	Massive		Limestone	
CC	3994971E	320544N	25	76	51	bedding	Shale	Fissile	Shaly		
CC	3994884E	320522N	26	75	60	bedding	Shale				
CC	3993034E	320886N	27	56	56	bedding					
CC	3992616E	320994N	28	56	72	overturned bedding	Shale				
CC	3992340E	321664N	29	52	15	bedding					
CC	3993474E	321028N	30	75	30	bedding	Limestone	Massive			
CC	3993549E	320997N	31	70	35	bedding	Limestone	Massive			
CC	3993640E	321095N	32	58	65	bedding	Limestone	Oolitic	Massive		
CC	3993504E	321101N	33	59	34	bedding	Limestone	Thrombolitic		Dolomite	
CC	3992742E	321025N	34	66	70	bedding	Limestone	Massive		Dolomite	
CC	3991537E	321279N	35	55	41	bedding	Limestone	Banded		Dolomite	
CC	3992418E	321616N	36	280	67	bedding	Dolomite				

QUAD	UTM Easting	UTM Northing	STATION	STRIKE	DIP	FEATURE	DOMINANT LITHOLOGY/UNIT	DESCRIPTION 1	DESCRIPTION 2	OTHER LITHOLOGY/UNIT 1	OTHER LITHOLOGY/UNIT 2
CC	3996808E	322274N	37	245	43	bedding	Limestone				
CC	3995402E	322377N	39	86	15	bedding	Dolomite				
CC	3995374E	322489N	40	155	35	bedding	Limestone				
CC	3995554E	322461N	41	304	28	bedding	Limestone				
CC	3992488E	323104N	42	55	39	bedding	Limestone			Dolomite	
CC	3991686E	322355N	43	54	75	bedding	Limestone	Ribboned	Interbedded	Dolomite	
CC	3991712E	322390N	44	54	35	bedding	Limestone	Ribboned	Interbedded	Dolomite	
CC	3991523E	322178N	45	325	35	bedding	Limestone			Dolomite	
CC	3990845E	321405N	46	36	25	bedding	Limestone	Banded	Ribboned	Dolomite	
CC	3990786E	321352N	47	59	31	bedding					
CC	3992162E	322145N	50	51	45	bedding	Limestone	Massive	Laminated		
CC	3992063E	322204N	54	310	50	bedding	Limestone				
CC	3995348E	322092N	56	33	26	bedding	Dolomite	Thrombolitic		Limestone	
CC	3995392E	321999N	58	65	62	bedding	Dolomite	Thrombolitic		Limestone	
CC	3995368E	321837N	62	65	67	bedding	Dolomite	Thrombolitic		Limestone	
CC	3995403E	321807N	64	213	11	bedding					
CC	3995461E	321782N	66	65	69	bedding	Dolomite			Limestone	
CC	3995472E	321888N	67	69	69	bedding	Dolomite			Limestone	
CC	3995205E	322128N	69	313	22	bedding	Dolomite			Limestone	
CC	3995165E	322006N	70	58	14	bedding	Dolomite			Limestone	
CC	3994944E	321803N	71	62	76	bedding	Dolomite			Limestone	
CC	3995284E	321998N	72	99	22	bedding	Dolomite			Limestone	
CC	3991040E	321538N	73	48	30	bedding	Dolomite	Massive			
CC	3991022E	321500N	74	49	30	bedding	Limestone	Interbedded	Massive	Dolomite	
CC	3990905E	321409N	78	45	35	bedding	Limestone	Massive	Interbedded	Dolomite	
CC	3991419E	322027N	79	278	62	bedding	Dolomite	Massive		Limestone	
CC	3995457E	324535N	80	250	69	bedding	Limestone	Oolitic	Shaly	Dolomite	
CC	3996215E	325801N	81	56	77	bedding	Limestone	Massive		Dolomite	
CC	3995525E	321383N	82	232	90	bedding	Limestone	Massive	Ribboned		
CC	3995567E	321374N	83	65	70	bedding	Shale	Calcareous	Fissile		
CC	3995556E	321430N	84	55	79	bedding	Limestone	Massive	Ribboned		
CC	3995280E	321102N	85	46	74	bedding	Shale	Fissile	Calcareous		
CC	3995339E	321293N	86	45	90	bedding	Limestone	Massive	Interbedded	Dolomite	
CC	3995236E	321222N	88	230	68	bedding	Limestone	Massive	Interbedded	Dolomite	
CC	3995102E	321030N	90	203	51	bedding	Limestone	Massive	Oolitic	Dolomite	

QUAD	UTM Easting	UTM Northing	STATION	STRIKE	DIP	FEATURE	DOMINANT LITHOLOGY/UNIT	DESCRIPTION 1	DESCRIPTION 2	OTHER LITHOLOGY/UNIT 1	OTHER LITHOLOGY/UNIT 2
CC	3995378E	321159N	94	46	90	bedding	Shale	Fissile	Calcareous		
CC	3995219E	320962N	95	64	54	bedding	Shale	Fissile	Calcareous		
CC	3995331E	320926N	96	59	32	bedding	Siltstone	Silty	Calcareous	Shale	
CC	3995425E	320921N	97	59	64	bedding	Shale	Fissile	Silty	Siltstone	
CC	3995512E	320915N	98	59	74	bedding	Shale	Fissile	Silty	Siltstone	
CC	3995652E	320952N	99	59	50	bedding	Shale	Fissile	Silty	Siltstone	
CC	3995708E	321079N	100	0	0	float	Sandstone	Sandy	Calcareous	Siltstone	
CC	3995747E	320948N	101	64	45	bedding	Siltstone	Silty	Calcareous		
CC	3995609E	320827N	102	58	66	bedding	Shale	Fissile	Silty	Siltstone	
CC	3995749E	320645N	103	0	0	float	Sandstone	Sandy	Calcareous	Siltstone	
CC	3995670E	320768N	104	66	62	bedding	Shale	Fissile	Silty	Siltstone	
CC	3995934E	321746N	106	326	74	bedding	Limestone	Massive	Interbedded	Dolomite	
CC	3995919E	321689N	107	305	41	bedding	Limestone	Massive	Interbedded	Dolomite	
CC	3991550E	322155N	108	29	34	bedding	Limestone	Banded	Shaly		
CC	3991458E	322338N	109	101	68	overturned bedding	Shale	Calcareous	Fissile	Siltstone	Nolichucky Shale
CC	3991471E	322391N	110	109	57	overturned bedding	Shale	Calcareous	Fissile	Siltstone	Nolichucky Shale
CC	3991469E	322478N	112	80	81	overturned bedding	Shale	Calcareous	Fissile	Siltstone	Nolichucky Shale
CC	3991581E	322668N	114	246	17	bedding	Limestone	Massive	Interbedded	Maynardville Limestone	Dolomite
CC	3991550E	322673N	115	74	69	overturned bedding	Shale	Fissile	Calcareous	Siltstone	Nolichucky Shale
CC	3991539E	322719N	116	55	29	overturned bedding	Shale	Fissile	Calcareous	Siltstone	Nolichucky Shale
CC	3991427E	322565N	118	69	64	bedding	Dolomite	Massive		Limestone	
CC	3990261E	322703N	119	206	46	bedding	Shale	Fissile	Calcareous	Siltstone	Nolichucky Shale
CC	3995842E	323086N	120	0	0	float	Dolomite	Massive		Limestone	
CC	3995993E	322831N	121	56	51	bedding	Dolomite			Limestone	
CC	3995951E	322930N	122	52	61	bedding	Dolomite	Interbedded	Massive	Limestone	
CC	3996074E	325481N	123	55	60	bedding	Limestone	Massive	Interbedded	Dolomite	
CC	3995499E	325040N	124	72	48	bedding	Limestone	Massive			
CC	3995436E	324975N	125	79	75	bedding	Limestone	Massive			
CC	3995351E	324881N	126	56	44	bedding	Limestone	Massive			
CC	3995197E	324707N	127	57	48	bedding	Dolomite	Massive		Limestone	
CC	3995150E	324655N	128	0	0	float	Sandstone	Sandy	Siliceous		
CC	3995106E	324606N	129	51	61	bedding	Limestone	Massive	Fissile	Dolomite	
CC	3994999E	324465N	130	45	50	bedding	Limestone	Massive		Dolomite	
CC	3994942E	324379N	131	43	56	bedding	Limestone	Massive		Dolomite	
CC	3994862E	324265N	132	55	56	bedding	Limestone	Massive		Dolomite	

QUAD	UTM Easting	UTM Northing	STATION	STRIKE	DIP	FEATURE	DOMINANT LITHOLOGY/UNIT	DESCRIPTION 1	DESCRIPTION 2	OTHER LITHOLOGY/UNIT 1	OTHER LITHOLOGY/UNIT 2
CC	3994861E	324217N	133	44	53	bedding	Sandstone	Sandy	Siliceous		
CC	3994864E	324118N	134	49	62	bedding	Limestone	Massive	Interbedded	Dolomite	
CC	3994825E	323911N	135	51	59	bedding	Limestone	Massive	Interbedded	Dolomite	
CC	3994818E	323848N	136	51	51	bedding	Limestone	Massive	Interbedded	Dolomite	
CC	3994848E	323768N	137	245	52	bedding	Limestone	Banded	Interbedded	Dolomite	
CC	3994914E	323758N	139	245	82	bedding	Limestone	Massive	Ribboned	Dolomite	
CC	3995007E	323934N	140	245	85	bedding	Limestone	Massive	Ribboned	Dolomite	
CC	3994958E	324003N	142	61	41	bedding	Limestone	Massive	Ribboned	Dolomite	
CC	3994886E	323872N	144	60	39	bedding	Limestone	Massive	Ribboned	Dolomite	
CC	3994851E	323649N	145	81	90	bedding	Limestone	Massive	Ribboned	Dolomite	
CC	3994914E	323589N	146	247	51	bedding	Limestone	Massive	Ribboned	Dolomite	
CC	3994266E	325337N	147	64	52	bedding	Limestone	Interbedded	Ribboned	Dolomite	
CC	3994195E	325347N	148	65	60	bedding	Dolomite	Massive			
CC	3994165E	325291N	149	65	57	bedding	Dolomite	Massive			
CC	3994113E	325207N	150	56	60	bedding	Dolomite	Massive			
CC	3994075E	325134N	151	53	56	bedding	Dolomite	Massive			
CC	3994047E	324932N	153	65	55	bedding	Limestone	Massive	Ribboned	Dolomite	
CC	3993968E	325033N	154	58	58	bedding	Limestone	Massive	Ribboned	Dolomite	
CC	3994141E	325120N	155	60	54	bedding	Limestone	Interbedded	Ribboned	Dolomite	
CC	3993765E	325354N	157	68	75	bedding	Dolomite	Massive	Silty	Dolomite	
CC	3993788E	325408N	158	95	76	bedding	Limestone	Ribboned		Dolomite	
CC	3993892E	325549N	159	31	54	bedding	Limestone	Ribboned	Silty	Dolomite	
CC	3994034E	325650N	160	49	71	bedding	Dolomite			Chepultepec Dolomite	
CC	3994164E	325397N	161	55	62	bedding	Limestone	Ribboned	Massive	Dolomite	
CC	3994276E	325518N	162	56	58	bedding	Dolomite				
CC	3994300E	325567N	163	56	60	bedding	Dolomite				
CC	3994336E	325657N	164	56	60	bedding	Dolomite				
CC	3992127E	323992N	165	338	51	bedding	Dolomite			Limestone	
CC	3992147E	324100N	166	101	74	bedding	Limestone	Ribboned	Massive	Dolomite	
CC	3992200E	324197N	167	75	69	bedding	Limestone	Ribboned	Massive	Dolomite	
CC	3992190E	324088N	168	105	75	bedding	Limestone	Interbedded	Ribboned	Dolomite	
CC	3992088E	323895N	169	332	70	bedding	Dolomite	Massive		Limestone	
CC	3992055E	323823N	170	284	70	bedding	Limestone	Interbedded	Ribboned	Dolomite	
CC	3991996E	323859N	171	313	67	bedding	Dolomite	Massive			
CC	3991930E	323864N	172	336	67	bedding	Limestone	Interbedded	Ribboned	Dolomite	

QUAD	UTM Easting	UTM Northing	STATION	STRIKE	DIP	FEATURE	DOMINANT LITHOLOGY/UNIT	DESCRIPTION 1	DESCRIPTION 2	OTHER LITHOLOGY/UNIT 1	OTHER LITHOLOGY/UNIT 2
CC	3991796E	323890N	173	75	63	bedding	Shale	Fissile	Calcareous	Siltstone	Nolichucky Shale
CC	3991795E	323841N	174	315	74	bedding	Siltstone	Fissile	Calcareous	Shale	Nolichucky Shale
CC	3991884E	323801N	175	343	57	bedding	Shale	Fissile	Calcareous	Siltstone	Nolichucky Shale
CC	3992316E	324418N	176	81	90	bedding	Dolomite	Ribboned	Massive	Limestone	
CC	3997034E	326925N	177	55	71	bedding	Limestone	Interbedded	Ribboned	Dolomite	
CC	3997233E	327168N	178	55	51	bedding	Limestone	Interbedded	Ribboned	Dolomite	
CC	3997305E	327236N	179	55	70	bedding	Limestone	Interbedded	Ribboned	Dolomite	
CC	3991740E	322502N	180	62	44	bedding	Limestone	Ribboned	Interbedded	Dolomite	Maynardville Limestone
CC	3991777E	322544N	181	312	81	joint	Limestone	Ribboned	Interbedded	Dolomite	Maynardville Limestone
CC	3991769E	322660N	183	49	27	bedding	Limestone	Ribboned	Interbedded	Dolomite	Maynardville Limestone
CC	3991763E	322697N	184	49	39	bedding	Limestone	Interbedded		Dolomite	
CC	3991819E	322778N	185	55	31	bedding	Dolomite	Interbedded	Ribboned	Limestone	
CC	3991916E	322609N	186	62	59	bedding	Dolomite	Fissile	Sandy		
CC	3991895E	322590N	187	0	0	float	Shale	Fissile	Calcareous	Nolichucky Shale	
CC	3991835E	322517N	188	48	38	bedding	Shale	Fissile	Calcareous	Nolichucky Shale	Dolomite
CC	3991791E	322418N	189	0	0	float	Shale	Fissile	Calcareous	Nolichucky Shale	Shale
CC	3991755E	322373N	190	58	30	bedding	Shale	Fissile	Calcareous	Nolichucky Shale	Siltstone
CC	3992573E	322472N	191	46	38	bedding	Limestone	Ribboned	Laminated	Dolomite	
CC	3992597E	322566N	192	49	44	bedding	Limestone	Ribboned	Massive	Dolomite	
CC	3992672E	322563N	193	49	44	bedding	Limestone	Ribboned	Laminated	Dolomite	
CC	3992755E	322655N	195	43	40	bedding	Limestone	Ribboned	Interbedded	Dolomite	
CC	3992836E	322750N	196	44	41	bedding	Limestone	Ribboned	Interbedded	Dolomite	
CC	3993399E	322461N	197	60	85	bedding	Limestone	Ribboned	Variegated	Dolomite	
CC	3993467E	322464N	198	60	86	bedding	Limestone	Ribboned	Variegated	Dolomite	
CC	3993558E	322415N	199	60	86	bedding	Limestone	Ribboned	Variegated	Dolomite	
CC	3993695E	322551N	200	60	84	bedding	Limestone	Ribboned	Variegated	Dolomite	
CC	3993315E	322472N	201	45	69	bedding	Limestone	Ribboned	Variegated	Dolomite	
CC	3993096E	322589N	202	0	0	float	Shale	Fissile		Nolichucky Shale	
CC	3994245E	323022N	203	55	44	bedding	Dolomite	Massive	Thrombolitic	Copper Ridge Dolomite	
CC	3994189E	322902N	205	61	54	bedding	Limestone	Massive	Ribboned	Dolomite	
CC	3994173E	322803N	206	0	0	float	Limestone	Ribboned	Interbedded	Dolomite	
CC	3994091E	322805N	207	0	0	float	Dolomite	Cherty		Limestone	
CC	3994087E	322900N	208	55	57	bedding	Limestone	Massive	Ribboned	Dolomite	
CC	3994169E	322978N	209	60	39	bedding	Limestone	Massive	Ribboned	Dolomite	
CC	3994156E	323136N	210	64	41	bedding	Limestone	Massive	Ribboned	Dolomite	Copper Ridge Dolomite

QUAD	UTM Easting	UTM Northing	STATION	STRIKE	DIP	FEATURE	DOMINANT LITHOLOGY/UNIT	DESCRIPTION 1	DESCRIPTION 2	OTHER LITHOLOGY/UNIT 1	OTHER LITHOLOGY/UNIT 2
CC	3994286E	323373N	211	58	47	bedding	Limestone	Shaly	Ribboned	Dolomite	
CC	3996843E	322916N	211	59	86	bedding	Jonesboro Limestone	Thrombolitic	Ribboned	Mascot Dolomite	
CC	3992474E	323598N	212	35	46	bedding	Dolomite	Interbedded	Sandy		
CC	3992398E	323634N	213	55	65	bedding	Limestone	Ribboned	Fossiliferous	Dolomite	Sandstone
CC	3992332E	323727N	214	280	76	bedding	Limestone	Ribboned		Dolomite	Breccia
CC	3992348E	323819N	215	62	46	bedding	Limestone	Ribboned	Interbedded	Dolomite	
CC	3991969E	323236N	217	51	55	bedding	Limestone	Ribboned	Interbedded	Dolomite	
CC	3991417E	320463N	218	54	38	bedding	Limestone	Cherty			
CC	3991597E	320595N	219	54	48	bedding	Limestone	Cherty			
CC	3991698E	320656N	220	44	40	bedding	Limestone	Cherty			
CC	3991886E	320705N	221	40	32	overturned bedding	Limestone	Cherty			
CC	3991892E	320557N	222	40	53	overturned bedding	Dolomite	Massive	Cherty	Limestone	
CC	3991933E	320471N	223	56	73	overturned bedding	Dolomite	Massive	Cherty	Limestone	
CC	3991922E	320327N	224	54	77	overturned bedding	Limestone	Ribboned	Massive	Dolomite	
CC	3991876E	320170N	225	44	45	bedding	Limestone	Ribboned	Massive	Dolomite	
CC	3991969E	320036N	226	54	24	bedding	Limestone	Cherty			
CC	3991741E	320067N	227	60	43	overturned bedding	Dolomite	Massive			
CC	3991166E	320429N	228	0	0	float	Other	Cherty			
CC	3991217E	320248N	229	0	0	float	Other	Cherty			
CC	3992791E	320455N	230	50	46	bedding	Limestone	Ribboned	Interbedded	Dolomite	
CC	3997428E	324282N	231	54	75	bedding	Limestone	Interbedded	Ribboned	Dolomite	Chepultepec Dolomite
CC	3997515E	324232N	232	0	0	float	Dolomite	Massive			
CC	3997523E	324324N	233	53	74	bedding	Dolomite	Massive			
CC	3997362E	324072N	234	56	74	bedding	Limestone	Massive	Interbedded	Dolomite	
CC	3997298E	324124N	235	57	83	bedding	Limestone	Massive	Interbedded	Dolomite	
CC	3997184E	324327N	236	54	54	bedding	Shale	Fissile	Silty	Nolichucky Shale	
CC	3997025E	323869N	237	240	70	cleavage	Shale	Fissile	Silty	Nolichucky Shale	
CC	3996735E	323191N	238	220	74	cleavage	Shale	Fissile	Silty	Nolichucky Shale	Coal
CC	3996316E	322796N	239	56	58	bedding	Shale	Fissile	Silty	Nolichucky Shale	Siltstone
CC	3996142E	322558N	240	65	65	bedding	Shale	Fissile	Silty	Nolichucky Shale	Siltstone
CC	3996144E	322450N	241	239	69	cleavage	Shale	Fissile	Silty	Nolichucky Shale	Siltstone
CC	3996144E	322450N	241	239	69	bedding	Shale	Fissile	Silty	Nolichucky Shale	Siltstone
CC	3996197E	322376N	242	66	70	bedding	Limestone	Interbedded	Massive	Dolomite	
CC	3996200E	329584N	243	53	73	bedding	Limestone	Ribboned	Massive	Dolomite	Sandstone
CC	3996140E	329468N	244	46	70	bedding	Limestone	Ribboned	Massive	Dolomite	Sandstone

QUAD	UTM Easting	UTM Northing	STATION	STRIKE	DIP	FEATURE	DOMINANT LITHOLOGY/UNIT	DESCRIPTION 1	DESCRIPTION 2	OTHER LITHOLOGY/UNIT 1	OTHER LITHOLOGY/UNIT 2
CC	3993233E	329395N	245	57	62	bedding	Shale	Fissile		Nolichucky Shale	
CC	3994285E	329731N	246	53	55	bedding	Limestone	Interbedded	Ribboned	Dolomite	
CC	3994163E	329713N	247	56	63	bedding	Limestone	Interbedded	Ribboned	Dolomite	
CC	3994025E	329605N	248	82	90	bedding	Limestone	Interbedded	Ribboned	Dolomite	Maynardville Limestone
CC	3994047E	329542N	249	250	64	bedding	Limestone	Interbedded	Ribboned	Dolomite	Maynardville Limestone
CC	3993977E	329645N	250	69	85	bedding	Limestone	Interbedded	Ribboned	Dolomite	Maynardville Limestone
CC	3991225E	326644N	252	106	64	bedding	Dolomite	Massive		Limestone	
CC	3993909E	329682N	253	71	74	bedding	Limestone	Ribboned	Massive	Dolomite	Sandstone
CC	3993626E	329787N	254	0	0	float	Other	Cherty		Copper Ridge Dolomite	
CC	3993821E	329788N	255	0	0	float	Other	Cherty			
CC	3994044E	329809N	256	72	69	bedding	Limestone	Ribboned	Interbedded	Dolomite	Maynardville Limestone
CC	3994457E	329782N	257	58	56	bedding	Limestone	Ribboned	Interbedded	Dolomite	Maynardville Limestone
CC	3994464E	329704N	258	60	41	bedding	Limestone	Ribboned	Interbedded	Dolomite	Maynardville Limestone
CC	3996399E	329351N	259	60	46	bedding	Dolomite	Shaly	Silty	Shale	
CC	3994330E	324663N	260	55	90	bedding	Limestone	Ribboned	Massive	Dolomite	Copper Ridge Dolomite
CC	3994538E	324593N	261	55	60	bedding	Limestone	Ribboned	Interbedded	Dolomite	
CC	3996936E	329962N	262	0	0	float	Shale	Fissile		Nolichucky Shale	
CC	3995578E	327393N	263	46	90	bedding	Limestone	Massive	Ribboned	Dolomite	Copper Ridge Dolomite
CC	3995609E	327324N	264	46	90	bedding	Limestone	Massive	Ribboned	Dolomite	Copper Ridge Dolomite
CC	3995130E	327217N	265	76	60	bedding	Limestone	Massive	Ribboned	Dolomite	Copper Ridge Dolomite
CC	3995306E	327335N	266	65	60	bedding	Limestone	Massive	Ribboned	Dolomite	Copper Ridge Dolomite
CC	3994006E	330019N	267	62	90	bedding	Limestone	Massive	Ribboned	Dolomite	Copper Ridge Dolomite
CC	3993436E	329937N	268	248	41	bedding	Shale	Fissile	Silty	Dolomite	Siltstone
CC	3993525E	330170N	269	0	0	float	Shale	Fissile	Silty	Dolomite	Siltstone
CC	3997045E	325604N	270	245	73	bedding	Dolomite	Banded	Massive	Limestone	
CC	3997182E	325487N	271	0	0	float	Other	Cherty	Sandy		
CC	3997011E	325669N	272	234	72	bedding	Limestone	Ribboned	Massive	Dolomite	
CC	3996976E	325725N	273	49	64	bedding	Limestone	Ribboned	Massive	Dolomite	
CC	3997523E	325493N	274	0	0	float	Limestone	Ribboned	Massive	Dolomite	
CC	3994120E	323557N	275	58	68	bedding	Limestone	Interbedded	Massive	Dolomite	
CC	3994046E	323608N	276	60	65	bedding	Limestone	Interbedded	Massive	Dolomite	
CC	3988060E	325177N	277	265	42	bedding	Dolomite	Sandy	Calcareous	Other	
CC	3988129E	325249N	278	255	60	bedding	Dolomite	Sandy	Calcareous	Other	
CC	3988155E	325351N	279	255	60	bedding	Dolomite	Shaly	Silty	Shale	
CC	3988186E	325429N	280	252	50	bedding	Dolomite	Shaly	Silty	Shale	

QUAD	UTM Easting	UTM Northing	STATION	STRIKE	DIP	FEATURE	DOMINANT LITHOLOGY/UNIT	DESCRIPTION 1	DESCRIPTION 2	OTHER LITHOLOGY/UNIT 1	OTHER LITHOLOGY/UNIT 2
CC	3988252E	325587N	281	244	51	bedding	Dolomite	Shaly	Silty	Shale	
CC	3988259E	325676N	282	256	59	bedding	Dolomite	Shaly	Silty	Shale	
CC	3988253E	325739N	283	270	31	bedding	Dolomite	Shaly	Silty	Shale	
CC	3988020E	325060N	284	265	40	bedding	Dolomite	Sandy	Silty		
CC	3987823E	325216N	285	49	40	bedding	Limestone	Laminated	Massive		
CC	3987473E	325370N	286	44	60	bedding	Shale	Fissile		Nolichucky Shale	
CC	3987473E	325370N	286	44	52	bedding	Shale	Fissile		Nolichucky Shale	
CC	3987473E	325370N	286	44	21	bedding	Shale	Fissile		Nolichucky Shale	
CC	3987473E	325370N	286	44	38	bedding	Shale	Fissile		Nolichucky Shale	
CC	3987488E	325355N	287	45	36	bedding	Dolomite	Massive	Ribboned		
CC	3987343E	325429N	288	0	0	float	Limestone	Ribboned	Massive	Dolomite	
CC	3994796E	327222N	289	66	66	bedding	Limestone	Interbedded	Ribboned	Dolomite	
CC	3994762E	327130N	290	70	59	bedding	Dolomite	Interbedded	Ribboned	Limestone	
CC	3994635E	327084N	291	56	55	bedding	Limestone	Banded	Interbedded	Dolomite	
CC	3995081E	328215N	292	59	66	bedding	Limestone	Ribboned		Dolomite	
CC	3995207E	328111N	293	62	67	bedding	Limestone	Ribboned	Cherty	Dolomite	
CC	3995100E	327973N	294	60	52	bedding	Limestone	Ribboned	Cherty	Dolomite	
CC	3993973E	328073N	295	64	58	bedding	Limestone	Ribboned		Dolomite	
CC	3997063E	328118N	296	259	41	bedding	Shale	Fissile	Calcareous	Lower Sevier Shale	
CC	3996990E	328074N	297	240	72	bedding	Shale	Fissile	Calcareous	Lower Sevier Shale	
CC	3996822E	328036N	298	58	72	bedding	Limestone	Massive		Dolomite	
CC	3996752E	327985N	300	59	90	bedding	Limestone	Interbedded	Massive	Dolomite	
CC	3995969E	327676N	301	62	74	bedding	Limestone	Ribboned	Interbedded	Dolomite	
CC	3991988E	327721N	302	65	63	bedding	Limestone	Massive	Interbedded	Dolomite	
CC	3991936E	327621N	303	0	0	float	Dolomite	Massive	Interbedded	Limestone	
CC	3998108E	329518N	304	62	90	bedding	Limestone	Massive	Ribboned	Dolomite	
CC	3998171E	329495N	305	62	90	bedding	Sandstone	Sandy	Massive	Limestone	Dolomite
CC	3998240E	329491N	306	62	90	bedding	Dolomite	Cherty	Interbedded	Limestone	
CC	3998216E	329395N	307	62	90	bedding	Limestone	Ribboned	Massive	Dolomite	
CC	3998172E	329706N	308	62	90	bedding	Limestone	Ribboned	Interbedded	Dolomite	
CC	3998301E	329714N	309	0	0	float	Sandstone	Sandy			
CC	3998325E	329682N	310	0	0	float	Dolomite	Cherty		Other	
CC	3998315E	329578N	311	60	90	bedding	Limestone	Ribboned	Massive	Dolomite	
CC	3998396E	329464N	312	0	0	float	Sandstone	Sandy		Dolomite	
CC	3998300E	329314N	313	231	67	bedding	Limestone	Ribboned	Massive	Dolomite	

QUAD	UTM Easting	UTM Northing	STATION	STRIKE	DIP	FEATURE	DOMINANT LITHOLOGY/UNIT	DESCRIPTION 1	DESCRIPTION 2	OTHER LITHOLOGY/UNIT 1	OTHER LITHOLOGY/UNIT 2
CC	3998269E	329366N	314	244	72	bedding	Limestone	Ribboned	Massive	Dolomite	
CC	3986559E	319842N	314	0	0	float	Nolichucky Shale	Fissile			
CC	3998966E	330327N	315	239	67	bedding	Shale	Fissile	Shaly	Sandstone	Lower Sevier Shale
CC	3986525E	319782N	315	0	0	float	Nolichucky Shale	Fissile			
CC	3998846E	330503N	316	57	90	bedding	Limestone	Ribboned	Massive	Dolomite	
CC	3998857E	330540N	317	60	90	bedding	Limestone	Ribboned	Massive	Dolomite	Sandstone
CC	3998891E	330607N	318	61	81	bedding	Limestone	Ribboned	Massive	Dolomite	Sandstone
CC	3998947E	330698N	319	65	76	bedding	Limestone	Ribboned	Massive	Dolomite	
CC	3998900E	330781N	320	61	90	bedding	Dolomite	Interbedded	Massive	Limestone	
CC	3998854E	330850N	321	57	81	bedding	Limestone	Ribboned	Interbedded	Dolomite	
CC	3998831E	328208N	322	66	28	bedding	Limestone	Interbedded	Cherty	Dolomite	
CC	3998915E	328296N	324	51	83	bedding	Limestone	Interbedded	Cherty	Dolomite	
CC	3998914E	328378N	325	57	36	bedding	Limestone	Interbedded	Cherty	Dolomite	
CC	3998951E	328389N	326	50	58	bedding	Limestone	Banded	Cherty	Dolomite	
CC	3999135E	328540N	327	56	56	bedding	Limestone	Banded	Cherty	Dolomite	
CC	3999192E	328487N	328	60	72	bedding	Limestone	Banded	Cherty	Dolomite	
CC	3999218E	328463N	329	216	75	bedding	Limestone	Ribboned	Interbedded	Dolomite	
CC	3999259E	328415N	331	216	82	bedding	Limestone	Ribboned	Massive	Dolomite	
CC	3999134E	328360N	332	222	70	bedding	Limestone	Ribboned	Cherty	Dolomite	Other
CC	3999063E	328343N	333	241	46	bedding	Limestone	Ribboned	Cherty	Dolomite	Other
CC	3999040E	330305N	334	59	64	bedding	Shale	Fissile		Lower Sevier Shale	
CC	3999108E	330335N	335	86	48	bedding	Shale	Fissile		Lower Sevier Shale	
CC	3999163E	330333N	336	216	66	bedding	Shale	Fissile		Lower Sevier Shale	
CC	3998928E	330385N	339	246	66	bedding	Shale	Fissile		Lower Sevier Shale	
CC	3998910E	330446N	340	240	70	bedding	Shale	Fissile		Lower Sevier Shale	
CC	3999003E	330265N	341	229	61	bedding	Shale	Fissile		Lower Sevier Shale	
CC	3999035E	330211N	343	56	90	bedding	Shale	Fissile		Lower Sevier Shale	
CC	3999080E	330178N	344	44	56	bedding	Shale	Fissile		Lower Sevier Shale	
CC	3995989E	330709N	345	56	71	bedding	Limestone	Ribboned	Interbedded	Dolomite	
CC	3995931E	330662N	346	48	79	bedding	Limestone	Ribboned	Interbedded	Dolomite	
CC	3991378E	321261N	347	55	49	bedding	Limestone	Massive	Calcareous		
CC	3991335E	321188N	348	59	51	bedding	Limestone	Massive	Calcareous		
CC	3991269E	321181N	349	56	44	bedding	Limestone	Massive	Calcareous		
CC	3991235E	321089N	350	64	52	bedding	Limestone	Massive	Calcareous		
CC	3991210E	321029N	351	66	60	bedding	Limestone	Ribboned	Massive	Dolomite	

QUAD	UTM Easting	UTM Northing	STATION	STRIKE	DIP	FEATURE	DOMINANT LITHOLOGY/UNIT	DESCRIPTION 1	DESCRIPTION 2	OTHER LITHOLOGY/UNIT 1	OTHER LITHOLOGY/UNIT 2
CC	3991333E	321311N	352	55	49	bedding	Limestone	Massive	Calcareous		
CC	3991299E	321336N	353	0	0	float	Limestone	Massive	Calcareous		
CC	3991222E	321446N	354	274	61	bedding	Limestone	Ribboned	Massive	Dolomite	
CC	3991169E	321429N	355	0	0	float	Limestone	Ribboned	Massive	Dolomite	
CC	3991289E	321423N	356	0	0	float	Limestone	Ribboned	Massive	Dolomite	
CC	3991467E	321383N	357	59	54	bedding	Limestone	Ribboned	Massive	Dolomite	
CC	3991471E	321439N	358	59	45	bedding	Limestone	Ribboned	Massive	Dolomite	
CC	3991461E	321234N	359	0	0	float	Shale	Shaly	Fissile	Nolichucky Shale	
CC	3991382E	321144N	360	0	0	float	Shale	Shaly	Fissile	Nolichucky Shale	
CC	3994056E	323894N	361	43	51	bedding	Limestone	Ribboned	Interbedded	Dolomite	Alluvium
CC	3993603E	324080N	362	50	75	bedding	Limestone	Massive	Oolitic	Maynardville Limestone	
CC	3993691E	324079N	363	44	43	bedding	Limestone	Ribboned	Oolitic	Maynardville Limestone	Dolomite
CC	3993687E	324116N	364	49	71	bedding	Limestone	Ribboned	Oolitic	Maynardville Limestone	Dolomite
CC	3993792E	323996N	365	0	0	float	Alluvium	Unconsolidated			
CC	3993460E	324084N	366	49	70	bedding	Shale	Shaly	Calcareous	Siltstone	
CC	3993485E	324132N	367	51	66	bedding	Shale	Shaly	Calcareous	Siltstone	
CC	3993535E	324161N	368	48	51	bedding	Dolomite	Shaly	Interbedded	Shale	Limestone
CC	3993513E	324206N	369	49	64	bedding	Limestone	Ribboned	Massive	Dolomite	
CC	3993386E	324425N	370	50	36	bedding	Limestone	Massive	Silty		
CC	3993116E	324254N	371	53	47	bedding	Limestone	Massive	Silty	Dolomite	
CC	3993457E	324301N	372	300	52	joint	Limestone	Massive	Oolitic	Dolomite	
CC	3993362E	324010N	373	50	66	bedding	Limestone	Ribboned	Massive	Dolomite	
CC	3994118E	324910N	374	0	0	float	Shale	Fissile		Nolichucky Shale	
CC	3994154E	324978N	375	0	0	float	Shale	Fissile		Nolichucky Shale	
CC	3994185E	325037N	376	0	0	float	Shale	Fissile		Nolichucky Shale	
CC	3991783E	322035N	378	46	45	bedding	Dolomite	Ribboned	Silty	Honaker Dolomite	
CC	3991726E	322054N	379	58	50	bedding	Dolomite	Ribboned	Massive	Honaker Dolomite	
CC	3991899E	322118N	380	70	56	bedding	Dolomite	Ribboned	Interbedded	Limestone	
CC	3992001E	322077N	382	348	28	bedding	Limestone	Ribboned	Interbedded	Dolomite	
CC	3991933E	322046N	383	68	46	bedding	Limestone	Ribboned	Interbedded	Dolomite	
CC	3996410E	326742N	384	42	55	bedding	Limestone	Ribboned	Calcareous	Dolomite	
CC	3988549E	326420N	385	0	0	float	Shale	Fissile		Nolichucky Shale	
CC	3988568E	326391N	386	0	0	float	Limestone	Massive		Maynardville Limestone	
CC	3991930E	327965N	387	37	62	bedding	Limestone	Massive			
CC	3991955E	327933N	388	39	60	bedding	Limestone	Massive			

QUAD	UTM Easting	UTM Northing	STATION	STRIKE	DIP	FEATURE	DOMINANT LITHOLOGY/UNIT	DESCRIPTION 1	DESCRIPTION 2	OTHER LITHOLOGY/UNIT 1	OTHER LITHOLOGY/UNIT 2
CC	3992562E	325706N	389	0	0	float	Limestone	Ribboned		Dolomite	
CC	3992628E	325647N	390	266	72	bedding	Limestone	Massive			
CC	3992747E	325746N	391	273	64	bedding	Limestone	Massive	Oolitic		
CC	3992688E	325678N	392	262	84	bedding	Limestone	Ribboned	Massive	Dolomite	
CC	3988115E	324386N	393	301	15	bedding	Limestone	Ribboned	Interbedded	Dolomite	Maryville Limestone
CC	3988077E	324281N	394	325	7	bedding	Limestone	Ribboned	Interbedded	Dolomite	Maryville Limestone
CC	3988178E	324488N	396	8	16	bedding	Limestone	Ribboned	Interbedded	Dolomite	Maryville Limestone
CC	3988292E	324305N	397	44	28	bedding	Limestone	Ribboned	Interbedded	Dolomite	Maryville Limestone
CC	3988198E	324254N	398	75	27	bedding	Limestone	Ribboned	Interbedded	Dolomite	Maryville Limestone
CC	3986588E	322226N	399	69	25	bedding	Limestone	Ribboned	Interbedded	Dolomite	Maryville Limestone
CC	3986587E	322367N	400	71	26	bedding	Limestone	Ribboned	Shaly	Dolomite	Maryville Limestone
CC	3986990E	325358N	401	68	66	bedding	Limestone	Ribboned	Banded	Dolomite	Maryville Limestone
CC	3986764E	324656N	402	0	0	float	Shale	Fissile		Nolichucky Shale	
CC	3991054E	328251N	403	57	67	bedding	Limestone	Interbedded		Dolomite	
CC	3988814E	323019N	404	0	0	float	Other	Cherty	Siliceous		
CC	3988832E	323184N	405	0	0	float	Other	Cherty	Unconsolidated		
CC	3989169E	322712N	406	218	65	bedding	Shale	Fissile		Nolichucky Shale	
CC	3989144E	322738N	407	38	64	overturned bedding	Dolomite	Shaly	Silty	Limestone	
CC	3989527E	326412N	408	38	64	bedding	Shale	Fissile		Nolichucky Shale	
CC	3987262E	326347N	410	323	90	joint	Dolomite	Massive			
CC	3987214E	326322N	411	52	50	bedding	Dolomite	Massive			
CC	3987415E	326393N	412	55	42	bedding	Dolomite	Ribboned	Massive		
CC	3987567E	326456N	413	52	36	bedding	Limestone	Ribboned	Cherty	Dolomite	
CC	3987661E	326476N	414	52	43	bedding	Limestone	Ribboned	Massive	Dolomite	
CC	3987735E	326506N	415	76	90	bedding	Limestone	Ribboned	Cherty	Dolomite	Copper Ridge Dolomite
CC	3987732E	326337N	417	0	0	float	Sandstone	Sandy		Middle Sevier Shale	
CC	3987797E	326443N	418	45	29	bedding	Limestone	Cherty	Ribboned	Dolomite	
CC	3987821E	326529N	419	49	22	bedding	Limestone	Cherty	Ribboned	Dolomite	
CC	3997414E	327848N	420	57	61	bedding	Limestone	Ribboned	Interbedded	Dolomite	
CC	3997188E	327901N	421	0	0	float	Other	Cherty		Copper Ridge Dolomite	
CC	3989459E	322819N	422	43	57	overturned bedding	Dolomite	Shaly			
CC	3989485E	322855N	423	0	0	float	Shale	Fissile		Nolichucky Shale	
CC	3989556E	322669N	424	0	0	float	Siltstone	Silty	Shaly	Dolomite	
CC	3989823E	322958N	425	50	25	bedding	Shale	Fissile		Nolichucky Shale	
CC	3989901E	323003N	426	0	0	float	Shale	Fissile	Shaly	Dolomite	

QUAD	UTM Easting	UTM Northing	STATION	STRIKE	DIP	FEATURE	DOMINANT LITHOLOGY/UNIT	DESCRIPTION 1	DESCRIPTION 2	OTHER LITHOLOGY/UNIT 1	OTHER LITHOLOGY/UNIT 2
CC	3989737E	322967N	428	0	0	float	Dolomite	Massive			
CC	3995718E	327314N	429	51	90	bedding	Dolomite	Massive			
CC	3995793E	327383N	431	57	90	bedding	Limestone	Ribboned		Dolomite	
CC	3995845E	327449N	432	56	90	bedding	Limestone	Ribboned		Dolomite	
CC	3995891E	327110N	433	0	0	float	Other	Cherty			
CC	3992012E	322249N	437	55	34	bedding	Limestone	Ribboned	Massive	Dolomite	
CC	3991908E	322231N	438	32	81	bedding	Dolomite	Massive			
CC	3992502E	322932N	440	40	75	bedding	Shale	Fissile		Nolichucky Shale	
CC	3993270E	320962N	442	54	39	bedding	Maryville Limestone	Ribboned	Banded	Limestone	Dolomite
CC	3993180E	321018N	443	49	26	bedding	Maryville Limestone	Ribboned	Banded	Limestone	Dolomite
CC	3993138E	320919N	445	53	35	bedding	Dolomite	Massive			
CC	3992667E	321267N	446	0	0	float	Dolomite	Massive			
CC	3992526E	321479N	447	169	58	bedding	Dolomite	Massive		Copper Ridge Dolomite	
CC	3992543E	321449N	448	274	90	bedding	Dolomite	Massive		Copper Ridge Dolomite	
CC	3992632E	321361N	449	0	0	float	Dolomite	Massive		Copper Ridge Dolomite	
CC	3993312E	320877N	450	0	0	float	Dolomite	Massive		Sandstone	
CC	3993395E	320929N	451	61	51	bedding	Dolomite	Massive	Massive		
CC	3993477E	320931N	453	178	52	joint	Limestone	Interbedded	Ribboned	Dolomite	
CC	3993530E	320879N	456	183	65	joint	Limestone	Interbedded	Ribboned	Dolomite	
CC	3993597E	320865N	457	75	75	bedding	Limestone	Interbedded	Ribboned	Dolomite	
CC	3993634E	320827N	458	75	90	bedding	Limestone	Interbedded	Ribboned	Dolomite	
CC	3993594E	320773N	459	76	90	bedding	Limestone	Interbedded	Ribboned	Dolomite	
CC	3993383E	320725N	463	59	29	bedding	Limestone	Interbedded	Ribboned	Dolomite	
CC	3993428E	320798N	464	59	32	bedding	Limestone	Interbedded	Ribboned	Dolomite	
CC	3993181E	320089N	465	0	0	float	Shale	Fissile		Nolichucky Shale	
CC	3993220E	320132N	466	0	0	float	Shale	Fissile		Nolichucky Shale	
CC	3993387E	320217N	467	0	0	float	Limestone	Massive	Ribboned	Dolomite	
CC	3993343E	320225N	468	246	45	bedding	Shale	Fissile	Silty	Nolichucky Shale	
CC	3993312E	320263N	469	0	0	float	Shale	Fissile		Nolichucky Shale	
CC	3993349E	320310N	470	46	26	bedding	Shale	Fissile		Nolichucky Shale	
CC	3993385E	320357N	471	0	0	float	Shale	Fissile		Nolichucky Shale	
CC	3993411E	320576N	472	57	40	bedding	Limestone	Massive	Ribboned	Dolomite	Maynardville Limestone
CC	3993389E	320600N	473	55	36	bedding	Limestone	Massive	Ribboned	Dolomite	Maynardville Limestone
CC	3993542E	320610N	474	60	69	bedding	Limestone	Massive	Ribboned	Dolomite	Maynardville Limestone
CC	3993543E	320611N	475	266	90	cleavage	Shale			Nolichucky Shale	

QUAD	UTM Easting	UTM Northing	STATION	STRIKE	DIP	FEATURE	DOMINANT LITHOLOGY/UNIT	DESCRIPTION 1	DESCRIPTION 2	OTHER LITHOLOGY/UNIT 1	OTHER LITHOLOGY/UNIT 2
CC	3993459E	320744N	476	60	62	bedding	Limestone	Interbedded	Ribboned	Dolomite	Sandstone
CC	3993568E	320702N	477	77	84	bedding	Limestone	Massive		Dolomite	Maynardville Limestone
CC	3993369E	320541N	478	358	76	cleavage	Limestone	Massive		Dolomite	Maynardville Limestone
CC	3993347E	320501N	479	60	43	bedding	Limestone	Massive		Dolomite	Maynardville Limestone
CC	3993273E	320544N	480	49	42	bedding	Limestone	Massive		Dolomite	
CC	3993186E	320599N	481	0	0	float	Sandstone	Sandy			
CC	3993269E	320709N	482	49	36	bedding	Dolomite	Massive	Interbedded	Limestone	Sandstone
CC	3993146E	320512N	483	0	0	float	Sandstone				
CC	3993299E	320433N	484	55	39	bedding	Limestone	Massive	Ribboned	Dolomite	
CC	3993353E	320391N	485	55	34	bedding	Dolomite	Shaly	Fissile	Shale	Nolichucky Shale
CC	3993447E	320503N	486	56	65	bedding	Shale	Fissile		Nolichucky Shale	
CC	3993884E	320700N	487	102	61	bedding	Limestone	Silty	Calcareous		
CC	3993864E	320645N	488	0	0	float	Sandstone	Sandy	Siliceous		
CC	3993763E	320582N	489	0	0	float	Limestone	Silty	Calcareous		
CC	3993734E	320440N	490	82	49	bedding	Dolomite	Shaly	Silty	Limestone	
CC	3993544E	320517N	491	0	0	float	Dolomite	Massive			
CC	3993617E	320451N	492	101	34	bedding	Limestone	Massive			
CC	3993686E	320407N	493	0	0	float	Other	Cherty			
CC	3993727E	320338N	494	100	33	bedding	Limestone	Shaly		Dolomite	
CC	3993831E	320306N	495	87	38	bedding	Limestone	Shaly		Dolomite	
CC	3990012E	321731N	496	0	0	float	Shale	Fissile		Lower Sevier Shale	
CC	3989897E	321723N	497	0	0	float	Limestone	Massive			
CC	3989658E	321645N	498	290	51	bedding	Dolomite	Ribboned	Ribboned	Dolomite	
CC	3989654E	321744N	499	301	24	bedding	Dolomite	Ribboned	Ribboned	Dolomite	
CC	3989531E	321997N	500	318	44	bedding	Shale	Fissile		Nolichucky Shale	
CC	3989286E	322074N	501	0	0	float	Dolomite	Massive			
CC	3989371E	322035N	502	0	0	float					
CC	3989450E	322023N	503	63	41	bedding	Shale	Fissile		Nolichucky Shale	
CC	3989754E	321943N	504	0	0	float	Other	Cherty			
CC	3990082E	321678N	505	75	31	bedding	Shale	Fissile		Lower Sevier Shale	
CC	3990164E	321622N	506	0	0	float	Shale	Fissile		Lower Sevier Shale	
CC	3989978E	321233N	507	101	65	bedding	Dolomite	Shaly			
CC	3990025E	320983N	509	0	0	float	Shale	Fissile		Lower Sevier Shale	
CC	3989995E	321061N	510	0	0	float	Shale	Fissile		Lower Sevier Shale	
CC	3993730E	328448N	512	64	55	bedding	Limestone	Ribboned	Massive	Dolomite	

QUAD	UTM Easting	UTM Northing	STATION	STRIKE	DIP	FEATURE	DOMINANT LITHOLOGY/UNIT	DESCRIPTION 1	DESCRIPTION 2	OTHER LITHOLOGY/UNIT 1	OTHER LITHOLOGY/UNIT 2
CC	3993739E	328493N	513	66	66	bedding	Limestone	Ribboned	Massive	Dolomite	
CC	3993775E	328383N	514	0	0	float	Dolomite	Massive			
CC	3993806E	322001N	515	62	50	bedding	Limestone	Ribboned	Interbedded	Dolomite	Conococheague Limestone
CC	3993803E	321871N	516	172	68	cleavage	Limestone	Ribboned	Interbedded	Dolomite	Conococheague Limestone
CC	3993725E	321863N	517	59	46	bedding	Limestone	Ribboned	Interbedded	Dolomite	Conococheague Limestone
CC	3993809E	321613N	520	0	0	float	Alluvium	Sandy	Siliceous		
CC	3993914E	321705N	521	0	0	float	Alluvium	Sandy	Siliceous		
CC	3993934E	321748N	522	65	65	bedding	Limestone	Ribboned	Interbedded	Dolomite	Conococheague Limestone
CC	3993937E	321846N	523	57	69	bedding	Limestone	Ribboned	Interbedded	Dolomite	Conococheague Limestone
CC	3993885E	321900N	524	62	51	bedding	Dolomite	Massive			
CC	3993898E	322053N	525	0	0	float	Limestone	Massive	Ribboned	Dolomite	Conococheague Limestone
CC	3993261E	321515N	526	0	0	float	Alluvium				
CC	3992996E	321339N	527	0	0	float	Alluvium				
CC	3992960E	321399N	528	56	64	bedding	Dolomite	Ribboned	Interbedded	Limestone	Conococheague Limestone
CC	3992861E	321894N	529	0	0	float	Alluvium				
CC	3992928E	321705N	530	0	0	float	Alluvium				
CC	3993168E	321646N	531	0	0	float	Alluvium				
CC	3993224E	321848N	532	72	70	bedding	Dolomite	Massive			
CC	3993428E	321788N	533	80	43	bedding	Limestone	Oolitic	Silty	Dolomite	
CC	3994075E	321674N	535	0	0	float	Alluvium				
CC	3994356E	321658N	536	0	0	float	Alluvium				
CC	3994364E	321696N	537	68	72	bedding	Limestone	Ribboned		Dolomite	
CC	3994085E	321939N	538	0	0	float	Limestone	Laminated		Conococheague Limestone	
CC	3994148E	322034N	539	69	90	bedding	Limestone	Ribboned	Interbedded	Conococheague Limestone	Dolomite
CC	3994277E	322142N	540	56	75	bedding	Limestone	Ribboned	Interbedded	Conococheague Limestone	Dolomite
CC	3994302E	322264N	541	240	68	bedding	Limestone	Ribboned	Interbedded	Conococheague Limestone	Dolomite
CC	3990798E	322113N	542	79	70	bedding	Limestone	Ribboned		Dolomite	Conococheague Limestone
CC	3990798E	322113N	542	79	70	overturned bedding	Limestone	Ribboned		Dolomite	Conococheague Limestone
CC	3990988E	321941N	543	39	33	bedding	Limestone	Ribboned	Interbedded	Dolomite	Jonesboro Limestone
CC	3991150E	322008N	544	41	42	bedding	Limestone	Ribboned	Interbedded	Dolomite	Jonesboro Limestone
CC	3991096E	321938N	545	352	90	joint	Limestone	Ribboned	Interbedded	Dolomite	Jonesboro Limestone
CC	3991042E	321928N	546	79	55	bedding	Limestone	Ribboned	Interbedded	Dolomite	Jonesboro Limestone
CC	3996855E	320278N	548	55	42	bedding	Dolomite	Massive		Limestone	Mascot Dolomite
CC	3996779E	320253N	549	55	50	bedding	Limestone	Massive		Limestone	Lenoir Limestone
CC	3996713E	320258N	551	67	59	cleavage	Shale	Fissile		Lower Sevier Shale	

QUAD	UTM Easting	UTM Northing	STATION	STRIKE	DIP	FEATURE	DOMINANT LITHOLOGY/UNIT	DESCRIPTION 1	DESCRIPTION 2	OTHER LITHOLOGY/UNIT 1	OTHER LITHOLOGY/UNIT 2
CC	3988605E	321473N	552	0	0	float	Shale	Fissile		Nolichucky Shale	
CC	3988672E	321001N	553	0	0	bedding	Limestone	Ribboned	Laminated	Dolomite	Shale
CC	3988820E	320656N	554	44	31	bedding	Limestone	Ribboned	Massive	Dolomite	Conococheague Limestone
CC	3989518E	320282N	555	91	90	bedding	Limestone	Interbedded	Ribboned	Dolomite	Jonesboro Limestone
CC	3989526E	320338N	556	21	35	joint	Limestone	Interbedded	Ribboned	Dolomite	Jonesboro Limestone
CC	3989400E	320428N	557	76	84	bedding	Limestone	Interbedded	Ribboned	Dolomite	Sandstone
CC	3989362E	320460N	558	72	72	bedding	Limestone	Interbedded	Ribboned	Dolomite	Sandstone
CC	3989310E	320469N	559	75	74	bedding	Limestone	Interbedded	Ribboned	Dolomite	Other
CC	3988091E	321112N	560	0	0	float	Conococheague Limestone	Ribboned		Limestone	
CC	3987963E	321106N	561	76	74	bedding	Shale	Interbedded	Calcareous	Lower Sevier Shale	Limestone
CC	3988027E	321117N	562	286	43	bedding	Shale	Interbedded	Calcareous	Lower Sevier Shale	Limestone
CC	3986777E	320699N	564	33	90	bedding	Shale	Silty	Fissile	Lower Sevier Shale	Nolichucky Shale
CC	3986868E	320643N	565	0	0	float	Shale	Fissile		Lower Sevier Shale	
CC	3986956E	320646N	566	0	0	float	Shale	Fissile		Lower Sevier Shale	
CC	3990833E	319914N	568	0	0	float	Other	Cherty			
CC	3990755E	319929N	569	0	0	float	Other	Cherty			
CC	3990787E	319841N	570	72	73	bedding	Shale	Fissile	Sandy	Nolichucky Shale	Sandstone
CC	3990756E	320463N	571	0	0	float	Conococheague Limestone	Cherty		Other	
CC	3995144E	325642N	572	60	62	bedding	Limestone	Massive	Calcareous		
CC	3995235E	325530N	573	0	0	float	Dolomite	Cherty		Other	
CC	3995427E	325626N	574	65	72	bedding	Limestone	Massive	Ribboned	Conococheague Limestone	Dolomite
CC	3995494E	325632N	575	0	0	float	Other	Cherty			
CC	3995685E	325480N	576	60	58	bedding	Limestone	Ribboned	Massive	Dolomite	Conococheague Limestone
CC	3996244E	325668N	577	50	56	bedding	Limestone	Ribboned	Massive	Dolomite	
CC	3996356E	325659N	578	54	42	bedding	Limestone	Ribboned	Massive	Dolomite	
CC	3996507E	325549N	580	0	0	float	Limestone	Ribboned	Massive	Dolomite	
CC	3996216E	325733N	581	52	45	bedding	Limestone	Ribboned	Massive	Dolomite	
CC	3996370E	325561N	582	50	42	bedding	Limestone	Ribboned	Massive	Dolomite	
CC	3996413E	325623N	584	315	58	joint	Limestone	Ribboned	Interbedded	Dolomite	
CC	3996592E	325520N	585	58	70	bedding	Limestone	Ribboned	Silty	Dolomite	
CC	3996631E	325501N	586	61	57	bedding	Limestone	Ribboned	Silty	Dolomite	
CC	3996836E	325356N	587	0	0	float	Limestone	Ribboned	Silty	Dolomite	
CC	3996855E	325431N	588	69	90	bedding	Limestone	Ribboned	Silty	Dolomite	
CC	3996869E	325621N	589	241	49	bedding	Limestone	Ribboned	Silty	Dolomite	
CC	3996783E	325667N	590	56	59	bedding	Limestone	Ribboned	Silty	Dolomite	

QUAD	UTM Easting	UTM Northing	STATION	STRIKE	DIP	FEATURE	DOMINANT LITHOLOGY/UNIT	DESCRIPTION 1	DESCRIPTION 2	OTHER LITHOLOGY/UNIT 1	OTHER LITHOLOGY/UNIT 2
CC	3996396E	326428N	591	246	54	bedding	Limestone	Ribboned	Cherty	Dolomite	
CC	3996359E	326365N	592	246	46	bedding	Limestone	Ribboned	Cherty	Dolomite	
CC	3991786E	322272N	593	68	50	bedding	Dolomite	Massive			
CC	3991718E	322257N	594	70	46	bedding	Shale			Nolichucky Shale	
CC	3996390E	325997N	597	48	54	bedding	Limestone	Ribboned	Interbedded	Dolomite	
CC	3996477E	326070N	599	50	55	bedding	Limestone	Ribboned	Interbedded	Dolomite	
CC	3996419E	325936N	600	52	58	bedding	Dolomite	Ribboned	Interbedded	Limestone	
CC	3996417E	325865N	601	58	40	bedding	Dolomite	Ribboned	Massive	Limestone	
CC	3996533E	325868N	602	0	0	float	Dolomite	Interbedded	Massive	Limestone	
CC	3996322E	325921N	603	55	57	bedding	Limestone	Ribboned	Massive	Dolomite	
CC	3992264E	323191N	605	39	51	bedding	Limestone	Ribboned	Massive	Dolomite	
CC	3992182E	323197N	607	41	53	bedding	Siltstone	Shaly	Laminated	Limestone	Dolomite
CC	3992188E	323123N	608	48	53	bedding	Dolomite	Interbedded	Ribboned	Limestone	
CC	3992186E	323047N	610	41	50	bedding	Limestone	Ribboned	Calcareous	Dolomite	
CC	3992211E	322999N	612	0	0	float	Shale	Fissile		Nolichucky Shale	
CC	3992122E	322993N	613	39	46	bedding	Limestone	Massive	Ribboned	Maynardville Limestone	
CC	3992030E	323000N	614	50	50	bedding	Limestone	Ribboned	Massive	Dolomite	
CC	3992114E	323180N	618	45	59	bedding	Limestone	Ribboned	Massive	Dolomite	
CC	3992081E	323210N	619	40	50	bedding	Dolomite	Shaly			
CC	3992182E	323296N	620	42	33	bedding	Dolomite	Shaly			
CC	3992543E	323740N	621	52	40	bedding	Limestone	Ribboned	Interbedded	Dolomite	Conococheague Limestone
CC	3992578E	323793N	622	51	60	bedding	Limestone	Interbedded	Ribboned	Dolomite	Conococheague Limestone
CC	3992630E	323858N	623	55	49	bedding	Limestone	Interbedded	Ribboned	Dolomite	Conococheague Limestone
CC	3992701E	324030N	624	57	52	bedding	Dolomite	Interbedded	Ribboned	Limestone	Conococheague Limestone
CC	3992746E	324139N	625	55	50	bedding	Dolomite	Interbedded	Ribboned	Limestone	Conococheague Limestone
CC	3992660E	324072N	626	50	47	bedding	Dolomite	Interbedded	Shaly	Limestone	Conococheague Limestone
CC	3992547E	323586N	627	70	53	bedding	Dolomite	Ribboned	Massive	Limestone	Conococheague Limestone
CC	3992779E	322962N	628	53	72	bedding	Dolomite	Massive	Massive	Honaker Dolomite	
CC	3993120E	323000N	632	47	34	bedding	Limestone	Banded	Ribboned	Dolomite	
CC	3992977E	322997N	634	40	51	bedding	Dolomite	Massive		Honaker Dolomite	
CC	3992798E	323199N	636	56	61	bedding	Shale	Silty	Fissile	Siltstone	Nolichucky Shale
CC	3990305E	320721N	639	0	0	float	Other	Cherty		Conococheague Limestone	
CC	3990259E	320610N	640	0	0	float	Other	Cherty		Jonesboro Limestone	
CC	3990045E	320850N	641	75	22	bedding	Shale			Dolomite	Lower Sevier Shale
CC	3990037E	320933N	642	0	0	float	Shale	Cherty	Fissile	Other	

QUAD	UTM Easting	UTM Northing	STATION	STRIKE	DIP	FEATURE	DOMINANT LITHOLOGY/UNIT	DESCRIPTION 1	DESCRIPTION 2	OTHER LITHOLOGY/UNIT 1	OTHER LITHOLOGY/UNIT 2
CC	3990762E	321973N	643	83	66	overturned bedding	Dolomite	Banded	Cherty	Limestone	Honaker Dolomite
CC	3990760E	321273N	644	50	41	bedding	Dolomite	Massive	Banded	Limestone	Honaker Dolomite
CC	3986868E	320211N	645	243	68	bedding	Siltstone	Silty	Silty	Limestone	
CC	3986897E	320057N	647	89	71	bedding	Dolomite	Shaly	Massive	Siltstone	Mascot Dolomite
CC	3987020E	319993N	648	95	79	bedding	Limestone	Calcareous	Shaly		
CC	3987052E	320117N	649	0	0	float	Lenoir Limestone	Cherty		Other	
CC	3987337E	319983N	651	2	25	bedding	Siltstone	Shaly	Silty	Shale	
CC	3987333E	319955N	652	66	40	bedding	Limestone	Massive	Thrombolitic		
CC	3987293E	320305N	653	66	74	bedding	Limestone	Massive			
CC	3987291E	320212N	654	89	31	bedding	Limestone	Massive		Dolomite	
CC	3987410E	320935N	655	0	0	float	Shale	Fissile		Lower Sevier Shale	
CC	3987503E	320962N	656	0	0	float	Siltstone	Silty		Other	
CC	3985675E	320512N	657	53	60	bedding	Limestone	Massive	Ribboned	Dolomite	Maynardville Limestone
CC	3985658E	319737N	658	55	90	bedding	Dolomite	Shaly		Siltstone	Honaker Dolomite
CC	3985640E	319812N	659	144	65	bedding	Dolomite	Shaly	Silty	Honaker Dolomite	
CC	3985682E	319897N	660	27	51	overturned bedding	Dolomite	Shaly		Siltstone	Honaker Dolomite
CC	3985719E	319877N	661	295	79	bedding	Siltstone	Silty		Shale	Dolomite
CC	3985723E	319957N	664	31	79	overturned bedding	Dolomite				
CC	3985611E	320105N	666	0	0	float	Other	Cherty			
CC	3985659E	320428N	667	55	51	bedding	Shale			Nolichucky Shale	Honaker Dolomite
CC	3985699E	320199N	669	0	0	float	Other	Cherty			
CC	3985762E	320112N	670	96	0	fold hinge	Dolomite	Massive	Silty	Honaker Dolomite	
CC	3985722E	320068N	671	39	54	overturned bedding	Dolomite	Massive	Silty	Honaker Dolomite	
CC	3985819E	320048N	672	229	85	bedding	Dolomite	Massive	Silty	Honaker Dolomite	
CC	3985861E	319975N	674	60	78	bedding	Shale	Fissile	Interbedded	Dolomite	Nolichucky Shale
CC	3985885E	319949N	675	312	73	bedding	Shale			Siltstone	Nolichucky Shale
CC	3985784E	319797N	677	0	0	float	Shale	Fissile		Siltstone	Nolichucky Shale
CC	3985819E	319781N	678	58	90	bedding	Shale	Fissile		Siltstone	Nolichucky Shale
CC	3985923E	319787N	679	61	54	bedding	Shale	Fissile	Interbedded	Siltstone	Limestone
CC	3986058E	319841N	680	0	0	float		Cherty			
CC	3986255E	320397N	681	0	0	float	Colluvium	Cherty		Other	
CC	3986126E	320348N	682	0	0	float	Shale	Silty		Nolichucky Shale	
CC	3986093E	320305N	683	0	0	float	Shale	Silty		Nolichucky Shale	
CC	3986412E	320626N	684	64	70	bedding	Shale	Fissile	Interbedded	Nolichucky Shale	Limestone
CC	3986439E	320833N	687	236	62	bedding	Dolomite	Laminated	Silty	Honaker Dolomite	

QUAD	UTM Easting	UTM Northing	STATION	STRIKE	DIP	FEATURE	DOMINANT LITHOLOGY/UNIT	DESCRIPTION 1	DESCRIPTION 2	OTHER LITHOLOGY/UNIT 1	OTHER LITHOLOGY/UNIT 2
CC	3986623E	320779N	688	0	0	float	Shale	Fissile		Nolichucky Shale	
CC	3986305E	320832N	689	53	41	bedding	Dolomite	Silty		Honaker Dolomite	
CC	3987046E	319956N	691	97	40	bedding	Conglomerate	Shaly	Interbedded	Dolomite	
CC	3986181E	321102N	692	68	48	bedding	Dolomite	Banded	Interbedded	Limestone	Honaker Dolomite
CC	3986135E	321171N	694	61	38	bedding	Siltstone	Fissile		Shale	Rogersville Shale
CC	3986052E	321139N	695	69	34	bedding	Dolomite	Banded	Interbedded	Limestone	Honaker Dolomite
CC	3986033E	321095N	696	71	44	bedding	Dolomite	Banded	Interbedded	Limestone	Honaker Dolomite
CC	3985753E	321623N	697	86	60	bedding	Limestone	Massive	Calcareous	Conococheague Limestone	Other
CC	3985759E	321678N	698	90	55	bedding	Limestone	Massive	Calcareous	Conococheague Limestone	
CC	3985778E	321799N	699	88	69	bedding		Ribboned	Banded		
CC	3985584E	321760N	700	82	66	bedding	Limestone	Ribboned	Interbedded	Dolomite	Conococheague Limestone
CC	3986581E	322589N	701	85	32	bedding	Dolomite	Shaly	Silty	Siltstone	
CC	3986549E	322053N	702	65	37	bedding	Dolomite	Massive		Limestone	Honaker Dolomite
CC	3986495E	321966N	704	65	43	bedding	Limestone	Banded	Interbedded	Dolomite	Honaker Dolomite
CC	3986464E	322022N	705	65	46	bedding	Siltstone	Silty		Dolomite	
CC	3986428E	322079N	706	65	38	bedding	Limestone	Ribboned	Calcareous	Dolomite	
CC	3986195E	321999N	707	67	21	bedding	Dolomite	Silty			
CC	3985856E	321906N	708	0	0	float	Shale	Fissile		Nolichucky Shale	
CC	3985827E	321831N	709	0	0	float	Shale	Fissile		Nolichucky Shale	
CC	3985906E	321914N	710	0	0	float	Dolomite	Massive		Honaker Dolomite	
CC	3986191E	321808N	711	50	31	bedding	Dolomite	Silty	Massive	Limestone	Honaker Dolomite
CC	3985797E	321548N	712	0	0	float	Shale	Fissile		Nolichucky Shale	
CC	3990029E	325382N	713	0	0	float	Shale	Fissile	Fissile		
CC	3989964E	325387N	714	0	0	float	Other	Cherty			
CC	3988832E	324009N	715	0	0	float	Shale	Fissile	Cherty		
CC	3989209E	324112N	716	219	41	bedding	Dolomite	Cherty	Massive	Limestone	Honaker Dolomite
CC	3989192E	324166N	717	69	39	bedding	Shale	Fissile	Silty	Nolichucky Shale	
CC	3989276E	323957N	718	0	0	float	Breccia	Interbedded	Massive	Dolomite	Limestone
CC	3988502E	325951N	720	252	35	bedding	Dolomite	Massive		Shale	Honaker Dolomite
CC	3988604E	325997N	722	253	37	bedding	Limestone	Ribboned	Massive	Dolomite	
CC	3988725E	326044N	723	237	38	bedding	Limestone	Ribboned	Cherty	Dolomite	Maynardville Limestone
CC	3988782E	326076N	725	255	40	bedding	Limestone	Massive	Ribboned	Dolomite	
CC	3988431E	326032N	726	0	0	float	Dolomite	Massive		Honaker Dolomite	
CC	3989569E	326313N	727	0	0	float	Dolomite	Massive		Honaker Dolomite	
CC	3988160E	326062N	728	0	0	float	Dolomite	Massive		Honaker Dolomite	

QUAD	UTM Easting	UTM Northing	STATION	STRIKE	DIP	FEATURE	DOMINANT LITHOLOGY/UNIT	DESCRIPTION 1	DESCRIPTION 2	OTHER LITHOLOGY/UNIT 1	OTHER LITHOLOGY/UNIT 2
CC	3988136E	326111N	730	34	49	bedding	Shale	Fissile	Interbedded	Nolichucky Shale	Siltstone
CC	3987924E	326123N	731	0	0	float	Conococheague Limestone				
CC	3988074E	325993N	732	22	35	bedding	Dolomite	Massive		Honaker Dolomite	
CC	3988676E	322122N	733	46	53	bedding	Limestone	Massive	Fissile	Nolichucky Shale	Shale
CC	3988652E	322300N	734	0	0	float	Limestone	Massive	Fissile	Nolichucky Shale	Shale
CC	3987880E	321373N	736	0	0	float	Shale	Fissile		Nolichucky Shale	
CC	3987398E	320270N	737	87	39	bedding	Limestone	Massive	Cherty	Breccia	
CC	3987441E	320221N	739	84	83	bedding	Limestone	Massive	Fissile	Dolomite	Shale
CC	3987326E	320304N	740	229	61	bedding	Limestone	Massive	Calcareous	Dolomite	
CC	3987758E	321046N	741	288	59	bedding	Siltstone	Silty	Shaly	Shale	
CC	3987585E	320654N	742	314	46	bedding	Limestone	Massive		Dolomite	Rutledge Limestone
CC	3987598E	320680N	743	22	25	bedding	Dolomite	Massive		Limestone	Honaker Dolomite
CC	3987528E	320525N	744	85	90	bedding	Limestone	Massive		Breccia	
CC	3987504E	320493N	745	0	0	float	Sandstone	Sandy			
CC	3986649E	320359N	746	15	79	bedding	Dolomite	Laminated		Honaker Dolomite	
CC	3986630E	320310N	747	95	90	cleavage	Siltstone	Silty		Dolomite	
CC	3986554E	320275N	748	0	0	float	Dolomite	Silty			
CC	3986532E	320213N	749	9	70	bedding	Dolomite	Silty			
CC	3986471E	320322N	750	11	90	bedding	Dolomite	Silty			
CC	3986140E	320156N	751	0	0	float	Other	Cherty			
CC	3986471E	320173N	752	21	68	bedding	Dolomite	Laminated			
CC	3992277E	331043N	753	82	69	bedding	Limestone	Interbedded		Dolomite	Conococheague Limestone
CC	3992344E	330762N	754	52	69	bedding	Dolomite			Honaker Dolomite	
CC	3992673E	330330N	755	82	0	fold hinge	Dolomite	Interbedded	Massive	Limestone	
CC	3992575E	330063N	756	0	0	float					
CC	3992413E	329973N	757	63	47	bedding	Dolomite	Interbedded		Limestone	
CC	3992186E	329800N	758	67	78	bedding	Limestone	Shaly		Shale	
CC	3991867E	329839N	759	67	77	bedding	Limestone	Interbedded	Silty	Limestone	Maryville Limestone
CC	3991831E	329858N	760	61	73	bedding	Limestone	Interbedded	Silty	Limestone	Maryville Limestone
CC	3991836E	329948N	761	53	83	bedding	Limestone	Interbedded	Massive	Dolomite	Honaker Dolomite
CC	3991744E	329979N	762	59	81	bedding	Limestone	Interbedded	Massive	Dolomite	Honaker Dolomite
CC	3991583E	329847N	763	52	83	bedding	Limestone	Interbedded	Massive	Dolomite	Honaker Dolomite
CC	3991604E	329771N	764	56	74	bedding	Limestone	Interbedded	Massive	Dolomite	Honaker Dolomite
CC	3991588E	329662N	765	68	76	bedding	Limestone	Interbedded	Massive	Dolomite	Honaker Dolomite
CC	3991620E	329527N	766	67	73	bedding	Dolomite	Interbedded	Massive	Limestone	Honaker Dolomite

QUAD	UTM Easting	UTM Northing	STATION	STRIKE	DIP	FEATURE	DOMINANT LITHOLOGY/UNIT	DESCRIPTION 1	DESCRIPTION 2	OTHER LITHOLOGY/UNIT 1	OTHER LITHOLOGY/UNIT 2
CC	3991625E	329350N	767	68	77	bedding	Dolomite	Interbedded		Honaker Dolomite	Limestone
CC	3991564E	329245N	768	63	73	bedding	Dolomite	Interbedded		Honaker Dolomite	Limestone
CC	3991403E	329095N	769	63	62	bedding	Dolomite	Interbedded		Honaker Dolomite	Limestone
CC	3991188E	329130N	770	58	62	bedding	Dolomite	Shaly	Interbedded	Shale	Honaker Dolomite
CC	3991054E	328755N	771	68	51	bedding	Dolomite	Interbedded	Interbedded	Limestone	Honaker Dolomite
CC	3991275E	328603N	772	57	57	bedding	Dolomite	Interbedded		Limestone	
CC	3991619E	328385N	773	296	84	bedding	Dolomite	Interbedded		Limestone	
CC	3996839E	321471N	774	75	75	bedding	Limestone	Thrombolitic	Massive	Dolomite	Jonesboro Limestone
CC	3996863E	321336N	775	69	55	bedding	Limestone	Thrombolitic	Massive	Dolomite	Jonesboro Limestone
CC	3996851E	321199N	776	0	0	float	Shale	Fissile	Shaly	Lower Sevier Shale	
CC	3996822E	321161N	777	235	51	bedding	Limestone			Lenoir Limestone	Lower Sevier Shale
CC	3996799E	321131N	778	91	69	bedding	Limestone			Lenoir Limestone	Lower Sevier Shale
CC	3996858E	320994N	779	0	0	float	Lower Sevier Shale				
CC	3996945E	320936N	780	0	0	float	Lower Sevier Shale				
CC	3997005E	320864N	781	56	75	cleavage	Lower Sevier Shale				
CC	3996995E	320845N	782	56	75	bedding	Lower Sevier Shale	Interbedded		Lenoir Limestone	
CC	3997046E	320898N	783	242	56	bedding	Lenoir Limestone	Massive			
CC	3997039E	320948N	784	0	0	float	Lower Sevier Shale				
CC	3996953E	321064N	785	54	60	bedding	Lower Sevier Shale				
CC	3996953E	321064N	785	255	68	cleavage	Lower Sevier Shale				
CC	3996921E	321140N	786	0	0	float	Lower Sevier Shale				
CC	3996909E	321197N	787	100	31	bedding	Lenoir Limestone				
CC	3996881E	321395N	788	81	65	bedding	Jonesboro Limestone	Massive	Thrombolitic		
CC	3997924E	322599N	789	0	0	float	Shale			Lower Sevier Shale	
CC	3996229E	321711N	790	88	55	bedding	Limestone			Jonesboro Limestone	
CC	3996229E	321711N	790	234	29	cleavage	Limestone			Jonesboro Limestone	
CC	3996269E	321820N	791	78	56	bedding	Jonesboro Limestone	Massive			
CC	3996363E	321659N	792	152	19	bedding	Limestone			Dolomite	Jonesboro Limestone
CC	3996399E	321583N	793	171	29	bedding	Limestone	Interbedded	Thrombolitic	Dolomite	Jonesboro Limestone
CC	3996366E	321638N	794	303	72	cleavage	Limestone	Interbedded	Thrombolitic	Dolomite	Jonesboro Limestone
CC	3996559E	321336N	795	49	61	bedding	Dolomite			Limestone	
CC	3996514E	321640N	796	0	0	float	Sandstone			Dolomite	
CC	3995198E	321925N	797	85	65	cleavage	Limestone				
CC	3998141E	322974N	798	71	90	cleavage	Lower Sevier Shale	Fissile			
CC	3997896E	322906N	799	54	41	bedding	Dolomite	Massive		Mascot Dolomite	

QUAD	UTM Easting	UTM Northing	STATION	STRIKE	DIP	FEATURE	DOMINANT LITHOLOGY/UNIT	DESCRIPTION 1	DESCRIPTION 2	OTHER LITHOLOGY/UNIT 1	OTHER LITHOLOGY/UNIT 2
CC	3998204E	323072N	800	0	0	float	Lower Sevier Shale	Fissile			
CC	3998757E	324024N	801	0	0	float	Lower Sevier Shale	Fissile			
CC	3998763E	324106N	802	135	55	bedding	Lower Sevier Shale	Fissile			
CC	3998763E	324106N	802	292	82	cleavage	Lower Sevier Shale	Fissile			
CC	3998895E	323967N	803	0	0	float	Lower Sevier Shale	Fissile			
CC	3998916E	323817N	804	0	0	float	Limestone	Massive		Lenoir Limestone	
CC	3998847E	323824N	805	0	0	float	Lower Sevier Shale	Fissile			
CC	3998620E	323738N	806	0	0	float	Other	Cherty			
CC	3996261E	322282N	807	0	0	float	Lower Sevier Shale	Fissile			
CC	3996103E	321733N	808	0	0	float	Lower Sevier Shale	Fissile			
CC	3996731E	323212N	809	81	45	bedding	Lower Sevier Shale	Fissile		Shale	
CC	3996144E	321181N	810	51	75	bedding	Shale	Fissile		Lower Sevier Shale	
CC	3996144E	321181N	810	174	74	cleavage	Shale	Fissile		Lower Sevier Shale	
CC	3996064E	320927N	811	89	55	bedding	Jonesboro Limestone	Cherty			
CC	3996028E	320911N	812	0	0	float	Shale			Lower Sevier Shale	
CC	3995980E	320907N	813	89	50	bedding					
CC	3995980E	320907N	813	109	76	cleavage					
CC	3996078E	320896N	814	0	0	float	Jonesboro Limestone				
CC	3996115E	320950N	815	85	50	bedding	Jonesboro Limestone			Dolomite	
CC	3996177E	321058N	816	70	48	bedding	Jonesboro Limestone	Thrombolitic	Ribboned	Dolomite	
CC	3996238E	320791N	817	48	90	cleavage	Lower Sevier Shale	Fissile			
CC	3996278E	320640N	818	0	0	float	Jonesboro Limestone				
CC	3996714E	320353N	819	240	54	bedding	Lower Sevier Shale	Fissile			
CC	3996725E	322005N	820	256	39	bedding	Lenoir Limestone	Massive	Calcareous	Limestone	
CC	3996626E	322046N	821	0	0	float	Dolomite			Jonesboro Limestone	
CC	3997054E	324971N	822	59	66	bedding	Conococheague Limestone	Ribboned		Limestone	Dolomite
CC	3997094E	324912N	823	82	57	bedding	Conococheague Limestone	Ribboned		Limestone	Dolomite
CC	3997196E	324816N	824	59	66	bedding	Conococheague Limestone	Massive		Limestone	Dolomite
CC	3997437E	324825N	825	54	75	bedding	Limestone	Thrombolitic	Massive	Dolomite	Jonesboro Limestone
CC	3997500E	324834N	826	0	0	float	Lower Sevier Shale				
CC	3997739E	324930N	827	0	0	float	Lower Sevier Shale				
CC	3997930E	325073N	828	0	0	float	Lower Sevier Shale				
CC	3999371E	324550N	829	0	0	float	Lower Sevier Shale				
CC	3999246E	324732N	830	242	72	bedding	Lower Sevier Shale	Fissile			
CC	3996764E	322539N	833	239	56	bedding	Limestone	Massive	Massive	Conococheague Limestone	

QUAD	UTM Easting	UTM Northing	STATION	STRIKE	DIP	FEATURE	DOMINANT LITHOLOGY/UNIT	DESCRIPTION 1	DESCRIPTION 2	OTHER LITHOLOGY/UNIT 1	OTHER LITHOLOGY/UNIT 2
CC	3996195E	322516N	834	0	0	float	Lower Sevier Shale				
CC	3996281E	322531N	835	51	50	bedding	Lenoir Limestone	Massive	Thrombolitic	Jonesboro Limestone	
CC	3996510E	322380N	836	59	79	bedding	Limestone	Ribboned	Massive	Jonesboro Limestone	
CC	3996856E	322918N	837	59	86	bedding	Jonesboro Limestone	Thrombolitic	Ribboned	Mascot Dolomite	
CC	3996939E	322825N	838	61	71	bedding	Limestone	Interbedded	Thrombolitic	Jonesboro Limestone	
CC	3996949E	322711N	839	235	52	bedding	Limestone	Thrombolitic	Cherty	Jonesboro Limestone	
CC	3996869E	322717N	840	0	0	float	Dolomite	Massive			
CC	3997136E	323021N	841	245	75	bedding	Jonesboro Limestone	Ribboned			
CC	3995778E	323146N	842	59	62	bedding	Conococheague Limestone	Massive	Cherty	Dolomite	Sandstone
CC	3995042E	323070N	843	240	75	bedding	Limestone	Thrombolitic	Ribboned	Dolomite	Jonesboro Limestone
CC	3995065E	322856N	844	242	82	bedding	Limestone	Thrombolitic	Ribboned	Dolomite	Jonesboro Limestone
CC	3994550E	323074N	845	80	53	bedding	Jonesboro Limestone	Cherty		Limestone	Dolomite
CC	3995612E	323952N	846	0	0	float	Limestone	Massive	Thrombolitic	Dolomite	Jonesboro Limestone
CC	3995481E	323767N	847	55	41	bedding	Limestone	Interbedded		Dolomite	
CC	3995183E	324048N	848	59	69	bedding	Limestone			Dolomite	
CC	3995158E	324267N	849	65	81	bedding	Limestone	Massive			
CC	3995357E	324539N	850	259	52	bedding	Limestone	Massive	Interbedded	Dolomite	
CC	3995615E	324244N	851	57	45	bedding	Limestone	Interbedded	Ribboned	Dolomite	
CC	3997605E	326494N	852	74	46	bedding	Dolomite	Silty		Conococheague Limestone	
CC	3997794E	326569N	853	74	35	bedding	Conococheague Limestone	Cherty		Limestone	
CC	3997720E	326567N	854	254	66	bedding	Conococheague Limestone	Cherty		Limestone	
CC	3998009E	326136N	855	35	51	bedding	Conococheague Limestone	Cherty		Dolomite	Limestone
CC	3998311E	325528N	856	60	86	bedding	Dolomite	Thrombolitic	Ribboned	Limestone	
CC	3998213E	325528N	857	60	70	bedding	Dolomite	Massive	Interbedded	Conococheague Limestone	Limestone
CC	3998284E	325644N	858	0	0	float	Shale			Lower Sevier Shale	
CC	3998462E	325537N	860	60	86	bedding	Dolomite	Massive	Interbedded		
CC	3997822E	326307N	861	60	40	bedding	Limestone	Interbedded	Cherty	Dolomite	
CC	3989285E	322690N	862	0	0	float	Nolichucky Shale				
CC	3989038E	322231N	863	0	0	float	Nolichucky Shale	Cherty			
CC	3988931E	322250N	864	0	0	float	Nolichucky Shale	Shaly			
CC	3988018E	321278N	865	0	0	float	Shale	Fissile		Nolichucky Shale	
CC	3987789E	320726N	866	0	0	float	Siltstone			Shale	
CC	3987592E	323670N	867	51	28	bedding	Limestone	Ribboned	Banded	Honaker Dolomite	Dolomite
CC	3988637E	323983N	868	49	59	bedding	Shale	Calcareous	Fissile		
CC	3988685E	323947N	869	0	0	float	Limestone	Cherty			

QUAD	UTM Easting	UTM Northing	STATION	STRIKE	DIP	FEATURE	DOMINANT LITHOLOGY/UNIT	DESCRIPTION 1	DESCRIPTION 2	OTHER LITHOLOGY/UNIT 1	OTHER LITHOLOGY/UNIT 2
CC	3988544E	323858N	870	0	0	float	Limestone			Shale	
CC	3986589E	323311N	871	61	60	bedding	Dolomite	Silty		Honaker Dolomite	
CC	3986615E	323367N	872	0	0	float	Limestone	Interbedded	Massive	Dolomite	
CC	3986473E	323346N	873	0	0	float	Shale	Fissile			
CC	3986435E	323338N	874	0	0	float	Shale	Fissile	Cherty		
CC	3986286E	323351N	875	48	77	bedding	Limestone	Interbedded	Ribboned	Conococheague Limestone	Maynardville Limestone
CC	3986411E	323346N	876	50	82	bedding	Maynardville Limestone	Massive		Limestone	
CC	3986271E	323354N	877	59	64	bedding	Limestone	Silty			
CC	3986183E	323371N	878	56	67	bedding	Conococheague Limestone	Ribboned	Massive	Limestone	Dolomite
CC	3986142E	323407N	879	58	42	bedding	Limestone	Interbedded		Dolomite	
CC	3985958E	323488N	880	0	0	float	Shale	Fissile		Nolichucky Shale	
CC	3985705E	323531N	881	0	0	float	Conococheague Limestone	Cherty			
CC	3985968E	323428N	882	0	0	float	Limestone	Massive			
CC	3986478E	323383N	883	0	0	float	Shale	Fissile		Nolichucky Shale	
CC	3989471E	326861N	884	335	10	bedding	Limestone	Ribboned		Dolomite	
CC	3989471E	326861N	884	256	67	cleavage	Limestone	Ribboned		Dolomite	
CC	3986725E	324494N	885	52	65	bedding	Limestone	Ribboned	Interbedded	Dolomite	Conococheague Limestone
CC	3986992E	325498N	886	50	43	bedding	Nolichucky Shale	Fissile			
CC	3987029E	325564N	887	51	40	bedding	Nolichucky Shale				
CC	3987029E	325564N	887	34	68	cleavage	Nolichucky Shale				
CC	3987029E	325564N	887	147	82	joint	Nolichucky Shale				
CC	3987079E	325563N	888	0	0	float	Limestone	Ribboned		Dolomite	
CC	3987093E	325541N	889	0	0	float	Shale				
CC	3986941E	325573N	890	0	0	float	Shale	Fissile		Nolichucky Shale	
CC	3986914E	325562N	891	0	0	float	Shale	Fissile	Cherty		
CC	3986813E	325729N	892	51	59	bedding	Limestone	Ribboned		Dolomite	Conococheague Limestone
CC	3986718E	325724N	893	49	35	bedding	Dolomite				
CC	3986698E	325855N	894	51	65	bedding	Limestone	Ribboned		Dolomite	
CC	3987156E	324549N	895	61	54	bedding	Dolomite	Massive		Honaker Dolomite	
CC	3987459E	324653N	896	57	46	bedding	Dolomite	Laminated	Silty		
CC	3987405E	324588N	897	61	48	bedding	Dolomite	Massive		Honaker Dolomite	
CC	3987332E	324819N	898	61	46	bedding	Dolomite	Massive		Honaker Dolomite	
CC	3987339E	322727N	899	0	0	float	Other			Conococheague Limestone	
CC	3987776E	322533N	900	0	0	float	Shale	Fissile	Cherty	Nolichucky Shale	
CC	3988312E	323496N	901	0	0	float	Shale	Fissile			

QUAD	UTM Easting	UTM Northing	STATION	STRIKE	DIP	FEATURE	DOMINANT LITHOLOGY/UNIT	DESCRIPTION 1	DESCRIPTION 2	OTHER LITHOLOGY/UNIT 1	OTHER LITHOLOGY/UNIT 2
CC	3988200E	323520N	902	0	0	float	Breccia	Calcareous	Cherty	Shale	Nolichucky Shale
CC	3988421E	323595N	903	0	0	float	Shale	Fissile		Breccia	Dolomite
CC	3988445E	323640N	904	55	49	bedding	Shale	Fissile			
CC	3988467E	323706N	905	15	29	bedding	Shale	Shaly		Dolomite	Breccia
CC	3988525E	323889N	906	32	72	bedding	Shale	Massive	Shaly	Dolomite	
CC	3987931E	323621N	907	35	40	bedding	Dolomite	Shaly		Shale	
CC	3991401E	325708N	908	265	63	bedding	Dolomite			Shale	Rogersville Shale
CC	3991434E	325761N	909	254	78	bedding	Rogersville Shale	Laminated		Dolomite	
CC	3991394E	325792N	910	63	29	bedding	Rogersville Shale	Laminated		Dolomite	
CC	3991405E	325798N	911	0	0	float	Limestone	Ribboned		Dolomite	
CC	3991431E	325799N	912	77	5	fold hinge	Dolomite	Laminated			
CC	3991431E	325799N	912	79	74	axial surface	Dolomite	Laminated			
CC	3991396E	325740N	913	65	35	bedding	Limestone	Ribboned		Dolomite	
CC	3991485E	325652N	914	0	0	float	Other				
CC	3991354E	325502N	915	250	66	bedding	Limestone			Limestone	Conococheague Limestone
CC	3991252E	325572N	916	0	0	float	Limestone	Thrombolitic		Dolomite	
CC	3991306E	325905N	917	0	0	float	Other				
CC	3991050E	325727N	918	0	0	float	Copper Ridge Dolomite				
CC	3991124E	325720N	919	80	90	bedding	Limestone	Ribboned		Dolomite	
CC	3991124E	325720N	919	348	77	cleavage					
CC	3991168E	325467N	920	342	22	bedding	Limestone	Ribboned	Massive	Dolomite	
CC	3991168E	325467N	920	122	82	cleavage	Limestone	Ribboned	Massive	Dolomite	
CC	3991107E	325449N	921	300	22	bedding	Dolomite				
CC	3991266E	325646N	922	64	41	bedding	Dolomite	Ribboned		Limestone	
CC	3991270E	325698N	923	31	32	bedding	Rogersville Shale			Dolomite	
CC	3991270E	325698N	923	288	72	cleavage	Rogersville Shale			Dolomite	
CC	3991270E	325698N	923	203	69	joint	Rogersville Shale			Dolomite	
CC	3989339E	324896N	924	0	0	float	Shale	Fissile		Rogersville Shale	Nolichucky Shale
CC	3989451E	325039N	925	27	53	bedding	Nolichucky Shale	Fissile	Laminated		
CC	3989338E	325088N	926	42	46	bedding	Limestone	Cherty	Laminated	Dolomite	
CC	3989266E	325285N	927	0	0	float	Other				
CC	3989726E	326860N	928	59	71	bedding	Limestone	Ribboned		Dolomite	
CC	3989739E	326821N	929	212	40	bedding	Limestone	Ribboned		Dolomite	
CC	3989900E	326925N	930	76	42	bedding	Limestone	Calcareous		Shale	
CC	3989892E	326859N	931	0	0	float	Nolichucky Shale				

QUAD	UTM Easting	UTM Northing	STATION	STRIKE	DIP	FEATURE	DOMINANT LITHOLOGY/UNIT	DESCRIPTION 1	DESCRIPTION 2	OTHER LITHOLOGY/UNIT 1	OTHER LITHOLOGY/UNIT 2
CC	3989882E	326852N	932	0	0	float	Nolichucky Shale				
CC	3989878E	326854N	933	62	59	bedding	Nolichucky Shale	Fissile			
CC	3989919E	326840N	934	0	0	float	Nolichucky Shale	Fissile			
CC	3989931E	326894N	935	0	0	float	Nolichucky Shale	Fissile			
CC	3989861E	327086N	936	53	45	bedding	Limestone			Dolomite	Sandstone
CC	3989719E	327033N	937	0	0	float	Limestone	Massive			
CC	3991164E	328136N	938	60	60	bedding	Limestone	Laminated	Massive	Dolomite	
CC	3991140E	328145N	939	162	86	joint	Limestone	Ribboned	Massive	Dolomite	
CC	3991083E	328150N	940	60	59	bedding	Limestone	Ribboned	Massive	Dolomite	
CC	3990998E	328171N	941	59	65	bedding	Maryville Limestone	Banded	Ribboned	Limestone	Dolomite
CC	3991018E	328057N	942	59	71	bedding	Maryville Limestone	Interbedded	Ribboned	Limestone	Dolomite
CC	3990923E	327947N	943	61	70	bedding	Maryville Limestone	Banded	Massive	Dolomite	
CC	3991200E	328100N	944	240	71	bedding	Rogersville Shale	Laminated	Cherty	Limestone	Dolomite
CC	3991200E	328100N	944	328	82	cleavage	Rogersville Shale	Laminated	Cherty	Limestone	Dolomite
CC	3991257E	328125N	945	59	82	bedding	Rogersville Shale	Calcareous	Fissile	Limestone	
CC	3991257E	328125N	945	328	58	cleavage	Rogersville Shale	Calcareous	Fissile	Limestone	
CC	3991299E	328067N	946	59	76	bedding	Rogersville Shale	Calcareous	Shaly	Limestone	
CC	3991517E	327999N	947	0	0	float	Shale	Fissile			
CC	3991428E	328030N	948	304	82	cleavage					
CC	3991428E	328030N	948	59	71	bedding					
CC	3991389E	328043N	949	238	80	bedding	Limestone			Rogersville Shale	
CC	3990831E	328295N	950	0	0	float	Nolichucky Shale	Fissile			
CC	3990875E	328273N	951	0	0	float	Nolichucky Shale	Fissile			
CC	3990910E	328276N	952	0	0	float	Nolichucky Shale	Fissile		Limestone	
CC	3990859E	328393N	953	54	66	bedding	Limestone	Massive		Maynardville Limestone	
CC	3990790E	328359N	954	0	0	float	Nolichucky Shale	Fissile	Interbedded		
CC	3992214E	328310N	955	44	48	bedding	Dolomite			Honaker Dolomite	
CC	3992172E	328327N	956	279	54	cleavage	Dolomite	Laminated		Honaker Dolomite	
CC	3992228E	328334N	957	0	0	float	Alluvium				
CC	3992358E	328339N	958	0	0	float	Alluvium				
CC	3989579E	321132N	959	268	54	bedding	Limestone	Ribboned		Dolomite	
CC	3989635E	321182N	960	272	49	bedding	Limestone	Ribboned		Dolomite	Kingsport Formation
CC	3989677E	321064N	961	275	40	bedding	Limestone	Ribboned		Dolomite	Kingsport Formation
CC	3989450E	321109N	962	324	55	bedding	Limestone	Thrombolitic		Dolomite	
CC	3989313E	321174N	963	166	79	cleavage	Limestone	Massive			

QUAD	UTM Easting	UTM Northing	STATION	STRIKE	DIP	FEATURE	DOMINANT LITHOLOGY/UNIT	DESCRIPTION 1	DESCRIPTION 2	OTHER LITHOLOGY/UNIT 1	OTHER LITHOLOGY/UNIT 2
CC	3989230E	321157N	964	50	18	bedding	Limestone	Massive			
CC	3989230E	321157N	964	30	90	cleavage	Limestone	Massive			
CC	3989230E	321157N	964	331	90	joint	Limestone	Massive			
CC	3989099E	321243N	965	61	26	bedding	Limestone	Massive			
CC	3989232E	320910N	966	29	90	cleavage	Limestone	Massive	Thrombolitic		
CC	3989191E	320926N	967	50	0	bedding	Limestone	Massive	Thrombolitic		
CC	3989412E	321230N	968	5	33	bedding	Limestone	Massive	Silty		
CC	3989412E	321230N	968	59	90	cleavage	Limestone	Massive	Silty		
CC	3989555E	321291N	969	265	53	bedding	Limestone	Massive		Lenoir Limestone	
CC	3991223E	326646N	970	104	64	bedding	Dolomite	Massive		Limestone	
CC	3988750E	327515N	971	204	46	bedding	Limestone	Ribboned	Massive	Dolomite	
CC	3988729E	327542N	972	58	48	bedding	Limestone	Ribboned	Massive	Dolomite	
CC	3988618E	327902N	973	44	0	bedding	Limestone	Ribboned		Dolomite	
CC	3988726E	327952N	974	46	9	bedding	Limestone	Ribboned		Dolomite	
CC	3988639E	327990N	975	44	32	bedding	Limestone	Ribboned		Dolomite	
CC	3991218E	324582N	976	24	35	bedding	Dolomite	Laminated	Interbedded	Conococheague Limestone	Limestone
CC	3991123E	324558N	977	25	36	bedding	Dolomite	Massive	Interbedded	Limestone	Mascot Dolomite
CC	3991202E	324409N	978	31	45	bedding	Dolomite	Massive			
CC	3991332E	324550N	979	24	49	bedding	Dolomite	Massive			
CC	3991327E	324625N	980	26	50	bedding	Dolomite	Massive			
CC	3991151E	324746N	981	0	0	float	Other	Cherty			
CC	3991191E	324852N	982	50	78	bedding	Sandstone	Sandy	Cherty		
CC	3991258E	324697N	983	22	39	bedding	Dolomite	Laminated	Massive		
CC	3991095E	324686N	984	25	35	bedding	Limestone	Massive			
CC	3991678E	324626N	985	251	63	bedding	Limestone	Interbedded	Ribboned	Dolomite	Conococheague Limestone
CC	3991650E	324549N	986	263	73	bedding	Dolomite	Laminated			
CC	3991650E	324549N	986	5	82	fold hinge	Dolomite	Laminated			
CC	3991650E	324549N	986	4	78	axial surface	Dolomite	Laminated			
CC	3991650E	324549N	986	226	71	cleavage	Dolomite	Laminated			
CC	3991711E	324526N	987	34	41	bedding	Dolomite	Massive			
CC	3991700E	324395N	988	0	0	float	Dolomite	Massive			
CC	3991626E	324285N	989	74	40	bedding	Shale			Nolichucky Shale	
CC	3991626E	324285N	989	173	75	cleavage	Shale			Nolichucky Shale	
CC	3991657E	324214N	990	321	46	bedding	Nolichucky Shale	Banded	Calcareous	Limestone	
CC	3991625E	324231N	991	281	70	bedding	Nolichucky Shale	Banded	Calcareous	Limestone	

QUAD	UTM Easting	UTM Northing	STATION	STRIKE	DIP	FEATURE	DOMINANT LITHOLOGY/UNIT	DESCRIPTION 1	DESCRIPTION 2	OTHER LITHOLOGY/UNIT 1	OTHER LITHOLOGY/UNIT 2
CC	3991623E	324247N	992	49	40	cleavage					
CC	3991594E	324242N	993	278	65	bedding	Limestone	Massive		Honaker Dolomite	Dolomite
CC	3991700E	324274N	994	0	0	float	Shale			Limestone	
CC	3991735E	324268N	995	45	43	bedding	Shale	Banded	Massive	Limestone	
CC	3991838E	324521N	996	291	47	bedding	Limestone	Ribboned	Massive	Dolomite	
CC	3991684E	324764N	997	55	69	bedding	Limestone	Ribboned	Massive	Dolomite	
CC	3991676E	324954N	998	55	56	bedding	Limestone	Laminated	Massive	Dolomite	Conococheague Limestone
CC	3991721E	324871N	999	0	0	float	Alluvium				
CC	3991595E	325125N	1000	0	0	float	Sandstone	Cherty	Sandy	Other	Copper Ridge Dolomite
CC	3991762E	325487N	1001	52	50	bedding	Limestone	Ribboned		Dolomite	
CC	3991664E	325422N	1002	50	47	bedding	Dolomite	Ribboned	Massive	Limestone	
CC	3991672E	325487N	1003	59	58	bedding	Dolomite	Ribboned	Massive	Limestone	
CC	3991744E	325677N	1004	51	56	bedding	Dolomite	Ribboned	Massive	Limestone	
CC	3991754E	327363N	1005	48	48	bedding	Dolomite	Massive	Laminated	Honaker Dolomite	
CC	3991701E	327351N	1006	51	59	bedding	Dolomite	Massive	Laminated	Honaker Dolomite	
CC	3992436E	327703N	1007	0	0	float	Alluvium				
CC	3992403E	327731N	1008	16	25	bedding	Limestone	Ribboned	Laminated	Dolomite	
CC	3992377E	327641N	1009	17	33	bedding	Limestone	Ribboned	Interbedded	Dolomite	Conococheague Limestone
CC	3992345E	327580N	1010	240	69	bedding	Limestone	Laminated		Alluvium	
CC	3992355E	327556N	1011	252	77	bedding	Limestone	Laminated		Alluvium	
CC	3992321E	327458N	1012	0	0	float	Other	Cherty			
CC	3992317E	327392N	1013	63	81	bedding	Limestone	Ribboned	Massive	Dolomite	Conococheague Limestone
CC	3992255E	327122N	1014	80	82	bedding	Limestone	Ribboned	Massive	Dolomite	Conococheague Limestone
CC	3992400E	326751N	1015	0	0	float					
CC	3992385E	327007N	1016	0	0	float	Sandstone			Alluvium	
CC	3991993E	326909N	1017	71	56	bedding	Limestone	Ribboned	Thrombolitic	Dolomite	Conococheague Limestone
CC	3991905E	326998N	1018	269	35	bedding	Limestone	Ribboned	Massive	Dolomite	Conococheague Limestone
CC	3991841E	326999N	1019	55	10	bedding	Limestone	Ribboned	Massive	Dolomite	Conococheague Limestone
CC	3991908E	326819N	1020	266	32	bedding	Limestone	Ribboned	Massive	Dolomite	Conococheague Limestone
CC	3992041E	326964N	1021	226	43	cleavage	Limestone	Ribboned	Massive	Dolomite	Conococheague Limestone
CC	3992314E	327846N	1022	28	51	bedding	Limestone	Interbedded	Cherty	Dolomite	
CC	3992276E	327878N	1023	0	0	float	Alluvium				
CC	3992154E	327826N	1024	0	0	float	Alluvium				
CC	3992109E	327790N	1025	52	55	bedding	Limestone	Ribboned	Massive	Dolomite	Conococheague Limestone
CC	3992589E	328084N	1026	32	18	bedding	Limestone	Ribboned	Massive	Dolomite	

QUAD	UTM Easting	UTM Northing	STATION	STRIKE	DIP	FEATURE	DOMINANT LITHOLOGY/UNIT	DESCRIPTION 1	DESCRIPTION 2	OTHER LITHOLOGY/UNIT 1	OTHER LITHOLOGY/UNIT 2
CC	3993273E	328336N	1027	82	90	bedding	Limestone	Ribboned	Massive	Dolomite	Conococheague Limestone
CC	3990164E	325752N	1028	0	0	float	Other	Cherty		Conococheague Limestone	
CC	3990239E	325828N	1029	0	0	float	Limestone	Massive		Conococheague Limestone	
CC	3990343E	325597N	1030	0	0	float	Shale	Fissile	Massive	Limestone	Nolichucky Shale
CC	3990280E	325666N	1031	47	90	cleavage	Nolichucky Shale	Fissile			
CC	3987923E	328557N	1032	51	66	bedding	Limestone	Interbedded		Jonesboro Limestone	
CC	3987939E	328647N	1033	50	66	bedding	Limestone	Ribboned	Massive	Dolomite	
CC	3987881E	328678N	1034	51	66	bedding	Limestone	Ribboned	Massive	Dolomite	
CC	3987848E	328731N	1035	48	62	bedding	Limestone	Massive	Sandy	Dolomite	Sandstone
CC	3987303E	328593N	1036	248	56	bedding	Limestone	Massive	Calcareous		
CC	3986742E	328038N	1037	240	59	bedding	Limestone	Banded	Silty	Limestone	
CC	3986804E	328036N	1038	245	65	bedding	Limestone	Banded	Silty	Limestone	
CC	3986702E	327917N	1039	246	68	bedding	Limestone	Banded	Silty	Limestone	
CC	3986521E	328909N	1040	64	46	bedding	Conococheague Limestone	Massive	Interbedded	Limestone	Dolomite
CC	3986637E	328970N	1041	64	52	bedding	Limestone	Ribboned		Dolomite	
CC	3986648E	329083N	1042	145	59	cleavage	Limestone	Ribboned		Dolomite	
CC	3986769E	328959N	1043	63	53	bedding	Limestone	Cherty			
CC	3986919E	329053N	1044	62	63	bedding	Limestone				
CC	3987164E	329148N	1045	258	55	bedding	Limestone	Ribboned		Dolomite	
CC	3987045E	329002N	1046	69	45	bedding	Limestone	Ribboned		Dolomite	
CC	3986928E	328884N	1047	275	90	cleavage	Limestone	Ribboned		Dolomite	
CC	3986412E	329167N	1048	52	48	bedding	Limestone	Massive			
CC	3986513E	329262N	1049	0	0	float	Colluvium				
CC	3986209E	329685N	1050	80	53	bedding	Limestone	Massive	Thrombolitic	Jonesboro Limestone	
CC	3986457E	330197N	1051	0	0	float	Colluvium				
CC	3986484E	330060N	1052	65	54	bedding	Jonesboro Limestone	Ribboned	Massive	Limestone	Dolomite
CC	3986933E	329973N	1053	0	0	float	Limestone			Colluvium	
CC	3987249E	329872N	1054	291	30	bedding	Limestone	Ribboned	Massive	Dolomite	
CC	3987283E	329779N	1055	0	0	float	Sandstone				
CC	3987537E	329588N	1056	280	38	bedding	Limestone	Ribboned	Massive	Dolomite	
CC	3987336E	329228N	1057	290	53	bedding	Limestone	Ribboned	Massive	Dolomite	Colluvium
CC	3987517E	329050N	1058	254	50	bedding	Limestone	Massive		Jonesboro Limestone	
CC	3987320E	328942N	1059	254	49	bedding	Limestone	Massive		Jonesboro Limestone	
CC	3989006E	329710N	1060	50	76	bedding	Jonesboro Limestone	Ribboned	Thrombolitic	Dolomite	
CC	3988903E	329446N	1061	51	80	bedding	Jonesboro Limestone	Ribboned	Thrombolitic	Dolomite	

QUAD	UTM Easting	UTM Northing	STATION	STRIKE	DIP	FEATURE	DOMINANT LITHOLOGY/UNIT	DESCRIPTION 1	DESCRIPTION 2	OTHER LITHOLOGY/UNIT 1	OTHER LITHOLOGY/UNIT 2
CC	3988830E	329742N	1062	49	65	bedding	Jonesboro Limestone	Ribboned	Thrombolitic	Dolomite	
CC	3990470E	329825N	1063	249	19	bedding	Limestone	Massive			
CC	3988938E	328525N	1064	57	66	bedding	Limestone	Ribboned	Thrombolitic	Dolomite	
CC	3990776E	329750N	1065	213	23	bedding	Limestone	Cherty	Sandy	Dolomite	Sandstone
CC	3990776E	329750N	1065	53	83	joint	Limestone	Cherty	Sandy	Dolomite	Sandstone
CC	3992030E	330595N	1066	51	70	bedding	Sandstone	Sandy	Shaly	Shale	Conococheague Limestone
CC	3992074E	330581N	1067	0	0	float	Alluvium				
CC	3992253E	330430N	1068	0	0	float	Alluvium				
CC	3990363E	324763N	1069	34	50	bedding	Dolomite	Massive		Honaker Dolomite	
CC	3990002E	324766N	1070	3	60	bedding	Dolomite	Shaly		Shale	Honaker Dolomite
CC	3990075E	324786N	1071	347	51	bedding	Shale	Shaly		Dolomite	
CC	3990113E	324908N	1072	0	0	float	Shale	Shaly	Cherty	Other	
CC	3990180E	324820N	1073	341	76	bedding	Dolomite	Shaly		Shale	Breccia
CC	3990488E	324674N	1074	128	24	bedding	Dolomite	Laminated	Massive	Honaker Dolomite	
CC	3990478E	324743N	1075	348	45	bedding	Limestone	Interbedded		Dolomite	Honaker Dolomite
CC	3987071E	328527N	1076	240	53	bedding	Limestone	Ribboned	Massive	Dolomite	Jonesboro Limestone
CC	3986076E	327698N	1077	252	50	bedding	Limestone	Ribboned	Thrombolitic	Dolomite	Jonesboro Limestone
CC	3985973E	325464N	1078	62	68	bedding	Limestone	Laminated	Banded	Dolomite	Conococheague Limestone

(End of Cedar Creek quadrangle data)

QUAD	STATION	STRIKE	DIP	FEATURE	DOMINANT LITHOLOGY/UNIT	DESCRIPTION 1	DESCRIPTION 2	OTHER LITHOLOGY/UNIT 1	OTHER LITHOLOGY/UNIT 2
NM	1	50	56	bedding	Limestone		Interbedded	Dolomite	
NM	2	52	51	bedding	Limestone		Interbedded	Dolomite	
NM	3	0	0	float	Nolichucky Shale				
NM	4	290	55	bedding	Limestone	Silty	Cherty	Dolomite	
NM	5	60	60	bedding	Dolomite			Honaker Dolomite	
NM	6a	31	0	fold hinge	Dolomite			Honaker Dolomite	
NM	6b	23	62	axial surface	Dolomite			Honaker Dolomite	
NM	6c	23	85	cleavage	Dolomite			Honaker Dolomite	
NM	7	124	70	bedding	Dolomite	Massive		Honaker Dolomite	
NM	8	81	90	bedding	Dolomite	Cherty		Honaker Dolomite	
NM	9	55	67	bedding	Dolomite	Cherty		Honaker Dolomite	
NM	10a	221	51	bedding	Dolomite	Cherty		Honaker Dolomite	Siltstone
NM	10b	0	0	float	Dolomite			Honaker Dolomite	
NM	11	0	0	float	Dolomite			Honaker Dolomite	
NM	12	56	55	bedding	Dolomite	Interbedded		Limestone	
NM	13	44	51	bedding	Siltstone	Silty		Dolomite	Shale
NM	14	46	55	bedding	Shale	Massive		Nolichucky Shale	Dolomite
NM	15	0	0	float	Shale			Dolomite	
NM	16	58	54	bedding	Dolomite			Siltstone	
NM	17	73	76	bedding	Nolichucky Shale	Fissile			
NM	18	190	28	cleavage	Dolomite				
NM	19	49	74	overturned bedding	Dolomite				
NM	20	55	71	overturned bedding	Dolomite				
NM	21	0	0	float	Breccia				
NM	22a	88	40	bedding	Limestone	Ribboned			
NM	22b	210	66	cleavage	Limestone	Thrombolitic			
NM	23	59	49	bedding	Limestone			Sandstone	
NM	24	0	0	float		Shaly			
NM	25	85	66	bedding	Dolomite	Shaly			
NM	26	55	50	bedding	Nolichucky Shale	Fissile			
NM	27	0	0	float	Nolichucky Shale	Fissile			
NM	28	30	14	bedding	Nolichucky Shale				
NM	29	56	45	bedding	Dolomite	Interbedded		Limestone	
NM	30	45	43	bedding	Dolomite	Cherty			
NM	31	56	56	bedding	Limestone				

QUAD	STATION	STRIKE	DIP	FEATURE	DOMINANT LITHOLOGY/UNIT	DESCRIPTION 1	DESCRIPTION 2	OTHER LITHOLOGY/UNIT 1	OTHER LITHOLOGY/UNIT 2
NM	32	48	57	bedding	Dolomite	Calcareous		Rogersville Shale	
NM	33	54	55	bedding	Limestone				
NM	34	48	49	bedding	Rogersville Shale	Interbedded		Dolomite	
NM	35	50	63	bedding	Maryville Limestone	Interbedded		Dolomite	
NM	36	50	62	bedding	Maryville Limestone	Interbedded		Dolomite	
NM	37	51	55	bedding	Dolomite	Massive		Sandstone	
NM	38	221	26	cleavage	Dolomite				
NM	39	292	41	fold hinge	Limestone				
NM	40	46	58	bedding	Limestone			Dolomite	
NM	41	45	51	bedding	Siltstone			Dolomite	
NM	42	50	58	bedding	Dolomite				
NM	43	46	60	bedding	Limestone	Ribboned		Dolomite	
NM	44	49	55	bedding	Dolomite				
NM	45	0	0	float	Limestone	Massive		Dolomite	
NM	46	46	52	bedding	Limestone	Thrombolitic		Dolomite	Jonesboro Limestone
NM	47	45	69	bedding	Limestone	Thrombolitic		Dolomite	Jonesboro Limestone
NM	48	0	0	float	Dolomite				
NM	49	0	0	float	Dolomite				
NM	50	48	65	bedding	Dolomite				
NM	51	44	28	bedding	Limestone	Calcareous		Dolomite	Breccia
NM	52	0	0	float	Limestone				
NM	53	85	50	bedding	Dolomite				
NM	54	62	64	bedding	Limestone			Dolomite	
NM	55	59	64	bedding	Dolomite				
NM	56	324	69	bedding	Dolomite			Jonesboro Limestone	
NM	57	347	65	bedding	Dolomite				
NM	58	59	46	bedding	Dolomite				
NM	59	59	43	bedding	Limestone			Dolomite	
NM	60	61	36	bedding	Limestone			Dolomtie	
NM	61	53	53	bedding	Limestone	Interbedded		Dolomite	
NM	62	49	52	bedding	Limestone			Dolomite	
NM	63	51	28	bedding	Limestone			Dolomite	
NM	64	0	0	float	Limestone				
NM	65	0	0	float	Limestone	Cherty			
NM	66	40	41	bedding	Limestone	Thrombolitic			

QUAD	STATION	STRIKE	DIP	FEATURE	DOMINANT LITHOLOGY/UNIT	DESCRIPTION 1	DESCRIPTION 2	OTHER LITHOLOGY/UNIT 1	OTHER LITHOLOGY/UNIT 2
NM	67	0	0	float	Limestone	Thrombolitic			
NM	68	43	21	bedding	Limestone	Thrombolitic			
NM	69	50	47	bedding	Limestone				
NM	70	47	41	bedding	Limestone	Cherty			
NM	71	43	45	bedding	Limestone			Dolomite	
NM	72	0	0	float	Limestone	Cherty		Dolomite	
NM	73	37	35	bedding	Dolomite	Calcareous		Limestone	
NM	74	50	35	bedding	Limestone			Dolomite	
NM	75	48	33	bedding	Dolomite			Limestone	
NM	76	37	35	bedding	Limestone	Thrombolitic		Dolomite	
NM	77	0	0	float	Rogersville Shale	Silty			
NM	78	177	78	bedding	Dolomite	Silty		Rogersville Shale	
NM	79	355	66	overturned bedding	Rogersville Shale			Dolomite	
NM	79	214	50	cleavage	Rogersville Shale				
NM	80	22	45	bedding	Dolomite	Cherty		Maryville Limestone	
NM	81	35	57	bedding	Limestone	Interbedded		Maryville Limestone	
NM	82	16	56	bedding	Limestone	Ribboned		Maryville Limestone	
NM	83	0	0	float	Honaker Dolomite				
NM	84	140	81	bedding	Dolomite	Shaly			
NM	85	0	0	float	Shale	Fissile		Rogersville Shale	
NM	86	10	68	overturned bedding	Rogersville Shale	Fissile			
NM	87	0	0	float	Rogersville Shale	Fissile			
NM	88	46	35	bedding	Limestone	Massive		Mascot Dolomite	Dolomite
NM	89	0	0	float	Mascot Dolomite	Massive			
NM	90	44	39	bedding	Mascot Dolomite	Massive		Dolomite	Limestone
NM	91	44	38	bedding	Mascot Dolomite	Massive		Dolomite	
NM	92	31	34	bedding	Limestone	Ribboned		Dolomite	
NM	93	36	51	bedding	Mascot Dolomite			Kingsport Formation	
NM	94	28	38	bedding	Dolomite				
NM	95a	356	68	bedding	Siltstone	Silty		Dolomite	Rogersville Shale
NM	95b	250	45	cleavage	Siltstone			Rogersville Shale	
NM	96	0	0	float	Dolomite				
NM	97	156	57	bedding	Rogersville Shale	Siltstone			
NM	98	30	25	bedding	Limestone	Massive		Dolomite	
NM	99	29	40	bedding	Limestone	Ribboned		Dolomite	

QUAD	STATION	STRIKE	DIP	FEATURE	DOMINANT LITHOLOGY/UNIT	DESCRIPTION 1	DESCRIPTION 2	OTHER LITHOLOGY/UNIT 1	OTHER LITHOLOGY/UNIT 2
NM	100	29	35	bedding	Dolomite	Interbedded		Limestone	
NM	102	0	0	float	Rogersville Shale				
NM	103	8	53	bedding	Dolomite	Fissile		Shale	
NM	104	50	35	bedding	Rogersville Shale	Silty		Dolomite	Siltstone
NM	105	349	43	bedding	Dolomite			Honaker Dolomite	
NM	106a	348	37	bedding	Rome Formation			Dolomite	
NM	106b	223	28	fold hinge					
NM	106c	249	60	cleavage					
NM	107	317	17	bedding	Shady Dolomite				
NM	108	64	64	bedding	Rome Formation			Sandstone	
NM	109	286	82	bedding	Rome Formation				
NM	110	41	46	bedding	Limestone			Dolomite	
NM	111	130	56	bedding	Limestone	Thrombolitic		Dolomite	
NM	112	137	30	bedding	Limestone	Thrombolitic		Dolomite	
NM	113	0	0	float	Dolomite				
NM	118	0	0	float		Cherty			
NM	119	114	47	bedding	Limestone	Calcareous		Dolomite	Nolichucky Shale
NM	120	74	39	bedding	Limestone	Siliceous		Siltstone	Nolichucky Shale
NM	121	58	52	bedding	Limestone				
NM	122	63	63	bedding	Dolomite	Cherty		Limestone	
NM	123	57	59	bedding	Limestone			Dolomite	
NM	124	66	50	bedding	Limestone	Interbedded		Dolomite	
NM	125	0	0	float	Shale	Fissile		Rogersville Shale	
NM	126a	120	61	bedding	Sandstone	Sandy		Shale	Rome Formation
NM	126b	16	49	joint	Sandstone	Sandy		Shale	Rome Formation
NM	127c	0	0	float	Dolomite	Massive			
NM	128	324	68	bedding	Limestone	Banded		Dolomite	Maryville Limestone
NM	129	315	73	bedding	Limestone	Ribboned		Dolomite	
NM	130	319	66	bedding	Limestone	Ribboned		Dolomite	
NM	131	0	0	float	Shale	Fissile		Rogersville Shale	
NM	132	331	68	bedding	Dolomite	Cherty			
NM	133	0	0	float	Shale	Fissile		Siltstone	Rogersville Shale
NM	134	350	50	bedding	Siltstone	Silty		Shale	Rogersville Shale
NM	135	355	59	bedding	Limestone	Interbedded		Dolomite	
NM	136	28	44	bedding	Limestone	Ribboned		Dolomite	

QUAD	STATION	STRIKE	DIP	FEATURE	DOMINANT LITHOLOGY/UNIT	DESCRIPTION 1	DESCRIPTION 2	OTHER LITHOLOGY/UNIT 1	OTHER LITHOLOGY/UNIT 2
NM	137	0	0	float	Dolomite				
NM	138	0	0	float	Shale	Fissile			
NM	139	51	46	bedding	Limestone	Interbedded		Dolomite	Maryville Limestone
NM	140	65	46	bedding	Limestone	Ribboned		Dolomite	Maryville Limestone
NM	141	57	42	bedding	Siltstone	Fissile		Shale	Limestone
NM	142	29	46	bedding	Limestone	Banded		Dolomite	Maryville Limestone
NM	143	322	66	bedding	Limestone	Banded		Dolomite	Maryville Limestone
NM	144	331	60	bedding	Dolomite				
NM	145	0	0	float	Shale	Fissile			
NM	146	29	49	bedding	Dolomite				
NM	147	0	0	float	Dolomite	Massive			
NM	148	0	0	float	Limestone	Ribboned		Dolomite	Maryville Limestone
NM	149	64	61	bedding	Dolomite				
NM	150a	75	20	fold hinge					
NM	150b	66	79	axial surface					
NM	151	55	51	bedding	Dolomite	Laminated			
NM	152	56	69	bedding	Dolomite	Siliceous		Limestone	
NM	153	44	62	bedding	Dolomite	Shaly			
NM	154	92	90	bedding	Dolomite	Laminated		Honaker Dolomite	
NM	155	0	0	float	Limestone	Calcareous			
NM	156	114	90	bedding	Dolomite	Laminated			
NM	157	0	0	float	Sandstone	Sandy		Limestone	
NM	158	0	0	float	Sandstone	Silty		Shale	Rome Formation
NM	159	0	0	float	Shale	Shaly		Rome Formation	Pumpkin Valley Shale?
NM	160	0	0	float	Dolomite				
NM	161	23	67	bedding	Dolomite				
NM	162	37	60	bedding	Dolomite				
NM	163	12	69	bedding	Dolomite	Silty			
NM	164	39	65	bedding	Limestone	Ribboned		Dolomite	
NM	165	0	0	float	Shale	Fissile			
NM	166	0	0	float	Shale	Fissile		Pumpkin Valley Shale?	
NM	167	148	45	bedding	Limestone	Calcareous		Dolomite	
NM	168	0	0	float	Sandstone	Sandy		Colluvium	Alluvium
NM	169	47	36	bedding	Dolomite				
NM	170	0	0	float	Sandstone			Colluvium	

QUAD	STATION	STRIKE	DIP	FEATURE	DOMINANT LITHOLOGY/UNIT	DESCRIPTION 1	DESCRIPTION 2	OTHER LITHOLOGY/UNIT 1	OTHER LITHOLOGY/UNIT 2
NM	171	0	0	float	Sandstone			Rome Formation	
NM	172	0	0	float	Shale	Fissile		Pumpkin Valley Shale?	
NM	173	72	52	bedding	Sandstone	Sandy		Dolomite	Rome Formation
NM	174	39	51	bedding	Limestone	Calcareous		Rome Formation	Breccia
NM	175	39	65	bedding	Limestone	Calcareous		Breccia	
NM	176	0	0	float	Dolomite	Cherty		Limestone	
NM	177	30	67	bedding	Limestone	Cherty		Dolomite	
NM	178	0	0	float	Rome Formation	Sandy			
NM	179	31	70	bedding	Sandstone			Rome Formation	
NM	180	0	0	float	Shale	Fissile		Rome Formation	
NM	181	73	63	bedding	Rome Formation			Sandstone	
NM	182	0	0	float	Shale	Fissile			
NM	183	0	0	float	Rome Formation				
NM	184	0	0	float	Other	Sandy			
NM	185	0	0	float	Limestone	Sandy		Breccia	Colluvium
NM	186	0	0	float	Siltstone			Sandstone	Rome Formation
NM	187	0	0	float	Colluvium				
NM	188	8	72	bedding	Limestone	Calcareous			
NM	189	1	50	bedding	Rome Formation	Sandy			
NM	190	49	45	bedding	Limestone	Calcareous		Kingsport Formation	
NM	191	45	46	bedding	Limestone	Ribboned		Dolomite	
NM	192	39	46	bedding	Limestone	Calcareous		Dolomite	
NM	193	50	41	bedding	Limestone			Kingsport Formation	
NM	194	48	38	bedding	Limestone	Calcareous		Dolomite	
NM	195	48	48	bedding	Limestone	Calcareous		Dolomite	
NM	196	0	0	float	Sandstone	Sandy			
NM	197	0	0	float	Colluvium			Other	
NM	198	31	56	bedding	Limestone				
NM	199	0	0	float	Limestone	Variegated		Dolomite	Breccia
NM	200	0	0	float	Shale	Sandy		Siltstone	
NM	201	0	0	float	Shale	Sandy		Siltstone	
NM	202	0	0	float	Shale	Sandy		Siltstone	Rome Formation
NM	203	0	0	float	Other	Cherty			
NM	204	0	0	float	Limestone	Massive		Kingsport Formation	
NM	205	0	0	float	Breccia	Siliceous		Other	

QUAD	STATION	STRIKE	DIP	FEATURE	DOMINANT LITHOLOGY/UNIT	DESCRIPTION 1	DESCRIPTION 2	OTHER LITHOLOGY/UNIT 1	OTHER LITHOLOGY/UNIT 2
NM	206	27	67	bedding	Limestone	Calcareous			
NM	207	0	0	float	Shale	Shaly		Pumpkin Valley Shale?	
NM	208	61	38	bedding	Limestone	Calcareous			
NM	209	53	53	bedding	Limestone	Ribboned		Dolomite	
NM	210	54	46	bedding	Limestone	Ribboned		Dolomite	
NM	213	58	90	bedding	Limestone	Oolitic		Sandstone	Jonesboro Limestone
NM	214a	41	42	bedding	Limestone	Thrombolitic		Dolomite	
NM	214b	260	14	fold hinge	Sandstone				
NM	215	51	49	bedding	Limestone			Dolomite	Sandstone
NM	216	35	55	bedding	Limestone	Cherty		Breccia	Dolomite
NM	217	0	0	float	Limestone			Dolomite	
NM	218	76	78	bedding	Limestone	Massive		Dolomite	
NM	219	102	76	bedding	Limestone	Silty		Siltstone	
NM	220	106	72	bedding	Limestone	Massive			
NM	221	41	62	bedding	Limestone	Massive			
NM	222	305	66	bedding	Limestone	Thrombolitic		Dolomite	
NM	223	346	55	bedding	Limestone	Thrombolitic		Dolomite	
NM	224	296	90	bedding	Limestone	Massive		Dolomite	
NM	225a	12	52	bedding	Limestone	Interbedded		Dolomite	Sandstone
NM	225b	358	85	cleavage					
NM	226	329	53	bedding	Shale	Shaly		Siltstone	
NM	227	71	63	bedding	Sandstone			Conglomerate	
NM	228	169	67	bedding	Sandstone			Conglomerate	
NM	229	0	0	float	Shale	Shaly			
NM	230	0	0	float	Quartzite			Colluvium	
NM	231	42	45	bedding	Sandstone			Conglomerate	
NM	232	79	59	bedding	Sandstone				
NM	233	76	53	bedding	Shale	Fissile			
NM	234	0	0	float	Shale				
NM	235	62	59	bedding	Shale			Siltstone	
NM	253	34	40	bedding	Limestone	Ribboned		Kingsport Formation	Dolomite
NM	254	0	0	float	Sandstone	Sandy			
NM	255	34	40	bedding	Limestone	Massive		Kingsport Formation	
NM	256	0	0	float	Sandstone				
NM	257	20	24	bedding	Limestone	Calcareous		Copper Ridge Dolomite	

QUAD	STATION	STRIKE	DIP	FEATURE	DOMINANT LITHOLOGY/UNIT	DESCRIPTION 1	DESCRIPTION 2	OTHER LITHOLOGY/UNIT 1	OTHER LITHOLOGY/UNIT 2
NM	258	19	12	bedding	Limestone	Massive			
NM	259	33	15	bedding	Limestone	Interbedded		Dolomite	
NM	260	35	0	bedding	Limestone	Ribboned		Dolomite	
NM	261	60	52	bedding	Limestone	Ribboned		Dolomite	
NM	262	250	22	bedding	Limestone	Thrombolitic		Limestone	
NM	263	41	33	bedding	Limestone	Interbedded		Dolomite	Copper Ridge Dolomite
NM	264	45	52	bedding	Limestone	Massive		Dolomite	Copper Ridge Dolomite
NM	265	43	53	bedding	Limestone	Ribboned		Dolomite	
NM	266a	250	52	bedding	Limestone	Massive			
NM	266b	61	52	cleavage	Limestone	Massive			
NM	267	255	65	bedding	Limestone	Massive			
NM	268a	255	52	overturned bedding	Limestone	Massive			
NM	268b	60	43	cleavage	Limestone	Massive			
NM	269	250	77	bedding	Dolomite	Interbedded		Limestone	
NM	270	55	19	bedding	Limestone	Thrombolitic		Dolomite	
NM	271	41	71	bedding	Limestone	Thrombolitic		Dolomite	
NM	272	52	90	bedding	Limestone	Ribboned		Dolomite	
NM	273	229	85	bedding	Limestone	Sandy		Dolomite	Other
NM	274	20	15	bedding	Limestone	Cherty		Dolomite	
NM	275	300	12	bedding	Limestone	Laminated			
NM	276	235	12	bedding	Limestone	Laminated		Dolomite	
NM	277	30	45	bedding	Limestone	Ribboned		Dolomite	
NM	278	30	37	bedding	Limestone	Ribboned		Dolomite	
NM	279	41	36	bedding	Limestone	Ribboned		Dolomite	
NM	280	35	35	bedding	Limestone	Massive			
NM	281	40	47	bedding	Limestone	Interbedded		Dolomite	
NM	282	20	28	bedding	Limestone	Interbedded		Dolomite	
NM	283	29	36	bedding	Limestone	Interbedded		Dolomite	
NM	284	38	47	bedding	Limestone	Interbedded		Dolomite	
NM	285	34	32	bedding	Limestone	Ribboned		Dolomite	
NM	286	34	37	bedding	Limestone	Ribboned		Dolomite	
NM	287	31	35	bedding	Limestone	Ribboned		Dolomite	
NM	288	30	40	bedding	Limestone			Dolomite	
NM	289	14	28	bedding	Limestone	Ribboned		Dolomite	
NM	290	14	16	bedding	Limestone	Ribboned		Dolomite	

QUAD	STATION	STRIKE	DIP	FEATURE	DOMINANT LITHOLOGY/UNIT	DESCRIPTION 1	DESCRIPTION 2	OTHER LITHOLOGY/UNIT 1	OTHER LITHOLOGY/UNIT 2
NM	291	20	20	bedding	Limestone	Ribboned		Dolomite	
NM	292	25	35	bedding	Limestone	Ribboned		Dolomite	
NM	293	25	0	bedding	Limestone	Ribboned		Dolomite	
NM	294	47	47	bedding	Limestone	Ribboned		Dolomite	
NM	295	40	45	bedding	Limestone	Ribboned		Dolomite	
NM	296	47	51	bedding	Limestone	Ribboned		Dolomite	
NM	297	246	35	bedding	Limestone	Ribboned		Dolomite	
NM	298	248	35	bedding	Limestone	Ribboned		Dolomite	
NM	299	249	59	bedding	Limestone	Interbedded		Limestone	
NM	300	245	68	bedding	Limestone	Massive		Limestone	
NM	301	262	59	bedding	Limestone	Massive		Dolomite	
NM	302	262	35	bedding					
NM	303	0	0	float					
NM	304	45	43	bedding	Limestone	Ribboned		Dolomite	
NM	305	25	60	cleavage	Nolichucky Shale	Fissile		Limestone	Shale
NM	316	50	45	bedding	Dolomite	Massive			
NM	317	41	60	bedding	Limestone	Ribboned		Dolomite	
NM	318a	213	37	joint	Limestone	Ribboned		Dolomite	
NM	318b	45	59	bedding	Limestone	Ribboned		Dolomite	
NM	319	50	50	bedding	Limestone	Ribboned		Dolomite	
NM	320	54	61	bedding	Limestone	Thrombolitic		Dolomite	
NM	321	55	59	bedding	Limestone	Cherty		Limestone	
NM	322	45	50	bedding	Limestone	Massive		Dolomite	
NM	323	38	49	bedding	Limestone	Massive		Dolomite	
NM	324	35	55	bedding	Limestone	Massive		Sandstone	
NM	326	37	49	bedding	Conococheague				
NM	328	33	50	bedding	Conococheague				
NM	329	0	0	float		Cherty			
NM	330	40	31	bedding	Limestone	Ribboned		Dolomite	
NM	332	38	44	bedding	Limestone	Ribboned		Dolomite	
NM	333	59	42	bedding	Limestone	Ribboned		Conococheague	
NM	334	0	0	float		Cherty		Conococheague	
NM	335	35	42	bedding	Conococheague				
NM	337	36	65	bedding	Limestone			Dolomite	
NM	338	78	55	bedding	Limestone				

QUAD	STATION	STRIKE	DIP	FEATURE	DOMINANT LITHOLOGY/UNIT	DESCRIPTION 1	DESCRIPTION 2	OTHER LITHOLOGY/UNIT 1	OTHER LITHOLOGY/UNIT 2
NM	339a	54	60	bedding	Limestone				
NM	339b	52	55	bedding	Limestone				
NM	340	328	21	bedding	Conococheague				
NM	341	0	0	float	Dolomite				
NM	342	0	0	float	Sandstone				
NM	343	335	40	bedding	Dolomite				
NM	344	0	0	float	Sandstone				
NM	345a	6	37	bedding	Limestone	Ribboned		Dolomite	
NM	345b	45	64	cleavage	Limestone				
NM	346	315	20	bedding	Limestone	Massive		Maynardville Limestone	
NM	347	0	0	float	Sandstone				
NM	348	32	38	bedding	Limestone				
NM	349	26	39	bedding	Maynardville	Massive		Dolomite	
NM	350	45	39	bedding	Maynardville	Fossiliferous		Limestone	
NM	351	61	42	bedding	Maynardville			Limestone	
NM	352	22	37	bedding	Maynardville				
NM	353a	13	26	bedding	Maynardville				
NM	353b	46	74	cleavage	Maynardville				
NM	354	50	36	bedding	Maynardville				
NM	357a	293	31	bedding	Maynardville				
NM	357b	60	74	cleavage	Limestone				
NM	358	253	47	bedding					
NM	359	0	0	float	Sandstone				
NM	362	241	87	bedding	Jonesboro?				
NM	364	247	55	bedding	Maynardville?				
NM	366	74	57	bedding	Limestone			Dolomite	
NM	367	55	60	bedding	Limestone	Ribboned		Dolomite	
NM	368	0	0	float	Sandstone	Cherty			
NM	369	0	0	float	Sandstone				
NM	370	41	39	bedding	Limestone				
NM	371	42	39	bedding	Limestone			Jonesboro	
NM	372	0	0	float	Sandstone				
NM	373	0	0	float		Cherty			
NM	374	0	0	float		Cherty			
NM	375	36	45	bedding	Limestone	Cherty		Longview	Jonesboro

QUAD	STATION	STRIKE	DIP	FEATURE	DOMINANT LITHOLOGY/UNIT	DESCRIPTION 1	DESCRIPTION 2	OTHER LITHOLOGY/UNIT 1	OTHER LITHOLOGY/UNIT 2
NM	376	37	43	bedding	Chepultepec				
NM	377	38	43	bedding	Chepultepec	Massive		Limestone	
NM	378	44	90	bedding	Chepultepec				
NM	379	38	45	bedding					
NM	380	49	70	bedding					
NM	391	0	0	float					
NM	392	46	64	bedding	Limestone	Massive			
NM	393	0	0	float	Sandstone				
NM	394	47	65	bedding	Limestone	Cherty			
NM	400	48	75	bedding	Limestone			Dolomite	Jonesboro
NM	401	48	65	bedding	Limestone				
NM	402	73	85	bedding	Limestone	Ribboned			
NM	403	246	73	bedding	Conococheague				
NM	404	50	63	bedding	Conococheague				
NM	406	55	75	bedding					
NM	407	72	80	bedding	Limestone	Massive			
NM	408	248	55	bedding	Limestone	Ribboned		Dolomite	
NM	409	75	90	bedding		Cherty			
NM	410	291	35	bedding					
NM	411	279	65	bedding	Limestone	Ribboned			
NM	412	279	30	bedding	Dolomite			Limestone	Sandstone
NM	413	0	0	float	Sandstone				
NM	414	239	53	bedding	Dolomite	Massive			
NM	415	240	60	bedding	Dolomite				
NM	416	241	63	bedding	Dolomite				
NM	417	267	62	bedding	Dolomite	Laminated			
NM	419	265	75	bedding					
NM	420a	240	55	bedding					
NM	420b	262	70	bedding	Dolomite				
NM	421	35	24	bedding	Jonesboro?				
NM	422	34	26	bedding	Limestone				
NM	423	60	16	bedding	Dolomite			Limestone	
NM	424	59	7	bedding					
NM	425	35	42	bedding					
NM	426	39	40	bedding					

QUAD	STATION	STRIKE	DIP	FEATURE	DOMINANT LITHOLOGY/UNIT	DESCRIPTION 1	DESCRIPTION 2	OTHER LITHOLOGY/UNIT 1	OTHER LITHOLOGY/UNIT 2
NM	427	36	55	bedding	Limestone				
NM	428	38	43	bedding					
NM	429a	38	40	bedding					
NM	429b	39	66	bedding					
NM	430	263	40	bedding					
NM	431	75	60	cleavage					
NM	432	255	55	bedding					
NM	433	245	50	bedding					
NM	434	215	50	bedding					
NM	435a	65	65	bedding	Sandstone			Limestone	
NM	435b	60	55	bedding	Limestone			Dolomite	
NM	435c	61	58	bedding	Limestone				
NM	435d	60	60	bedding	Copper Ridge Dolomite				
NM	436	55	50	bedding	Limestone			Sandstone	
NM	437	61	62	bedding	Limestone			Dolomite	
NM	438	50	82	bedding					
NM	439	52	72	bedding					
NM	440	55	55	bedding	Jonesboro Limestone				
NM	441	60	65	bedding	Jonesboro Limestone				
NM	442	47	50	bedding					
NM	443	50	60	bedding	Limestone			Jonesboro Limestone	
NM	444	65	45	bedding	Limestone	Ribboned		Dolomite	
NM	445	59	24	bedding	Limestone				
NM	446	0	0	float	Sandstone				
NM	447a	56	68	bedding	Sandstone				
NM	447b	52	66	bedding	Limestone				
NM	447c	50	55	bedding					
NM	448a	48	55	bedding	Sandstone			Limestone	
NM	448b	50	55	bedding	Limestone			Sandstone	
NM	448c	50	62	bedding	Limestone			Dolomite	
NM	449d	49	39	bedding	Limestone			Dolomite	Jonesboro Limestone
NM	449	49	40	bedding	Limestone			Dolomite	
NM	450a	42	58	bedding	Limestone	Thrombolitic		Dolomite	
NM	450b	48	40	bedding					
NM	451	42	58	bedding	Limestone	Ribboned		Dolomite	

QUAD	STATION	STRIKE	DIP	FEATURE	DOMINANT LITHOLOGY/UNIT	DESCRIPTION 1	DESCRIPTION 2	OTHER LITHOLOGY/UNIT 1	OTHER LITHOLOGY/UNIT 2
NM	452	52	47	bedding	Limestone	Laminated			
NM	453	56	72	bedding					
NM	454	50	57	bedding	Limestone			Jonesboro Limestone?	
NM	455	0	0	float	Sandstone				
NM	456	235	76	bedding	Limestone	Massive			
NM	457	56	68	bedding	Limestone			Dolomite	
NM	458a	49	80	bedding	Limestone			Dolomite	
NM	458b	49	75	bedding					
NM	459	0	0	float	Sandstone				
NM	460	240	85	bedding	Limestone			Dolomite	
NM	461	240	86	bedding	Limestone				
NM	462	0	0	float	Sandstone				
NM	463	66	41	bedding	Limestone				
NM	464	148	23	bedding	Sandstone				
NM	465a	55	90	bedding	Limestone				
NM	465b	57	90	bedding	Limestone				
NM	466	41	72	bedding	Limestone			Dolomite	
NM	467a	35	59	bedding	Limestone				
NM	467b	41	61	bedding	Limestone				
NM	468	0	0	float	Sandstone				
NM	469	0	0	float	Sandstone			Conglomerate	
NM	470a	51	64	bedding	Limestone				
NM	470b	48	65	bedding	Limestone				
NM	471	45	62	bedding	Limestone			Sandstone	
NM	472	303	64	bedding	Limestone	Cherty	Massive		
PR	1	69	65	bedding	Dolomite	Massive	Calcareous	Limestone	Honaker Dolomite
PR	2	75	54	bedding	Dolomite	Laminated		Honaker Dolomite	
PR	3	62	56	bedding	Dolomite	Laminated		Honaker Dolomite	Maryville Limestone
PR	4	325	87	cleavage	Dolomite	Laminated		Honaker Dolomite	Maryville Limestone
PR	5	49	52	bedding	Nolichucky Shale	Fissile	Massive	Maynardville Limestone	
PR	6	49	55	bedding	Maynardville Limestone	Massive			
PR	7	64	50	bedding	Limestone	Interbedded		Dolomite	
PR	8	58	58	bedding	Maynardville Limestone	Massive			
PR	9	61	54	bedding	Limestone				
PR	10	62	58	bedding	Honaker dolomite	Laminated		Dolomite	

QUAD	STATION	STRIKE	DIP	FEATURE	DOMINANT LITHOLOGY/UNIT	DESCRIPTION 1	DESCRIPTION 2	OTHER LITHOLOGY/UNIT 1	OTHER LITHOLOGY/UNIT 2
PR	11	55	60	bedding	Limestone	Massive		Dolomite	
PR	12	70	46	bedding	Rogersville Shale	Laminated	Fissile	Dolomite	
PR	13	210	52	cleavage	Rogersville Shale	Laminated	Fissile	Dolomite	
PR	14	0	0	float	Nolichucky Shale	Fissile		Shale	
PR	15	55	50	bedding	Conococheague Limestone	Ribboned	Interbedded	Limestone	Dolomite
PV	1	295	60	bedding	Limestone	Ribboned	Massive	Dolomite	Conococheague Limestone
PV	2	295	54	bedding	Limestone	Massive		Dolomite	
PV	3	272	30	bedding	Limestone	Laminated	Massive	Dolomite	Sandstone
PV	4	81	42	bedding	Limestone		Calcareous	Breccia	
PV	5	43	61	bedding	Limestone	Fissile	Massive	Shale	Nolichucky Shale
PV	6	0	0	float	Shale	Fissile		Nolichucky Shale	
PV	7	0	0	float	Shale		Fissile	Nolichucky Shale	
PV	8	31	28	bedding	Limestone	Massive	Ribboned	Dolomite	
PV	9	80	64	bedding	Limestone	Ribboned	Shaly	Dolomite	
PV	10	35	37	bedding	Dolomite	Interbedded		Limestone	

VITA

Phillip Michael Derryberry was born in Nashville, Tennessee, on September 12, 1986, to Gary and Virginia Derryberry. He was raised in Hendersonville, Tennessee, and graduated from Hendersonville High School in May 2004. In August 2005, just like his sister Jennifer Derryberry before him, he enrolled at Tennessee Technological University with plans on becoming a history major. He quickly changed his career path after discovering a passion for geology (a different kind of history). In his first year, he won the "Freshman of the Year Award in Geology" and went on to meet great success and opportunities in the remaining years, receiving his Bachelor of Science degree in Geosciences in May 2008. That following August, he entered the University of Tennessee, Knoxville, and started working toward his Master of Science Degree in Geology under Dr. Hatcher. A fascination with Valley and Ridge geology led him to stay in northeast Tennessee for his research.